SAE Aerospace
An SAE International Group

AEROSPACE INFORMATION REPORT

SAE AIR5020 | REV. A

Issued 1996-12
Reaffirmed 2004-11
Stabilized 2012-05

Superseding AIR5020

Time-Dependent In-Flight Thrust Determination

RATIONALE

The overall objectives and approach described in this document were intended to provide guidance and benchmarking. Readers may refer to this approach and practice guidance for application, comparison, or extension to their specific related tasks, using the appropriate technical data, requirements and the most current applicable references. The general approach and guidance are considered stable in regards to the above stated intent.

STABILIZED NOTICE

This document has been declared "Stabilized" by the SAE E-33 In-Flight Propulsion Measurement Committee and will no longer be subjected to periodic reviews for currency. Users are responsible for verifying references and continued suitability of technical requirements. Newer technology may exist.

SAENORM.COM : Click to view the full PDF of air5020a

SAE Technical Standards Board Rules provide that: "This report is published by SAE to advance the state of technical and engineering sciences. The use of this report is entirely voluntary, and its applicability and suitability for any particular use, including any patent infringement arising therefrom, is the sole responsibility of the user."

SAE reviews each technical report at least every five years at which time it may be revised, reaffirmed, stabilized, or cancelled. SAE invites your written comments and suggestions.

Copyright © 2012 SAE International

All rights reserved. No part of this publication may be reproduced, stored in a retrieval system or transmitted, in any form or by any means, electronic, mechanical, photocopying, recording, or otherwise, without the prior written permission of SAE.

TO PLACE A DOCUMENT ORDER: **Tel: 877-606-7323 (inside USA and Canada)**
Tel: +1 724-776-4970 (outside USA)
Fax: 724-776-0790
Email: CustomerService@sae.org
SAE WEB ADDRESS: **http://www.sae.org**

SAE values your input. To provide feedback on this Technical Report, please visit
http://www.sae.org/technical/standards/AIR5020A

INTRODUCTION

AIR1703 (Reference 1.1)[1] reviews the principles of thrust/drag accounting for wing-mounted and buried propulsion installations, and discusses thrust-method options, calibration techniques, and data acquisition, test planning and analysis guidelines. The material presented is circa 1980's state-of-the-art. Essentially, AIR1703 is limited to flight operations and associated ground calibrations in steady-state conditions: mainly fixed-throttle, level flight. As such, discussion of alternative flight techniques involving changes with time is purposely limited, it being assumed that the methods developed may be applied using the "quasi-steady" assumption (i.e., that time-variant conditions can be determined using steady-state analyses). The uncertainty considerations of AIR1678 (Reference 1.2)[1] are also consistent with the steady-state approach.

With time-variant flight conditions and either fixed- or variable-throttle engine operation, deviations of several percent from fundamental steady-state concepts and assumptions can occur, depending upon the nature of the transient - its duration and rate of change. A rigorous development requires that nonstationary mass, force, and energy terms in the governing performance equations be considered. The quasi-steady assumption may not be appropriate if flight and propulsion system parameters change sufficiently rapidly. Changes in aircraft and engine geometrical shape due to time-variant aerothermal loads may also need to be considered with the flight condition changes.

The practice of determining aircraft performance involves the determination of thrust minus drag (F_{EX}) through the measurement of aircraft acceleration and use of the quasi-steady assumption for aircraft vehicle aerodynamics and propulsion system thrust. It is important to realize in this connection that "thrust" includes engine net thrust ("standard" net thrust as defined in AIR1703) and propulsion system

---

[1] A review of AIR1703 is a prerequisite to reading this document since the present results and recommendations are based on evaluating the effects of time-variant deviations in the steady-state relationship established in AIR1703. AIR1703, which was issued in November 1985, provides engineering information for use as a reference and for guiding efforts to determine steady-state in-flight propulsion system thrust for fixed and variable sweep-wing aircraft employing turbofan or turbojet engines.The companion report, AIR1678, provides a methodology for estimating the "measurement" error involved in the ground calibration, flight, and posttest phases of the process.

SAENORM.COM : Click to view the full PDF of air5020a

INTRODUCTION (Continued)

throttle-dependent terms appropriate to the air intake spillage drag and afterbody jet interference force. Engine calibrations from the ground-level test stand and altitude test facility are utilized to evaluate "modified" net thrust as defined in AIR1703. The results of wind tunnel tests on intake and afterbody models are utilized to evaluate the throttle-dependent force terms. In maneuvering flight, the test data are obtained with higher response instrumentation to correct for time-dependent changes in flight condition. To date, flight tests have been conducted almost exclusively with fixed throttle to minimize engine transient effects on test data.

Typically, maneuvering flight methods encompass:

a. Level flight accelerations and decelerations
b. Climbs and descents
c. Push-overs and pull-ups
d. Wind-up turns and wind-down turns

To recover the steady drag polar from measurements obtained during time-variant test conditions, the rates of flight maneuvers are limited as required to avoid departure from quasi-steady conditions. The extent to which the quasi-steady assumption contributes to the data scatter and the limits to which the maneuvers must be maintained to yield acceptable results is far from clear. Prospectively, significant improvements in data accuracy and in the efficiency of flight data acquisition can be made if transient effects can be better accounted. A further technology advance could be made if reliable variable-throttle methods could be developed.

Ground-based techniques (i.e., engine sweep testing) for calibrating engine steady performance during transient conditions have been demonstrated in an effort aimed at reducing facility air-on time. This is accomplished through the use of controlled engine power lever transients, high-response instrumentation, and calibrated engine cycle models. Technology developments, together with the advance in instrumentation, fast data acquisition, and processing technologies, are determinants and provide incentive and impetus for an effort aimed at achieving these aims in flight testing.

The E-33 Committee debated the extension of its charter into the time-dependent thrust domain and determined that work would be warranted in view of the interest expressed in the subject. Therefore, it was proposed that a subcommittee, E-33E, be established to define guidelines for the determination of in-flight, time-variant thrust (i.e., net thrust and throttle-dependent forces) in order to enable the evaluation of aircraft drag and engine performance during time-variant operating conditions. The proposal was endorsed by the Propulsion Division of SAE. The first meeting took place in May 1986 under the chairmanship of Mr. E. C. Rooney, representing the Naval Air Systems Command, and this report documents the subcommittee's findings from the ensuing years.

Reference terms used in this report (and consistent with AIR1703) to describe engine and aircraft operating conditions are as follows:

SAENORM.COM : Click to view the full PDF of air5020a

INTRODUCTION (Continued)

a. Engine:

Steady-State: Fixed throttle and fixed flight conditions with no time-variant changes in engine aerodynamic and thermal performance.

Quasi-Steady: Operation where time-variant changes in engine aerodynamic and thermal performance are sufficiently slow to assume steady-state operating conditions at specified time.

Transient: Variable throttle and/or flight conditions where time-variant changes in engine aerodynamic or thermal performance must be accounted. The term "unsteady" in AIR1703 is used synonymously with transient engine operation.

Dynamic: Refers to engine high-frequency aerodynamic characteristics associated with combustor/augmentor instabilities and component highly turbulent/separated flows. Engine dynamic considerations are not included in this report.

b. Aircraft:

Steady-State: Fixed attitude and flight conditions with no time-variant changes in aircraft performance.

Quasi-Steady: Operation where time-variant changes in aircraft performance are sufficiently slow to assume steady-state operation at the specified time.

Dynamic: Variable maneuver and/or flight conditions where time-variant changes in aircraft performance must be accounted. Note, the term "dynamic" is used to describe time-variant aircraft operation and not "transient" as used for engine time-variant operation.

Unsteady: Refers to high-frequency aerodynamic flow-field characteristics associated with separated flows and boundary-layer flow interactions. Unsteady flow-field characteristics are not included in this report.

This report reviews the major aspects of processes that must be considered for the determination of in-flight time-variant thrust. Since thrust and drag are first-order interrelations, the concept of drag is introduced into the report, but only as required to understand aircraft thrust-drag polar resolutions. The report is organized into seven major sections (absent the Introduction and Reference sections and the Appendices) comprising the following topics:

SAENORM.COM : Click to view the full PDF of air5020a

INTRODUCTION (Continued)

a. Scope (Section 1): Presents the goal of the E-33E Subcommittee effort, outlines the specific objectives of the report, and documents limitations with respect to conclusions and recommendations.

b. Time-Dependent Thrust Considerations (Section 3): Discusses the theoretical basis and first-order considerations for determining time-dependent thrust. A review of force and drag accounting increments is provided. Results based on time-dependent analyses, wave propagation considerations, and test operational experience are used to estimate aircraft and engine operational limits for application of quasi-steady thrust determination methodologies.

c. In-Flight Thrust Methods (Section 4): Reviews individual methods available for the determination of time-dependent in-flight thrust and identifies the merits and limitations of each method.

d. Test Facilities (Section 5): Reviews the use of ground-level test stands and altitude test facilities to quantify engine time-dependent operational performance, including the use of wind tunnels, aircraft installed facilities, and aircraft to support final integration of airframe and engine performance.

e. Test Data Acquisition (Section 6): Describes the instrumentation and measurement systems necessary for obtaining data under time-variant test conditions. Measurement considerations that are unique to ground facilities and flight environment are identified. The data processing of both ground and flight information are presented, and typical measurement uncertainties of thrust-related parameters are listed.

f. Flight Testing (Section 7): Describes the procedures and use of ground and flight test programs to isolate and correct errors and improve confidence in test results including:

   (1) The equations and methodology used for aircraft performance measurement (lift, drag, thrust, and excess thrust) and maneuvers employed in the evaluation of these elements for time-dependent aircraft operating conditions,

   (2) Data consistency checks and validation of test data that are accomplished to enhance confidence in the vehicle thrust measurements,

   (3) Evaluation of the validity of the quasi-steady assumption for fixed-throttle engine operation, and

   (4) Validation procedures for time-variant thrust measurement (variable-throttle engine operation).

g. Guidelines for Time-Dependent Thrust Determination (Section 8): Summarizes ground and flight test planning considerations for test techniques, instrumentation, and data analysis required to assess time-variant in-flight thrust.

SAENORM.COM : Click to view the full PDF of air5020a

FOREWORD

Industry and government agencies concerned with aircraft flight performance evaluation recognize a need to improve technology and methods for the assessment of thrust during aircraft maneuvers and transient engine operation. Building on the in-flight steady-state thrust and uncertainty work of the E-33 Committee, published in AIR1703 and AIR1678, the E-33 Committee undertook to determine whether an information report on time-dependent thrust methods and associated uncertainty was warranted.

To address this issue, Subcommittee E-33E was formed in 1986 with Mr. Eugene C. Rooney appointed as chairman and Mr. Darrel Williams appointed as vice chairman. In addition, members representing a cross section of industry and government concerned with flight performance evaluation were selected to serve on this subcommittee.

The E-33E Subcommittee, in its proceedings, produced a considerable body of information which reviewed flight maneuvers and addressed from fundamental principles the question of engine time-dependent thrust and propulsion system throttle-dependent force terms. The subcommittee determined that this information, organized into a generally-available document, would provide a source of knowledge for engineers. Accordingly, AIR5020 was prepared. Significant comments and opinions obtained from wide circulation of the report in the U.S. and Europe have been taken into consideration. A list of the individuals and their sponsoring organizations who contributed many hours of work in the compilation of the report is provided on the following page.

SAENORM.COM : Click to view the full PDF of air5020a

SAE E-33E SUBCOMMITTEE MEMBERSHIP

Ms. J. Baer-Riedhart, NASA Dryden Flight Research Center
Mr. J. D. Dinkel, Northrop-Grumman Aerospace Corporation
Mr. G. Kamphaus, Aeronautical Systems Center, Wright-Patterson AFB
Mr. R. F. Lauer, Jr., Micro Craft Technology, AEDC Operations
Mr. M. A. Luter, Naval Air Systems Command
Mr. J. McCrillis, Naval Air Warfare Center, Aircraft Division
Mr. S. L. Parker, McDonnell Douglas Aerospace
Mr. R. J. Ray, NASA Dryden Flight Research Center
Mr. J. H. Roberts, Chairman E-33, Pratt & Whitney Commercial Engine Business
Mr. E. C. Rooney, Chairman E-33E, Naval Air Systems Command (Retired)
Mr. P. Singshinsuk, Naval Air Systems Command
Dr. W. G. Steenken, GE Aircraft Engines
Mr. M. Thompson, Naval Air Warfare Center, Aircraft Division
Mr. W. S. Thompson, Pratt & Whitney Government Engine and Space Propulsion
Mr. E. C. Wantland, Sverdrup Technology, Inc., AEDC Division
Mr. A. T. Webb, ENF Flight Dynamics, USAF, Edwards AFB
Mr. S. Wehofer, Sponsor E-33E, Sverdrup Technology, Inc., AEDC Division
Mr. D. D. Williams, Rolls Royce Limited (Retired)
Mr. C. E. Wilt, Naval Air Systems Command (Retired)

SAENORM.COM : Click to view the full PDF of air5020a

TABLE OF CONTENTS

SAENORM.COM : Click to view the full PDF of air5020a

TABLE OF CONTENTS (CONTINUED)

SAENORM.COM : Click to view the full PDF of air5020a

TABLE OF CONTENTS (CONTINUED)

SAENORM.COM : Click to view the full PDF of air5020a

1. SCOPE:

The purpose and intent of Subcommittee E-33E's effort, the reporting objectives, and the limitations inherent in the reported findings and recommendations are reviewed since these factors are the basis of the information contained in this document.

SAE E-33E Subcommittee was formed to assess the level of industry experience that exists in the area of thrust determination during aircraft time-variant operating conditions. A prime objective was to provide a center for gathering expertise and to be a forum for the exchange of ideas and viewpoints. The committee recognized that a practice for the rigorous treatment of time-dependent thrust did not exist and that several critical aspects of its accounting would need to be investigated.

The specific objectives of this document are:

a. To examine aircraft and engine operating conditions under which the quasi-steady thrust assumption is valid.

b. To determine the extent to which time-dependent (nonstationary) force accounting for engine net thrust and propulsion system throttle-dependent terms is required, consistent with existing and developing thrust-minus-drag techniques.

c. To report time-dependent thrust methodologies and measurement techniques used for flight and ground testing.

d. To present the results of a data review of state-of-the-art methodology appropriate to the determination of aircraft-installed thrust during quasi-steady and dynamic maneuvers.

e. To provide guidelines for validating and improving time-dependent thrust determination as appropriate to a specific program.

1.1 Limitations:

This document addresses definitions of thrust, force, and drag from test principles (when possible) based on steady practices as defined in AIR1703. It is limited to fixed-wing and variable swept wing aircraft employing turbojet or turbofan engines with nonvectoring or fixed vectored nozzle position but not with time-variant vectoring terms. It is not the purpose of this document to detail onboard high-response data systems or develop new in-flight thrust methodologies. Conclusions and recommendations are valid only where criteria and data for a specific program or application have been identified and measurement uncertainty aspects of the data understood. It is anticipated that this document will be updated periodically as new developments in ground and flight testing occur.

SAENORM.COM : Click to view the full PDF of air5020a

2. REFERENCES:

2.1 Applicable Documents:

The following publications form a part of this document to the extent specified herein. The latest issue of SAE publications shall apply. The applicable issue of other publications shall be the issue in effect on the date of the purchase order. In the event of conflict between the text of this document and references cited herein, the text of this document takes precedence. Nothing in this document, however, supersedes applicable laws and regulations unless a specific exemption has been obtained.

2.1.1 Section 1:

1.1 "In-flight Thrust Determination." SAE, AIR1703, November 1985.

1.2 "Uncertainty of In-Flight Thrust Determination." SAE, AIR1678, November 1985.

2.1.2 Section 3:

3.1 Covert, E. E., et al. "Thrust and Drag: Its Prediction and Verification." Progress in Astronautics and Aeronautics, Vol. 98, Chap. 2, AIAA, New York, 1985.

3.2 Shames, Irving H. Engineering Mechanics. Vol. II, Dynamics, Prentice-Hall Engineering Science Series, 1966.

3.3 Van Wylen, Gordon J. and Sonntag, Richard E. Fundamentals of Classical Thermodynamics. Series in Thermal and Transport Sciences, Wiley & Sons, Inc., 1968.

3.4 Dunlap, Everett W. and Porter, Milton B. "Theory of the Measurement and Standardization of In-Flight Performance of Aircraft." Air Force Flight Test Center, FTC-TD-71-1, April 1971.

3.5 Etkin, Bernard. "Dynamics of Atmospheric Flight." John Wiley & Sons, Inc., 1972.

3.6 "Gas Turbine Engine Performance Station Identification and Nomenclature." SAE, ARP755A; April 15, 1974.

3.7 "Gas Turbine Engine Steady State Performance Presentation for Digital Computer Programs." SAE, AS 681C; April 15, 1974.

3.8 Sverdrup Technology, Inc., internal memorandum from F. C. Loper to S. Wehofer, dated May 1991, Subject: "One-Dimensional Time Dependent Equations for a Flow Through Nacalle with Fuel Injection."

SAENORM.COM : Click to view the full PDF of air5020a

2.1.3 Section 4:

4.1 Baer-Riedhart, Jennifer L. "Evaluation of a Simplified Gross Thrust Calculation Method for a J85-21 Afterburning Turbojet Engine in an Altitude Facility." AIAA Paper 82-1044, June 1982.

4.2 Kurtenbach, Frank J. and Burcham, Frank W., Jr. "Flight Evaluation of a Simplified Gross Thrust Calculation Technique Using An F100 Tubofan Engine in an F15 Airplane." NASA TP 1782, June 1981.

4.3 Alexander, R. I. and Ray, R. J. "Development and Flight Test of a Real-Time Thrust Measurement Technique on the X-29A/F404 Advanced Technology Demonstrator." NASA TM 101707, September 1989.

4.4 Huges, Donald L. "Comparison of Three Thrust Calculation Methods Using In-Flight Thrust Data," NASA TM 81360, July 1981.

4.5 AS681D, "Gas Turbine Engine Transient Performance Presentation for Digital Computer Programs." 1983.

4.6 Khalid, S. J. and Hearne, R. E. "Enhancing Dynamic Model Fidelity for Improved Prediction of Turbofan Engine Transient Performance." AIAA-80-1083.

4.7 Hutcheson, L. C. "AEDC Development and Validation of a J79 Engine Status Deck for the AFFTC Dymotech Program" presented at the 2nd Annual Dynamic Workshop held at AEDC, May 8-9, 1979.

4.8 Khalid, S. J. "Role of Dynamic Simulation in Fighter Engine Design and Development." AIAA-89-2467.

4.9 Khalid, S. J. and Faherty, M. F. "Propulsion System Flight Test Analysis Using Modeling Techniques." AIAA-90-3288.

4.10 Shaefer, H. J. "Measurements of a Mean-Flow and Turbulence Characteristics in a Turbojet Exhaust Using a Laser Velocimeter." N89-28519#, September 1988.

4.11 Johnson, D. A. "Doppler Anemometry." N89-28739#, May 1989.

4.12 Elena, M. "Laser Doppler Anemometry in Supersonic Flows." Problems of Seeding and Angular Bias," N89-28740#, May 1989.

4.13 Dopheide, D. et al. "The Use of High-Frequency Pulsed Laser Diodes in Fringe Type Laser Doppler Anemometer." N89-28826#, September 1988.

SAENORM.COM : Click to view the full PDF of air5020a

2.1.3 (Continued):

4.14 Leland, R. "Wind Profile Estimation from Point Laser Distortion Data." N89-28990#, August 1989.

2.1.4 Section 5:

5.1 Kimzey, W. F. and Wantland, E. C. "Short Duration Turbine Engine Testing for Energy Conservation." AIAA-77-991, July 1977.

5.2 Overall, B. W. and Harper, R. E. "The Airjet Distortion Generator System: A New Tool for Aircraft Turbine Engine Testing." AIAA-77-993, July 1977.

5.3 Duesterhaus, D. A. and Maywald, P. V. "Free-jet Test Capability for the Aeropropulsion Systems Test Facility." AIAA-89-2537, July 1989.

5.4 Wantland, E. C. "Turbine Engine Operability Test and Evaluation Techniques." AIAA-91-2277, June 1991.

5.5 Chappell, M. A. and McKamey, R. S. "Adjusting Turbine Engine Transient Performance for the Effects of Environmental Variances." AIAA-90-2501, July 1990.

5.6 "Aeronautical Facilities Catalogue, Volume 1, Wind Tunnels." NASA RP-1132, January 1985.

2.1.5 Section 6:

6.1 MIL-STD-1553B, "Aircraft Internal Time Division Command/Response Multiplex Databus." 21 Sept 1978.

6.2 Whitmore, S. A., "Formulations of a General Technique for Predicting Pneumatic Attenuation Errors in Airborne Pressure Sensing Devices." NASA TM 100450, May 1988.

6.3 Edwards, J. L., "Guide to Temperature Monitoring in Aircraft Gas Turbine Engines." SAE Technical Paper Series 871730, 1987.

6.4 "Guide to the Measurement of the Tranisent Performance of Aircraft Turbine Engines and Components." AGARD, AR-320, March 1994.

6.5 Hicks, J. W. and Huckabone, T., "Preliminary Flight-Determined Subsonic Lift and Drag Characteristics of the X-29A Forward-Swept-Wing Airplane." NASA TM 100409, August 1989.

6.6 "Flying Qualities Theory and Flight Test Techniques." Dynamic Parameters Analysis, USAF Test Pilot School, Aug 1978. (Requests for this document must be referred to USAFTPS/TENC, Edwards AFB, CA).

SAENORM.COM : Click to view the full PDF of air5020a

2.1.5 (Continued):

6.7 Abernethy, R. B. and Thompson, J. W., Jr. Handbook, Uncertainty in Gas Turbine Measurements, AEDC-TR-73-5, February 1973.

6.8 Fluid Flow Measurement Uncertainty, ISO/DIS 5168 for International Organization for Standardization Committee, May 1987.

2.1.6 Section 7:

7.1 Pueschel, P. "Development of Dynamic Methods of Performance Flight Testing." Report No. ADR-07-01-70, Grumman Aerospace Corporation, Bethpage, New York, August 1970.

7.2 "Performance." Report No. FTC-T1H-70-1001, Air Force Aerospace Research Pilot School, Edwards Air Force Base, CA, February 1970.

7.3 Perkins, C. D. and Hage, R. E. "Airplane Performance Stability and Control." John Wiley and Sons, Inc., New York, 1949.

7.4 Rooney, E. C. and Craig, R. E. "Development of Techniques and Correlation of Results to Accurately Establish the Lift/Drag Characteristics of an Air Breathing Missile from Analytical Predictions, Sub-scale and Full Scale Wind Tunnel Tests and Flight Tests." Presentation No. 16 at the Specialists' Meeting on "Aircraft Performance Prediction Methods" sponsored by the AGARD Flight Mechanics Panel at Paris, France, 11-13 October 1977.

7.5 Rooney, E. C. "Development of Techniques to Measure In-flight Drag of a U. S. Navy Fighter Airplane and Correlation of Flight Measured Drag with Wind Tunnel Data." Presentation No. 24 at the Specialists' Meeting on "Aerodynamic Drag," sponsored by the AGARD Fluid Dynamics Panel at Izmir, Turkey, 10-13 April 1973.

7.6 Hicks, J. W. and Moulton, B. J. "Effects of Maneuver Dynamics on Drag Polars of the X-29 Forward-Swept-Wing Aircraft With Automatic Wing Camber Control." NASA TM 100422, June 1988.

7.7 Herman, J. F. and Washington, E. S. "Wind Tunnel Measurements of Aerodynamic Hysteresis on the F4C Aircraft, and Its Effects on Aircraft Motion." AEDC-TR-80-10, 1980.

7.8 Symposium on Transonic Aircraft Technology (TACT) held Lancaster, CA, 15-17 August 1978, AFFDL-TR-78-100.

7.9 Ray, R. J. "Evaluation of Various Thrust Calibration Techniques on an F404 Engine." NASA TP 3001, April 1990.

SAENORM.COM : Click to view the full PDF of air5020a

2.2 Symbols:

TABLE 1A - Roman

Description	Units	U.S. Common Units	SI Units
A	Area	ft^2	m^2
a	Acceleration	ft/s^2	m/s^2
A/B	Afterburner or Augmentor	-	-
B	Bias or Systematic error	-	-
BAA	Body axis accelerometer	-	-
C_D	Discharge coefficient or drag coefficient	-	-
C_f	Flow coefficient	-	-
C_G	Gross thrust coefficient	-	-
C_L	Lift coefficient	-	-
C_V	Specific thrust coefficient based on ideal flexible convergent-divergent nozzle expansion		
CVV	Compressor variable vane setting	deg	deg
D	Drag force	lbf	N
D_{AFS}	Aircraft system drag at full-scale operating conditions	lbf	N
D_{REFOP}	Aircraft system reference drag at full-scale operating reference conditions	lbf	N
dt	Derivative with respect to time	s	s
E	Energy	ft-lbf	m-N
EPR	Engine pressure ratio	-	-
f( )	Function of argument within ( )	-	-
F	Force or absolute stream force	lbf	N
FPA	Flight path accelerometer	-	-
F_{EX}	Excess thrust (i.e., thrust minus drag)	lbf	N
F/AP	Ideal gross thrust parameter, "pressure area" formulation	-	-
$F/W\sqrt{T}$	Ideal gross thrust parameter, "flow temperature" formulation	-	-
F_G	Gross thrust and gauge stream force	lbf	N
F_{IPF}	Installed propulsive force	lbf	N
F_M	Measured test stand force	lbf	N
F_N	Net thrust between Stations 0 and 9 for single-stream engine (Figure 2)	lbf	N
F',N	Overall net thrust between Stations 0 and 00 (Figure 2)	lbf	N
$\dot{F}_N$	Modified net thrust	lbf	N
$F_{N,int}$	Intrinsic net thrust between Stations 1 and 9 (Figure 2)	lbf	N
F_R	Ram drag and free-stream momentum	lbf	N
FRL	Fuselage reference line	-	-
FS	Full scale	-	-
F_T	Trunnion thrust	lbf	N
FVV	Fan variable vane setting	deg	deg
g	Gravitation constant	ft/s^2	m/s^2
H	Altitude	ft	m
Hz	Frequency	s^{-1}	s^{-1}
IRT	Intermediate rated thrust	lbf	N
k	Thousand	-	-
KE	Kinetic energy	ft/lbf	m-N
L	Aircraft lift force or	lbf	N
	length	ft	m
L_X	Distance from aircraft nose to engine face	ft	m
LPC	Low pressure compressor	-	-
M	Mach number	-	-
m	Mass	slug	kg
MAX	Maximum afterburner thrust	lbf	N

SAENORM.COM : Click to view the full PDF of air5020a

TABLE 1A (Continued)

Description	Units	U.S. Common Units	SI Units
N	Engine rotor speed	rpm	rpm
NC	Corrected rotor speed	rpm	rpm
NPR	Nozzle pressure ratio	-	-
N_x	Aircraft longitudinal acceleration	g	g
N_y	Aircraft lateral acceleration	g	g
N_z	Aircraft normal acceleration	g	g
PE	Potential energy	ft/lbf	m-N
PLA	Power lever angle	deg	deg
PLF	Power for level flight	lbf	N
P_S	Specific excess power (Equation 43)	ft/s	m/s^2
P_ψ	Percent change in P_{t2} lapse rate with aircraft attitude = $dP_{t2}/d\psi$	deg^{-1}	deg^{-1}
P_∞	Free-stream static pressure	lbf/ft^2	N/m^2
P	Static pressure	lbf/ft^2	N/m^2
P_t	Total pressure	lbf/ft^2	N/m^2
q	Free-stream dynamic pressure	lbf/ft^2	N/m^2
R	Gas constant	ft-lbf/lbm-R	J/kg K
rad	Radian	rad	rad
RN	Reynolds number	-	-
rpm	Revolution per minute	min^{-1}	min^{-1}
S	Surface/reference area or	ft^2	m^2
	precision/random error	-	-
s	Second	s	s
SGTM	Simplified gross thrust method	-	-
SLM	Simplified linear model	-	-
SNTM	Simplified net thrust method	-	-
SPS	Samples per second	s^{-1}	s^{-1}
SVM	State variable model	-	-
T_t	Total temperature	°R	°K
t	Time	s	s
U	Measurement uncertainty at 95% confidence level	-	-
u	Axial velocity	ft/s	m/s
V	Velocity or flight speed	ft/s	m/s
v	Specific volume	$(slug/ft^3)^{-1}$	$(slug/ft^3)^{-1}$
W	Mass flow rate or	slug/s	kg/s
	aircraft weight	lbm	N
W_c	Corrected mass flow rate	slug/s	slug/s
WB	Bleed flow rate	lbm/h	kg/s
WCL3	Compressor bleed cooling flow	lbm/h	kg/s
WF	Fuel mass flow rate	lbm/h	kg/s
WFA/B	Augmentor fuel flow rate	lbm/h	kg/s
W_{RF}	Afterburner fuel mass flow rate	lbm/h	kg/s
X	Axial distance or	ft	m
	flight path longitudinal axis	-	-
Z	Flight path normal axis	-	-

SAENORM.COM : Click to view the full PDF of air5020a

TABLE 1B - Greek

α	Angle of attack or	deg	deg
	nozzle force vertical vector angle	deg	deg
$\dot{\alpha}$	Angle of attack change rate	deg/s	deg/s
γ	Specific heat ratio = C_p/C_v	-	-
	or aircraft flight path angle	deg	deg
δ	Nondimensional pressure = $P/P_{SL, STD}$	-	-
Δ	Parameter incremental change	-	-
η_R	Intake pressure recovery = P_{t2}/P_{t0}	-	-
β_{eff}	Nozzle effective yaw angle	deg	deg
β	Angle of sideslip	deg	deg
θ	Nondimensional temperature = $T/T_{SL, STD}$ or	-	-
	aircraft pitch attitude	deg	deg
θ_{CR}	Exhaust nozzle flap metal angle	deg	deg
θ_{EFF}	Effective exhaust nozzle vector angle based on force vectors	deg	deg
ϕ	Axial gauge force on a body or streamtube surface	lbf	N
ϕ_{post}	Axial gauge force on post exit streamtube between Stations 9 and 00 (Figure 2)	lbf	N
ϕ_{pre}	Axial gauge force on pre-entry streamtube between engine Stations 0 and 1 (Figure 2)	lbf	N
ϕ_{pylon}	Axial gauge force on pylon surface within bypass streamtube	lbf	N
τ	Longitudinal thrust inclination angle	deg	deg
ψ	Aircraft attitude = $(\alpha^2 + \beta^2)^{1/2}$	deg	deg
$\dot{\psi}$	Aircraft attitude change rate	deg/s	deg/s
ω	Angular frequency	rad/s	rad/s
∂t	Partial with respect to time	s	s
Λ	Wing sweep angle	deg	deg
ρ	Density	$slug/ft^3$	kg/m^3
σ	Standard deviation	-	-
Σ	Summation	-	-

SAENORM.COM : Click to view the full PDF of air5020a

TABLE 1C - Subscripts

0,1,2,etc.	Station designations (see Figure 1)
AB	Afterbody (i.e., nozzle/afterbody drag)
AC	Aircraft
act	Actual value (distinguished from "ideal")
aft	Aft facing position
AMB	Ambient
AVG	Average
C	Corrected
calc	Calculated
con	Convergent ideal nozzle
CV	Control volume
eff	Effective value of V at exit from a con-di nozzle which, when multiplied by W_{act}, gives $F^{G, act}$, or effective flow area
EXH	Exhaust
flex-con-di	Flexible convergent-divergent ideal nozzle
FPA	Flight path acceleration
FRL	Fuselage reference line
fwd	Forward facing position
g	Gas
H	High-pressure engine spool
id	Ideal value (distinguished from "actual")
int	Internal
INL	Inlet
J	Jet exhaust
L	Low-pressure engine spool
L/H	Left-hand engine
M	Measured
max, MAX	Maximum
min,MIN	Minimum
OP	Operating condition
ref, REF	Reference value or conditions
R/H	Right-hand engine
RN	Reynolds number
STD	Standard (temperature or pressure)
t	Total conditions
t/c	Time constant
TRIM	Aircraft trim related
WL	Wing length
X	Flight path longitudinal axis
Y	Flight path lateral axis
Z	Flight path normal axis
∞	Free-stream

SAENORM.COM : Click to view the full PDF of air5020a

3. TIME-DEPENDENT THRUST CONSIDERATIONS:

The theoretical basis and first-order considerations for determining time-dependent thrust are reviewed in this section. Force accounting development and application are presented, one-dimensional time-dependent analyses results are evaluated, and practical considerations and operational experience for determination of time-dependent thrust are provided.

3.1 Thrust/Drag Accounting:

Accurate prediction of air vehicle performance, tracking, and evaluation of the elements of performance and correlation between prediction and flight measurements requires definition of a thrust-drag accounting or "bookkeeping" system which clearly defines the treatment of all the aerodynamic and propulsion-related forces acting on the system. The variety of actual and possible aerodynamic and propulsion system configurations makes it impractical to specify a single rigorous accounting system. The accounting methodology should be tailored to the requirements, details of the aerodynamic/ propulsion configuration, and resources of each development program. However, the chosen methodology should address the following characteristics: (1) consistency, (2) visibility given to the performance of the elements of the airplane system, (3) selection of realistic reference conditions, and (4) suitability and consistency for tracking the integrated propulsion/airframe performance throughout the aircraft development program.

3.1.1 Basic Equations: As developed in AIR1703, the breakout of forces, definition of terms, and reference conditions applicable to the fully integrated propulsion configuration where the effects of the inlet and exhaust nozzle can be determined separately and combined linearly are repeated herein (see Section 2.2 of AIR1703 for additional discussion and Reference 3.1 for handling of alternate aerodynamic and propulsion configurations). Considering an aircraft in level flight, the simplified force equation applied in the flight direction for dynamic aircraft conditions takes the form:

$$F_{EX} = F_{IPF} - D_{AFS} \qquad \text{(Eq.1)}$$

where:

F_{EX} = Imbalance (total force) between the engine thrust and aircraft drag forces in the light direction at given aircraft and engine operating conditions.
F_{IPF} = Installed net propulsive force that is obtained from net thrust, with adjustment for deviations from full-scale operating reference conditions.
D_{AFS} = Airframe system drag force at full-scale operating conditions.

Additional forces are included in the F_{IPF} (Thrust) and D_{AFS} (Drag) terms to account for defined or chosen reference full-scale operating conditions and excursions from the full-scale operating conditions. These additional forces are discussed in the following subsections.

SAENORM.COM : Click to view the full PDF of air5020a

3.1.2 Installed Net Propulsive Force: The installed propulsive force is defined to be equal to the installed net thrust at the full-scale reference conditions, and accounts for all propulsive forces acting on the aircraft. For excursions from the full-scale reference conditions, incremental forces must be considered. These throttle-dependent forces are included as adjustments to develop the installed propulsive force:

$$F_{IPF} = F_N^* - \Delta F_{INL} - \Delta F_{EXH} - \Delta F_{TRIM} \quad \text{(Eq.2)}$$

where:

F_N^* = Modified net thrust, accounting for installation effects of inlet internal performance, bleed air extractions, and shaft power extractions.

ΔF_{INL} = External force increment between full-scale reference and any given operating condition due to the inlet (see Figure 2.7 in AIR1703).

ΔF_{EXH} = External force increment between full-scale reference and any given operating condition due to the exhaust system (see Figure 2.8 in AIR1703).

ΔF_{TRIM} = External control surface trim force increment associated with operating the propulsion system at other than the chosen propulsion system reference conditions.

3.1.3 Airframe System Drag Force: The derivation of D_{AFS} accounts for the nonthrottle-dependent differences in the drag polar between the aerodynamic model reference conditions and the full-scale operating conditions, as follows:

$$D_{AFS} = D_{REF} + \Delta D_{INL} + \Delta D_{EXH} + \Delta D_{TRIM} + \Delta D_{RN} \quad \text{(Eq.3)}$$

where:

D_{REF} = External airframe drag at the aerodynamic model reference conditions adjusted to the reference full-scale Reynolds number and complete full-scale airframe configuration.

ΔD_{INL} = Nonthrottle-dependent external force increment between the aerodynamic model reference conditions and the chosen full-scale reference operating conditions due to the inlet (see Figure 2.7 in AIR1703).

ΔD_{EXH} = Nonthrottle-dependent external force increment between the aerodynamic model reference conditions and the chosen full-scale reference operating conditions due to the exhaust system (see Figure 2.8 in AIR1703).

ΔD_{TRIM} = Nonthrottle-dependent external force increment between the full-scale reference condition and any given operating condition due to control surface changes for trim.

ΔD_{RN} = External force increment associated with Reynolds number differences (skin friction drag) between the full-scale reference conditions and any given flight operating condition.

SAENORM.COM : Click to view the full PDF of air5020a

3.1.4 Force Accounting Development and Application: The preceding breakout of force increments is not all-inclusive, but is representative of the kinds of items that must be included. Additional items such as drag increments due to inlet and exhaust secondary airflows may be required for a particular aerodynamic/propulsion configuration. Separate tests and/or analytic calculations are required to develop the information required to support the chosen force accounting system. Generally, wind tunnel tests are conducted to determine the incremental drag forces attributable to the inlet and afterbody geometry, inlet mass flow ratio, nozzle pressure ratio, and control surface effects on vehicle trim. The applicability of these force increments, derived under steady-state conditions, to time-variant aircraft and engine operating conditions is discussed in 3.2 through 3.5.

3.2 Propulsion System Net Thrust:

The basic premise used to establish the steady-state in-flight thrust methodology in SAE AIR1703, "In-Flight Thrust Determination," was to define a propulsion system thrust and associated aircraft drag with the thrust axis parallel to the flight path so thrust and drag are equal in level, nonaccelerating flight. The steady-state installed propulsive force provided in AIR1703 is defined by Equation 2. The terms ΔF_{INL}, ΔF_{EXH}, ΔF_{TRIM} [Equation 2)] are referred to as aircraft throttle-dependent forces, and F_N^* as the propulsion system modified net thrust. Ideally, the determination of time-variant propulsive force would expand on the basic methodology developed for steady-state in-flight thrust by the algebraic addition of the time-dependent force terms to the steady-state definition. Initially, it was intended to utilize the generalized three-dimensional equations of motion, including energy transfer, for a propulsion system during an aircraft maneuver and, through linearization, to quantify the magnitude of the time-dependent forces acting on the propulsion system (refer to Appendix A regarding these initial efforts). However, after conducting a literature survey (References 3.2 through 3.5) and completing discussions with industry and university personnel, it was determined that the development of the general equations was beyond the scope and resources of the committee. Instead, the approach by the committee was to use one-dimensional, time-dependent analyses to quantify the relative effect of time-variant maneuvers and throttle movement on the magnitude of propulsion system net thrust, and to use wave propagation and volumetric time considerations to quantify the relative effect of time-variant effects on throttle-dependent forces and aircraft performance.

Prior to discussing a methodology for estimating the magnitude of time-dependent influences on propulsion system net thrust, it is necessary to introduce a consistent station numbering system to define flow path locations ahead, within and aft of the propulsion system. Figure 1 presents a summary of the station numbering system used in this report. The designations in Figure 1 are consistent with SAE ARP755A and AS681C (References 3.6 and 3.7, respectively).

To identify the impact of transient operation on steady-state net thrust, consider the simple nacelle shown in Figure 2.

SAENORM.COM : Click to view the full PDF of air5020a

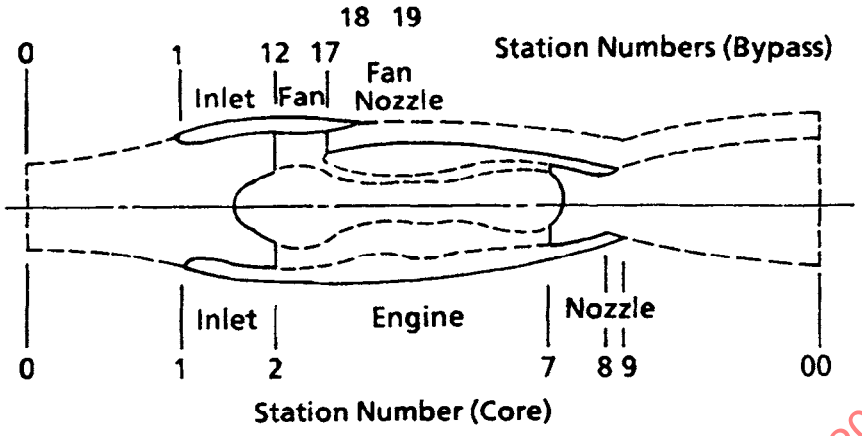

FIGURE 1 - Station Numbering System

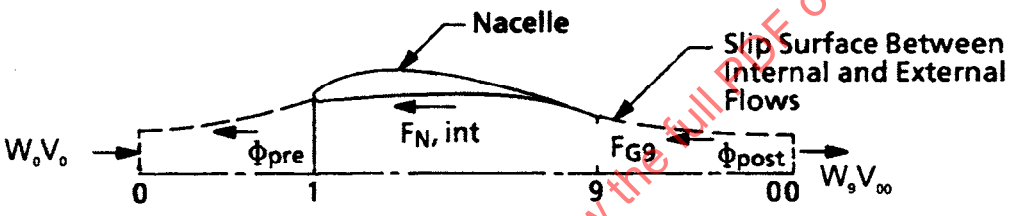

FIGURE 2 - Force Components for Simple Nacelle

3.2 (Continued):

The concept of steady-state net thrust is derived by the hypothesis of a slip surface so that drag can be equated to a momentum defect at a station far downstream (Sta. 00) and thrust may be equated to the momentum of the propulsive system exhaust stream at a station far downstream (Sta. 00) of the nozzle exit station (Sta. 9), less the momentum of the internal flow at a station far upstream (Sta. 0) of the engine inlet (Sta. 1). The overall modified net thrust of a single-stream propulsion system operating under steady-state conditions can therefore be represented by the expression:

$$F_N^* = W_9 V_{00} - W_0 V_0 \qquad \text{(Eq.4)}$$

The difference in Sta. 00 and Sta. 0 momentum is also equivalent of the sum of the forces ϕ_{pre}, $F_{N,int}$, and ϕ_{post} exerted on the streamtube bounding the flow between these two stations (Refer to Figure 2), or

SAENORM.COM : Click to view the full PDF of air5020a

3.2 (Continued):

$$F_N^* = \phi_{pre} + F_{N,int} + \phi_{post} \quad \text{(Eq.5)}$$

ϕ_{pre} and ϕ_{post} are the forces acting on the slip surface between Stations 0 and 1 and Stations 9 and 00, respectively. $F_{N,int}$ is the intrinsic net force exerted between the engine inlet and exit stations.

The propulsion system modified net thrust used in Equation 2 is obtained by accounting ϕ_{post} as a "drag" term, thereby avoiding the difficulty of evaluating ϕ_{post}. With the exclusion of ϕ_{post}, propulsion system modified net thrust is:

$$F_N^* = \phi_{pre} + F_{N,int} \quad \text{(Eq.6)}$$

Under actual test conditions, both ϕ_{pre} and $F_{N,int}$ are time-variant, and Equation 4 for modified net thrust is given by:

$$F_N^*(t) = W_9 V_{00} - W_0 V_0 + \frac{\partial}{\partial t}\int_0^9 \rho V dv \quad \text{(Eq.6a)}$$

The time-dependency results from aircraft power and/or flight changes and corresponding changes in environmental conditions that contribute to the storage or depletion of momentum within the propulsion system control volume. In the next sections, a means to estimate the effect of time-variant operation on propulsion net thrust is presented.

3.2.1 Inlet Streamtube Force: To estimate the time dependency of the inlet streamtube force, ϕ_{pre}, (and thereby inlet ram drag) the one-dimensional, time-dependent equations for the conservation of mass and momentum, are solved for the propulsion nacelle shown in Figure 2. The one-dimensional, time-dependent equations for the conservation of mass and momentum from Sta. 0 to Sta. 1 are (Reference 3.8):

$$\text{Mass} \quad \frac{\partial \rho A}{\partial t} + \frac{\partial \rho u A}{\partial x} = 0 \quad \text{(Eq.7)}$$

$$\text{Momentum} \quad \frac{\partial \rho u A}{\partial t} + \frac{\partial [A(\rho u^2 + P)]}{\partial x} = P\frac{\partial A}{\partial x} + f' A \quad \text{(Eq.8)}$$

In the momentum Equation 8, f′ is a "lumped" forcing term that represents viscous forces, gravity, and/or other forcing terms as appropriate for the particular application. Equations 7 and 8 are written in "weak" conservation law form with source/sink terms on the right-hand side of the equation. The advantage of the "weak" form is that supersonic flows can be solved numerically, and embedded shock/expansion waves can form and decay automatically without special interface discontinuity treatments. Now, by substituting

SAENORM.COM : Click to view the full PDF of air5020a

3.2.1 (Continued):

$$W = \rho u A \text{ and } \frac{\partial F}{\partial t} = P\frac{\partial A}{\partial x} + f' A \qquad \text{(Eq.8a)}$$

Equations 7 and 8 can be respectively expressed as:

$$\frac{\partial \rho A}{\partial t} + \frac{\partial W}{\partial x} = 0 \qquad \text{(Eq.9)}$$

$$\frac{\partial W}{\partial t} + \frac{\partial (Wu + PA)}{\partial x} = \frac{\partial F}{\partial X} \qquad \text{(Eq.10)}$$

By making a first-order assumption that W and ρA vary linearly from the free-stream (Sta. 0) to the inlet (Sta. 1) gives:

$$\frac{d(\rho_1 A_1)}{dt} + \frac{d(\rho_o A_0)}{dt} + \frac{W_1 - W_0}{0.5\Delta X} = 0 \qquad \text{(Eq.11)}$$

Then the time-variant force between Stations 1 and 0 (i.e. $\phi_{pre}(t)$ Figure 2) can be expressed by:

$$\phi_{pre}(t) = [F_1(t) - F_0(t)] = (P_1 A_1 + W_1 u_1) - (P_0 A_0 + W_0 u_0) + 0.5\Delta x\left(\frac{dW_1}{dt} + \frac{dW_0}{dt}\right) \qquad \text{(Eq.12)}$$

Ordinarily, the amount of error incurred from the linearity assumption will vary according to the amount of nonlinearity in W and ρA between Sta. 0 and Sta. 1, although it is theoretically possible to have small or even zero errors for highly nonlinear functions. The error, however, will always be zero if W and ρA are both linear.

The first two terms in Equation 12 are the steady-state force values at Sta. 1 and Sta. 0, respectively, at a specified time. The third term in Equation 12 is the time-dependency force term. The computer listing for the one-dimensional, time-dependent equations is provided in Appendix B.

SAENORM.COM : Click to view the full PDF of air5020a

3.2.2 Intrinsic Net Thrust: The intrinsic net thrust (and thereby the gross thrust) delivered by a gas turbine engine transiently passing through a given power setting differs from that produced under steady-state conditions at the same power setting. For transient rates produced by flight condition or power lever transients, the principal causes of this difference are transient inertia and thermal effects. As the power lever is advanced from a low to a high setting as shown in Figure 3A, the engine parameters (rotor speed, thrust) increase with some time lag. As shown in Figure 3A, key performance parameters reach a near-equilibrium condition in less than a minute; however, temperatures throughout the engine (Figure 3B) take longer to adjust. The engine gas temperatures adjust quickly to changes in flow conditions. Metal temperatures in heavy components take longer. The actual time periods required for these adjustments vary as a function of flight condition and rate of energy input change. Therefore, engine flow path and engine metal temperatures differ during transient operation, causing a different distribution of energy throughout the engine.

Principal energy input sources are engine fuel flow and the enthalpy of the inlet airstream. For power transients, both sources change because the engine accelerates as a result of increased fuel flow. For flight condition transients with fixed power lever setting, the enthalpy of the inlet air changes, and only the fuel flow rate is changed to accommodate the modified inlet conditions.

For a typical power lever change from a low to a high power setting, the energy added to the engine must be sufficient to:

a. Provide the basic steady-state required-to-run energy at the instantaneous operating point.
b. Accelerate the rotors by overcoming rotor inertia.
c. Make up for transient energy losses through heat transfer to the metal parts.
d. Make up for additional transient compressor work required during the acceleration because of higher backpressure on the compressor.
e. Make up for changed efficiencies because of transient tip and seal clearance changes.
f. Make up for component operating condition changes because of transient scheduling of engine variable geometry (jet nozzle, compressor vanes, and bleeds).
g. Make up for operating changes because of bleeds, power extraction, and inlet recovery.

For operation at steady-state conditions, the energy input (fuel flow) is required only for the first item. The remaining five energy items are transient effects.

Flight condition changes produce the same physical effects as shown in Figure 3, but usually to a much lesser degree because the maximum rate of energy input change is much less from flight maneuvers.

Two methods can be employed to account for transient effects: transient effects may be treated by either avoidance or compensation. In avoidance, flight and power maneuvers are restricted to rates which hold the effects to insignificant magnitudes. In compensation, engine transient simulation techniques are applied to correct for the effects. Nonlinear aerothermodynamic engine transient models are comprehensive representations of engine components which include transient energy terms (refer to 4.2). As such, an engine transient model which has been "trimmed" to experimental ground test data can be used to estimate the time-dependent force terms for engine intrinsic net thrust.

SAENORM.COM : Click to view the full PDF of air5020a

X(t) - Instantaneous Values

X_i - Initial (Idle) Value

X_{SS} - Steady-State Value After Transient

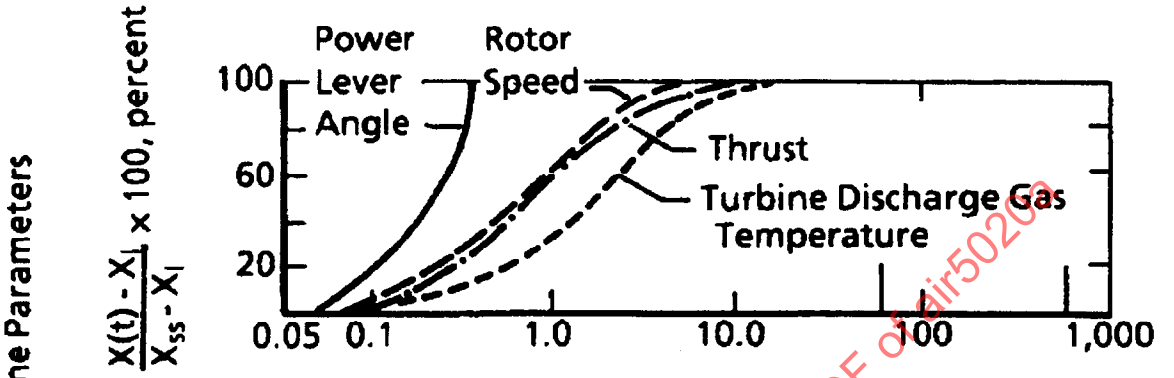

FIGURE 3A - Key Performance Parameters

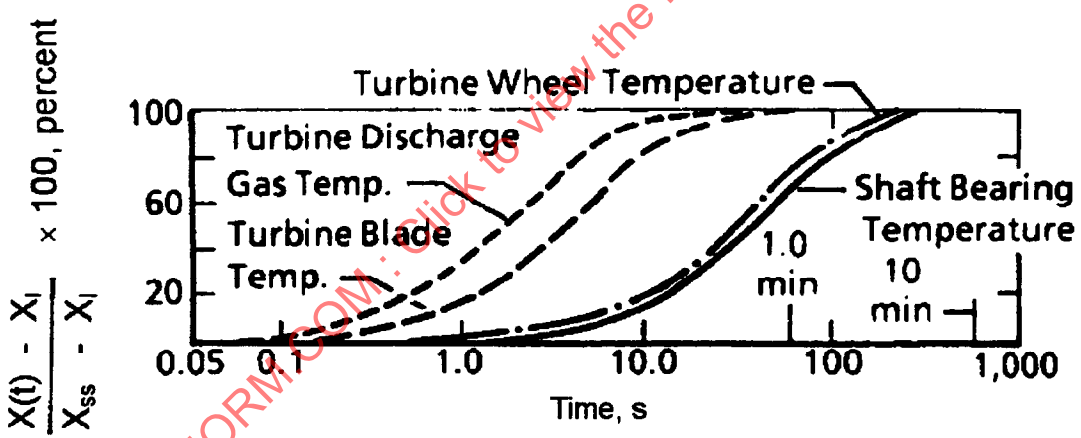

FIGURE 3B - Key Turbine Temperatures

FIGURE 3 - Behavior of Key Performance Parameters and Temperatures During a Rapid Throttle Transient for a Typical Turbine Engine at M = 1.0 at 36,000 ft

SAENORM.COM : Click to view the full PDF of air5020a

3.2.3 Quasi-Steady Limits: A tactical aircraft configuration (Figure 4) with a 20,000-lbf thrust class engine was used to quantify the effect of aircraft maneuvers on time-variant modified net thrust. Two flight maneuvers were considered in quantifying the effects of flight transients on propulsion system forces:

Case 1: An aircraft acceleration from Mach 0.8 to 1.8 at fixed altitude of 30,000 ft and fixed engine throttle at maximum power (Figure 5A).
Case 2: An aircraft climb from 20,000 ft to 40,000 ft at fixed Mach number of 0.8 and fixed engine throttle at maximum power (Figure 6A).

Equation 12 was used to quantify the inlet streamtube volumetric dynamics between Sta. 0 and Sta. 2. In making the inlet streamtube calculation, inlet losses were determined using MIL-E-5007D paragraph 3.2.1, and a distance of one aircraft length (50 ft) was used to define the region of uniform flow upstream of the inlet.

SAENORM.COM : Click to view the full PDF of air5020a

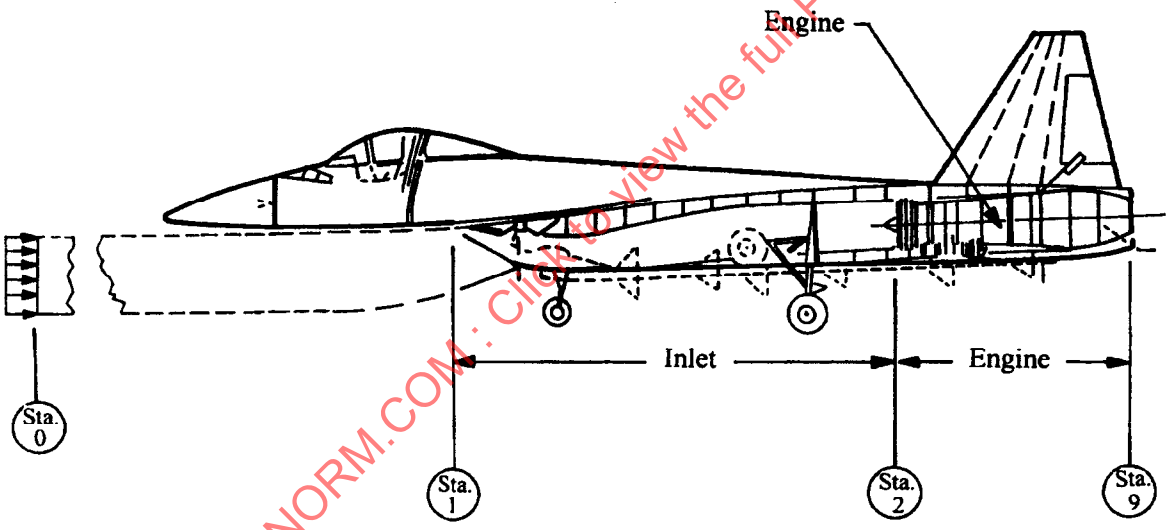

FIGURE 4 - Airplane Schematic Illustrating Inlet, Engine, and Exhaust Nozzle Stations

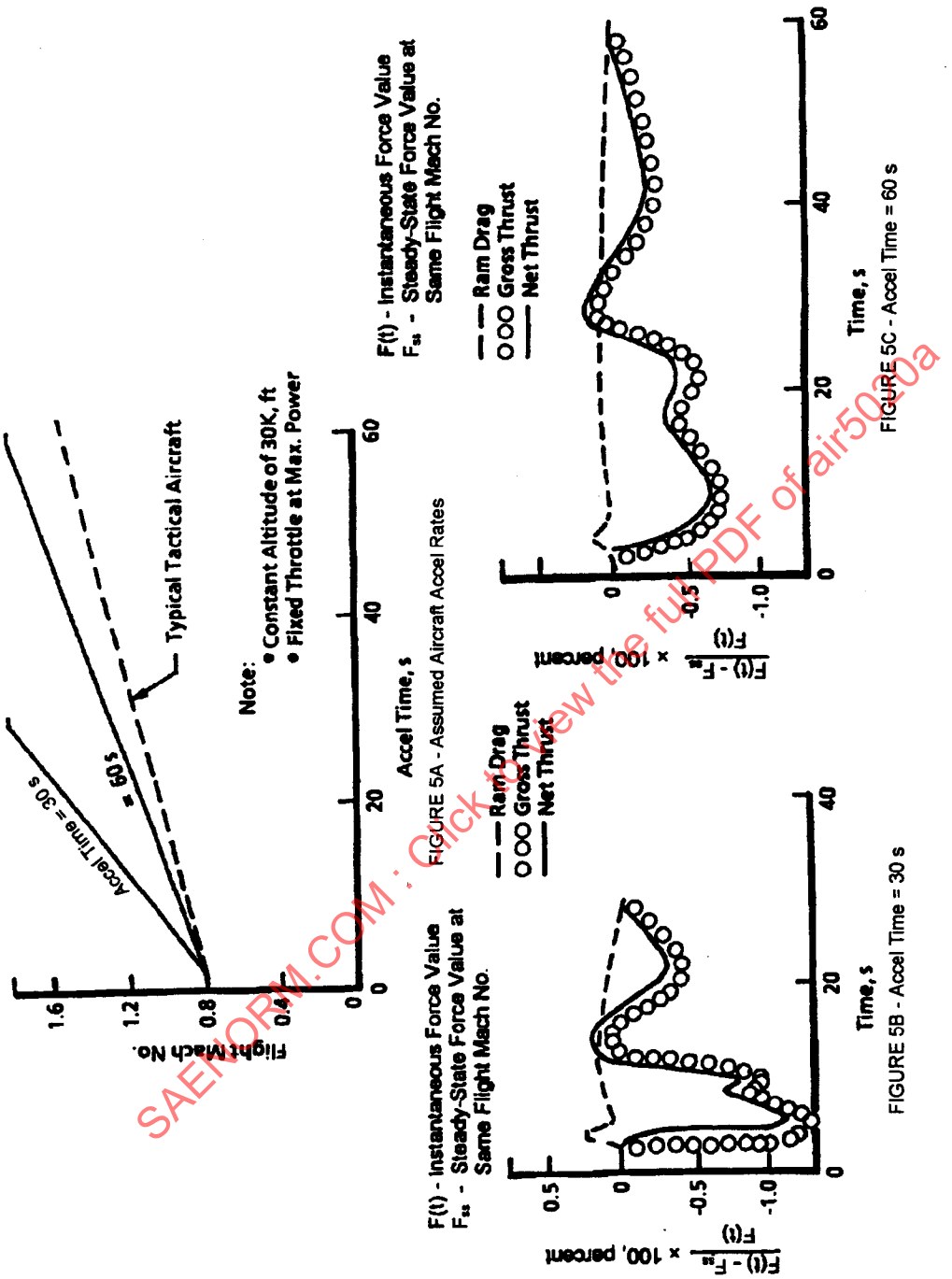

FIGURE 5A - Assumed Aircraft Accel Rates

FIGURE 5B - Accel Time = 30 s

FIGURE 5C - Accel Time = 60 s

FIGURE 5 - Time-Dependent Thrust Effects for Transonic Accel

SAENORM.COM : Click to view the full PDF of air5020a

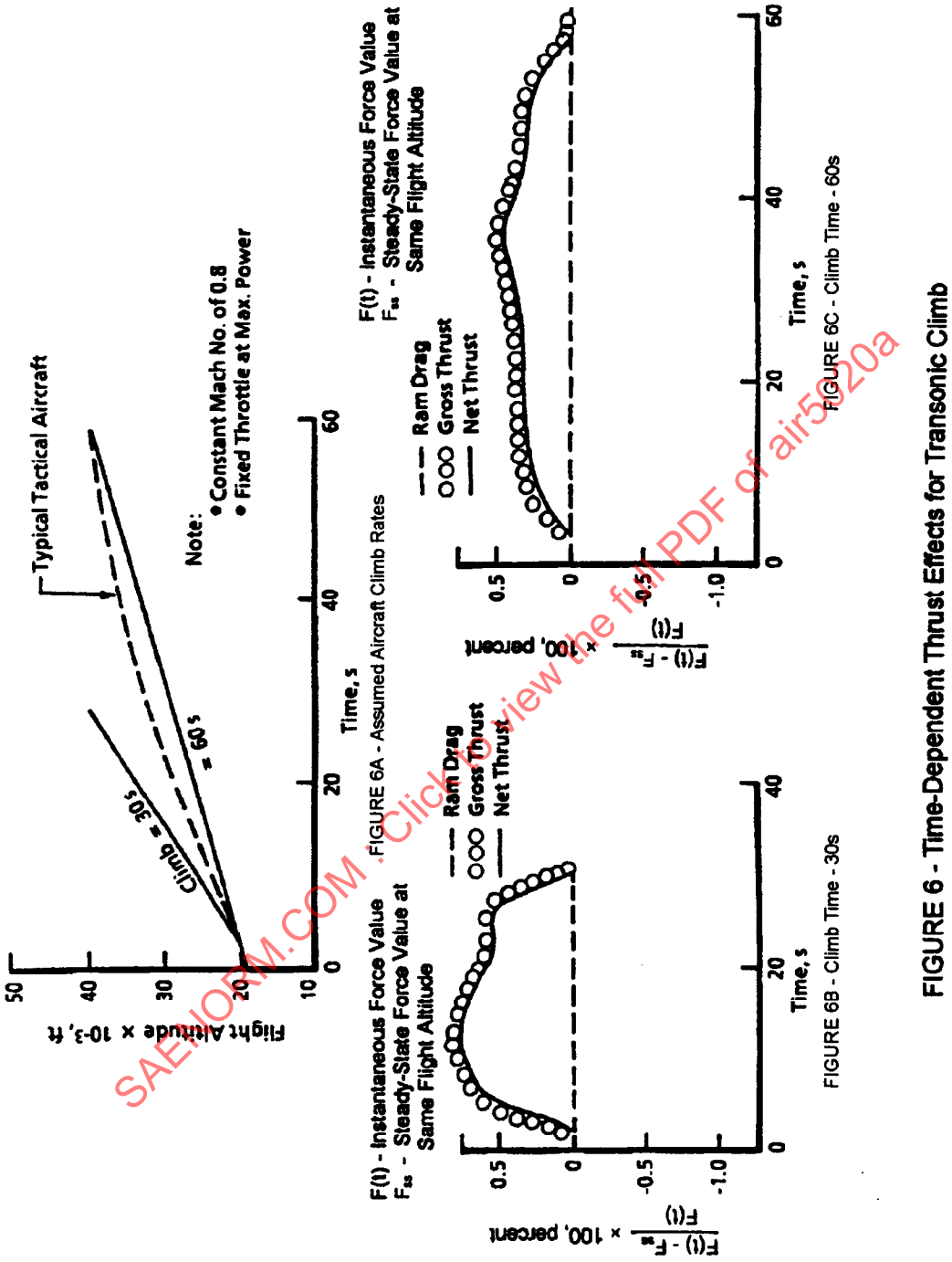

FIGURE 6A - Assumed Aircraft Climb Rates

FIGURE 6B - Climb Time - 30s

FIGURE 6C - Climb Time - 60s

FIGURE 6 - Time-Dependent Thrust Effects for Transonic Climb

SAENORM.COM : Click to view the full PDF of air5020a

3.2.3 (Continued):

A low-bypass turbofan engine transient simulation model validated with test data and which accounts for the energy effects listed in 3.2.2 was used to evaluate the engine volumetric and thermal dynamics between Stations 2 and 9. The engine transient model incorporated a fan speed control algorithm so that for fixed-throttle operation, engine fuel flow varied to maintain an inlet temperature versus fan speed schedule. An engine using an engine pressure ratio control algorithm would give a different time-variant result, but the magnitude of the transient terms is expected to be of the same order. The magnitude of the fixed-throttle engine time-variant effects was determined by evaluating engine gross thrust for both transient operation and steady-state operation at the same flight condition at a specified time.

For the max aircraft acceleration depicted in Figure 5B, the increase in uncertainty in net thrust is on the order of -1% and is almost entirely the result of the engine thermal effects (as discussed in 3.2.2) on gross thrust. The maximum ram drag difference for this case is on the order of +1/4%. For the more representative case of tactical aircraft (Figure 5C), increase in uncertainty in net thrust is reduced to about -1/2%. For the max aircraft climb depicted in Figure 6B, the increase in uncertainty in net thrust is on the order of +1% and, as in the case of the acceleration, is the result of engine thermal response to varying inlet conditions. For the case representative of current tactical aircraft (Figure 6C), the increase in uncertainty in net thrust is reduced to about +1/2%.

From the results on Figures 5 and 6, time-variant corrections to inlet ram drag are minimal for aircraft limiting climb and acceleration flight test maneuvers, but in-flight thrust methods based on steady-state engine calibrations could be in error by 0.5 to 1.0%. Selection of in-flight thrust methods to minimize engine thermal effects is discussed in Section 4.

Although no evaluations were made for a comparable deceleration and descent scenario, it is expected that the magnitude of the time-variant corrections to net thrust would be the same order as for the acceleration and climb scenarios.

3.3 Quasi-Steady Limits for Aircraft Dynamic Maneuvers:

As stated in the preface of AIR1703, in-flight thrust, or the determination thereof, is not an end unto itself, but rather is a piece of information which, when combined with other air vehicle energy state properties through a well-defined force accounting system (see Reference 3.1), yields the total air vehicle system drag. Typically, it is desirable to compare drag inferred from measured thrust with drag predictions from sub-scale tests and/or other steady-state sources. Thus, one must consider when it is proper to compare thrust-inferred drag with the predicted, steady-state, longitudinal air vehicle performance database. This becomes all the more necessary when one is considering transient engine/aircraft maneuvers rather than steady or quasi-steady conditions as in AIR1703.

SAENORM.COM : Click to view the full PDF of air5020a

3.3.1 Aircraft Performance: In an attempt to ascertain what magnitude of transient is sufficient to affect or render inappropriate the steady-state aerodynamic characteristics of an air vehicle, the time scale of the event must be considered. The critical time interval during which a maneuver would affect the aircraft aerodynamics is considered to be that required for the vehicle to pass a fixed point in space. In the present context, the transients of interest are changes in altitude, velocity (speed), and attitude. An acceptable error in the vehicle drag solely due to the transient event is assumed to be 0.5%. The threshold measurable performance affecting criteria that could result in a 0.5% drag error are: (1) A 0.5% change in static pressure due to an altitude change; (2) A 0.5% change in dynamic pressure resulting from an acceleration or deceleration, and (3) An attitude change rate that causes a 0.5% vehicle drag error. The acceptable attitude uncertainty is a function of both the vehicle and the test condition. It is on the order of 0.05 deg for a high-performance vehicle with low wing loading at cruise attitude (and less than 0.02 deg for a high-speed transport). It is believed that the effects of these transients on the aircraft aerodynamic performance characteristics would not be noticeable, but more rapid transients would begin to invalidate the use of the time-independent aerodynamic characteristics, thus the quasi-steady limit is defined.

The first of the above cases, static pressure change, is trivial and may be ignored: the maximum rate of change of pressure with altitude is 0.0047% per foot. Therefore, a 0.5% pressure change over the length of a vehicle is possible only if the altitude of the nose and tail are separated by more than 100 ft. Consequently, this criteria could be met only by an airplane with length greater than 100 ft, and then only when in a very steep climb or dive.

In trying to determine whether an aircraft acceleration results in a 0.5% uncertainty in dynamic pressure, one assumes that in the time interval it takes for the nose and the tail of an airplane to pass a common point in space, the velocity of the airplane has changed such that the dynamic pressure at the two velocities differs by 0.5%. At any given Mach number the acceleration is a function of the airplane excess thrust-to-weight ratio, the airplane length, and the temperature. The critical threshold values of the excess thrust-to-weight ratio and the airplane length as a function of the nominal Mach number are presented in Figure 7A for two ambient temperature conditions.

There is a possibility of exceeding the limiting quasi-steady acceleration criteria in the subsonic speed range with some present-day aircraft. For example, assume a 50-ft-long (L_{AC}), high-performance vehicle operating at standard day sea-level conditions, and at maximum power that airplane has an excess thrust (or thrust-minus-drag), F_{EX}, that is 70% of its weight (F_{EX}/W_{AC} = 0.70). Using Figure 7A, it is seen that that airplane can match the quasi-steady limiting criteria ($F_{EX} \times L_{AC}/W_{AC}$ = 0.70 x 50 = 35 ft). However, observing Figure 7A, it is seen that the limiting criteria rapidly increase with Mach number (and the available F_{EX} decreases), so there is virtually no chance of an airplane matching these criteria in the transonic speed range. This is particularly fortunate because the change in drag coefficient with Mach number is not too significant in the subsonic range, but becomes quite significant transonically. Thus, there does not seem to be a problem in confusing a pure dynamic pressure effect with a Mach number effect. Also, at any given Mach number the magnitude of the excess thrust, F_{EX}, is proportional to the ambient pressure, so F_{EX}/W_{AC} decreases as altitude is increased. Consequently, it appears that most velocity transients (within reason at the lower altitudes in the subsonic speed regime) will not invalidate the procedure of treating accelerating flight data in a quasi-steady manner.

SAENORM.COM : Click to view the full PDF of air5020a

3.3.1 (Continued):

It may be shown that the error in drag due to the uncertainty in angle of attack, α, is a direct function of the lift at any given attitude. If an aircraft is varying angle of attack, it is changing its lift and drag as a function of that pitch rate. The critical pitch rate is determined as follows: because of the rotation of an aircraft about its center of gravity during an attitude change, each point on the aircraft has a velocity normal to the flight path that is proportional to the longitudinal distance from the center of gravity. Consequently, each part of the vehicle is at a local angle of attack that is proportional to its longitudinal position, and the uncertainty in the vehicle angle of attack can be determined as the arc-tangent of the average differential velocity over the length of the lifting surface ratioed to the flight velocity. The critical pitch rate is defined when that angle (in radians), multiplied by the aircraft lift exceeds 0.5% of the vehicle drag. It is thus possible to determine the acceptable threshold rotation (attitude change) rate as a function of the vehicle velocity, lift-to-drag ratio, and lifting surface length for a given drag error (0.5% in this case) as is presented in Figure 7B. A simple example shows that these change rates may easily be exceeded in maneuvers: Consider the above case at 0.6 Mach number, sea-level standard day with the 50-ft-long airplane (assume the wing length to be 25 ft) cruising at a lift-to-drag ratio of eight (e.g., $C_D = 0.0250$ and $C_L = 0.200$). Using Figure 7B, it is seen that $\dot{\alpha} \times L_{WL} = 48$ ft-deg/s, and, therefore, a pitch rate of (48 ft-deg/s)/(25 ft) = 1.92 deg/s is sufficient to exceed the threshold criteria limit. In addition, it has long been known in the dynamic stability (flying qualities) field that there are real effects on lift, pitching moment, and elevator effectiveness during rapid pitch transients (e.g., see Reference 3.2). These facts, coupled with the fact that during an attitude transient the control surfaces are, by definition, not at a position for trimmed flight (though the effect of the displacement of the longitudinal control can be corrected) mean that the aircraft performance data acquired during attitude changes very well may differ from the steady-state database, except for during very mild changes on the order of those indicated in Figure 7B.

A note of caution should be added to the above discussion about attitude transients. For the example given, a pitch rate of 1.92 deg/s would not invalidate the quasi-steady assumption or use of the steady-state database. Taking this a step further, the effects of a transient rate of 4-5 deg/s probably would be hard to detect in the data, considering all of the other uncertainties, but the effects of a pitch rate of 20 or 30 deg/s in all probability would be quite noticeable. Thus, considerable discretion must be used when deriving aerodynamic performance from in-flight thrust measurements obtained during attitude transients greater than those presented in Figure 7B.

SAENORM.COM : Click to view the full PDF of air5020a

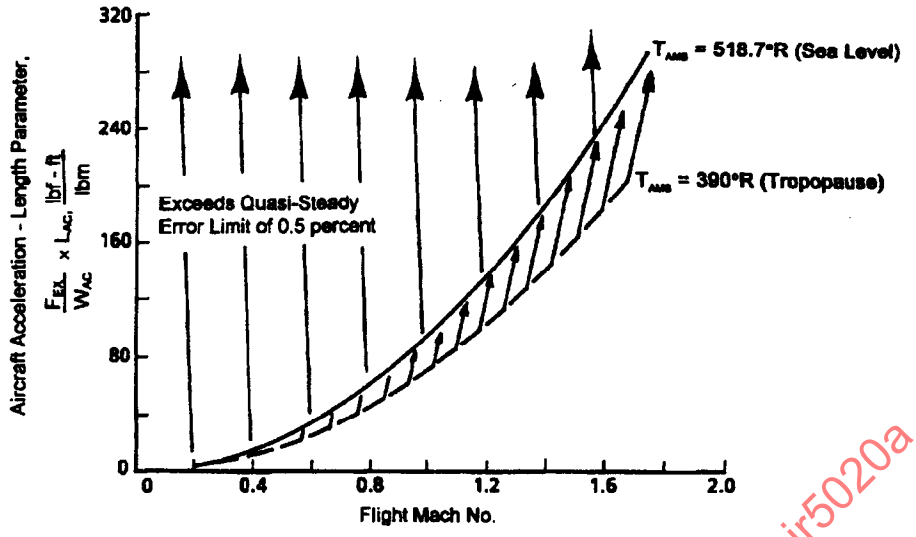

FIGURE 7A - Aircraft Acceleration Threshold

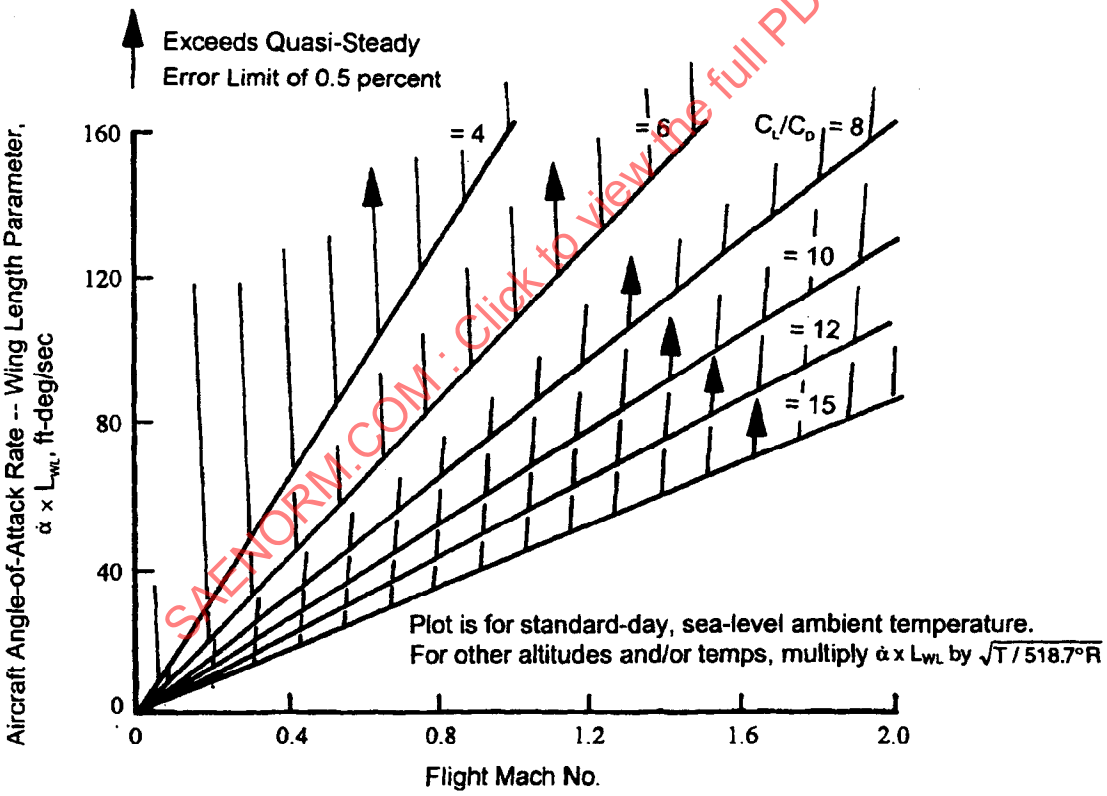

FIGURE 7B - Aircraft Attitude Change Threshold

FIGURE 7 - Threshold Transient Rates

SAENORM.COM : Click to view the full PDF of air5020a

3.3.1 (Continued):

There is one other flight transient, or effect resulting from a flight transient that should be avoided in performance flight testing. That involves obtaining performance flight test data, particularly in the transonic speed range, shortly after a significant change in vehicle surface temperature has occurred. If such a change results in wing surface heat transfer other than would be present at "temperature soaked" conditions, the state of the boundary layer would be changed from the steady-state case which could result in a displacement of the wing terminal normal shock-wave position, particularly on a vehicle with a supercritical wing. That, in turn, would affect the wing and air vehicle lift, drag, and pitching moment (uncorrected for longitudinal control repositioning). This problem could occur, for example, if an airplane had been temperature soaked at supersonic conditions and data were acquired as the airplane underwent a rapid deceleration to and through the transonic speed regime.

3.3.2 Installed Engine Net Thrust: The installation of an engine into an air vehicle and the transient operation of that air vehicle or engine has several effects on engine performance. Principal among these are the changes in the engine inlet properties that are a function of the air vehicle altitude, attitude, Mach number, and the engine corrected mass flow (or corrected speed). Additionally, the effect of the changing local nozzle exit ambient pressure with the above variables also must be considered. However, this effect is a problem only for unchoked, underexpanded nozzle cases where the net propulsive force is a function of the local nozzle pressure ratio. For situations with a choked throat and fully expanded divergent nozzle, knowing the internal engine pressures and the free-stream static pressure is sufficient to determine the net thrust in a bookkeeping system as described in AIR1703. For the unchoked nozzle, assuming that the local nozzle exit static pressure is measured, the effect of a transient (aircraft or engine) on that pressure is known.

The most significant effect of an aircraft or engine speed transient on the engine inlet flow properties is that on the spatially averaged engine face total pressure, P_{t2}. Coupled with the average P_{t2} value are the effects of the changing spatial total pressure distortion and bulk inlet swirl (which affects engines without inlet guide vanes). The rate of temperature change with altitude and/or Mach number is quite slow, well within the quasi-steady-state limits, and thus is not discussed herein. More rapid temperature transits resulting from gun firings or an aircraft-launched rocket exhaust are of such an isolated nature that they, too, are excluded from the discussion.

It is generally (intuitively) believed (though not rigorously proven) that engine net thrust is insensitive to the high-frequency (greater than a few percent of engine speed) spatial total pressure recovery and distortion variations to which the engine stability is quite sensitive. Thus, for frequencies on the order of a few Hertz, the "steady-state" values of distortion (usually as defined in subscale wind tunnel tests) are appropriate for defining the distortion for consideration in net thrust calculation. However, the effect of this distortion on engine re-match and performance often is poorly defined; consequently, the effects of the distortion usually are not considered in the net thrust calculation, with a resulting increase in uncertainty. Similarly, the effects of swirl on net thrust traditionally are not measured or accounted, and usually the magnitude of the swirl is not even defined in the inlet model wind tunnel tests.

SAENORM.COM : Click to view the full PDF of air5020a

3.3.2 (Continued):

The rate of change of the mass-averaged P_{t2} with any of the independent variables is a function of the specific air vehicle being considered. However, total pressure variations on the order of 0.5% per angle of attack or sideslip degree and 5% for an idle to maximum engine speed (airflow) change are possible. The effects of Mach number on total-pressure recovery usually are small at subsonic conditions and could only become a factor during rapid accelerations at supersonic Mach numbers where oblique and normal shock losses are significant. Thus, any Mach number effects would be quite configuration-dependent. Also, the effects of altitude change on total pressure are quite small (see 3.3.1) and not included here. Figure 8 is presented to illustrate the acceptable (0.5% uncertainty) magnitude of attitude change rate on net thrust, assuming that net thrust is directly proportional to P_{t2}. For example referring to Figure 8, a flight Mach number of 0.9 at sea-level gives an attitude rate parameter value of 500. Appling this value to an aircraft with an L_x (distance from nose to engine inlet) of 50 ft at a P_{t2} lapse rate with attitude of 0.5% per deg (P_ψ), results in a suggested attitude change rate limit of 20 deg/s for the determination of engine inlet pressure. In general, the quasi-steady limit for attitude changes is on the order of 10 deg/s for modern aircraft at lower subsonic Mach numbers and increases proportionally with Mach number. A similar plot could be prepared for the effect of engine corrected weight flow (speed) change. The critical length would be the inlet duct length, Mach number would be replaced with corrected airflow W_c, and lapse rate, $dP/d\psi$, replaced with dP/dW_c. However, because of the reduced length and lapse rate, the allowable transient rates are proportionally larger and the problem becomes insignificant.

It should be noted that the above discussion on the effect of engine inlet flow properties on net thrust is pertinent to those cases where net thrust is being determined by a method that assumes knowledge of engine inlet P_{t2} and its spatial distortion. If, for example, gross thrust is being determined from nozzle pressure/temperature/area measurements it is insensitive to engine inlet P_{t2} variations. A rematch of an engine from its calibration because of inlet distortion can affect the gross thrust calibration, but this is believed to be a second-order effect and is usually handled by independently measuring the core and bypass flow properties. The effects of inlet swirl (but not the swirl itself) will be reflected by the nozzle instrumentation. Both the P_{t2} and swirl effects can be significant if either the engine airflow or gross thrust is determined as a function of corrected engine speed.

SAENORM.COM : Click to view the full PDF of air5020a

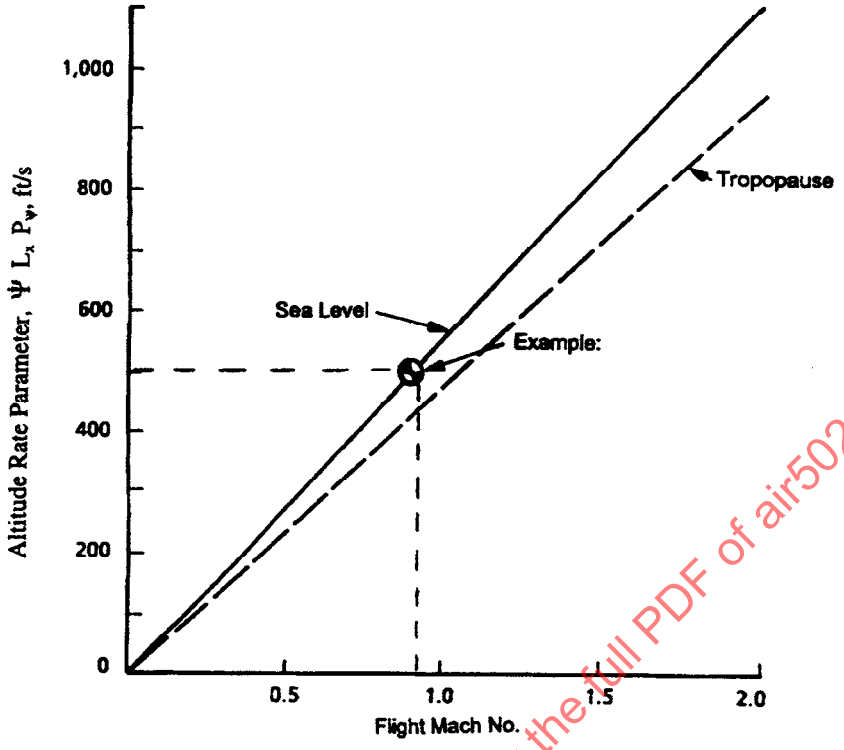

FIGURE 8 - Acceptable Attitude Change Rates for Determination of Engine Inlet Pressure

3.4 Quasi-Steady Engine Transient Limits for Throttle-Dependent Aerodynamic Forces:

The throttle-dependent forces (inlet spillage and nozzle-afterbody drag) that are considered a part of the net propulsive force can be on the order of 5 to 10% of the aircraft drag. The effects of an aircraft transient on these forces are considered to be negligible because these forces vary only slightly with Mach number and are generally insensitive to aircraft attitude. Thus, the effects of an aircraft transient could amount, at most, to only a few tenths of a percent.

A possible error in the throttle-dependent forces could result from an engine transient because of the time lag due to the wave propagation time from the engine to the affected surfaces. Considering the inlet spillage drag resulting from an engine airflow (speed) change, it may be shown as in 3.2 with the effect of airflow change on P_{t2}, that the effect is insignificant. The effects on afterbody drag due to nozzle pressure ratio changes are even less because of the natural proximity of the afterbody to the exit plane. The effects of nozzle position for a variable nozzle geometry engine are not considered herein because it is assumed that all of the data are time correlated and the nozzle position is known as a function of time. The effects of an engine transient on aircraft trim are not considered because those effects would be evident in the aircraft acceleration, pitch rate, and/or elevator position and would be thus accounted.

SAENORM.COM : Click to view the full PDF of air5020a

3.5 Summary:

Force accounting procedures for time-dependent aircraft motion and engine thrust operating conditions parallel those developed for steady-state aircraft maneuvers with fixed-throttle engine operation. Within the operational guidelines defined for quasi-steady-state flight testing, the element of installed net propulsive force and airframe system drag that make up aircraft excess thrust are applicable to time-dependent aircraft operating conditions providing that the time-dependent force and drag values are used in the evaluation. As for steady-state, the accounting methodology for time-dependent aircraft motion must be tailored to the requirements, program resources, and details of the aerodynamic and propulsion configuration being evaluated. The chosen methodology should, from the time-dependency standpoint, address the characteristics of consistency, visibility given to the performance elements of the airplane system, selection of reference conditions, and suitability and consistency for tracking the integrated propulsion and airframe performance throughout the aircraft development program.

Based on one-dimensional time-dependent flow equations and wave propagation considerations, quasi-steady assumptions should be applicable to determine net thrust for fixed throttle climb/descent and accel/decel aircraft maneuvers. For current tactical aircraft operating in the transonic and supersonic flight regimes, the magnitude of the time-dependent force terms on modified net thrust was determined to be of the order of 1% or less. For variable engine throttle operations, however, the magnitudes of the engine thrust time-dependent force terms can be significantly different than the corresponding steady-state value, (depending on the throttle rate change and the flight condition), and requires a calibrated engine transient simulation model to quantify the engine thrust levels.

Using aircraft threshold considerations enables one to estimate the effects of aircraft time-variant operation on in-flight thrust. For example, a change in throttle position will strongly affect engine thrust-level but have a lesser effect on aircraft throttle-dependent parameters. A change in aircraft altitude and Mach number will strongly affect the aircraft aerodynamic parameters but have a lesser effect on the engine thrust. Specific aircraft threshold transient values are extremely configuration and flight condition dependent, but by evaluating aircraft rate changes on flight performance, nominal threshold transient rates for deviations of less than 1% on in-flight thrust data have been estimated (Table 2).

SAENORM.COM : Click to view the full PDF of air5020a

TABLE 2 - Aircraft Quasi-Steady Threshold Limits (Fixed Throttle)

Type Maneuver	Speed Regime Subsonic	Speed Regime Transonic	Speed Regime Supersonic
Quasi Steady-State			
• Accel/Decel	$F_{EX}/W_{AC} > 0.5$	NA	NA
• Climb/Descent	NA	NA	NA
Dynamic			
• Pitch Rate (deg/s)	1-3	2-5	5-10

3.5 (Continued):

The effects of these same transients on the engine performance and the effect of engine transients on the aircraft throttle-dependent drag or engine ambient conditions are not presented because they have significantly higher threshold rates than those given for aircraft performance and are not critical to in-flight thrust data evaluation.

4. IN-FLIGHT THRUST METHODS:

The fundamental concepts discussed in Section 3 require the determination of modified net thrust, F_N^*. This chapter discusses methods used for the determination of F_N^* during transient operation for either fixed- or variable-throttle maneuvers. This is accomplished by reviewing the transient engine considerations and how they apply to various thrust calculation techniques. Gas path methods, transient engine simulations, and engine independent techniques are discussed, as well as the validation and calibration procedures. Examples of the application to flight test data are shown, along with the benefits and limitation of each method of thrust determination.

4.1 Gas Path Methods:

Gas path methods of in-flight thrust determination as discussed in AIR1703 are techniques which use measured flow properties throughout the engine to determine nozzle gross thrust and inlet ram drag. The procedures used to make these calculations are correlations based on steady-state data from ground and altitude test facilities. Application of these steady-state correlations to flight testing has generally been successful for fixed-throttle operation at quasi-steady and dynamic aircraft flight conditions (see Section 7).

For variable throttle or rapidly changing flight conditions, the uncertainty with gas path methods can increase significantly. This is caused by the implicit steady-state assumptions contained in the stabilized test data used to develop the correlations. The additional time-variant factors that must be considered are the transient energy terms, transient component performance changes, and instrumentation lags in the measurement system.

4.1.1 $F/W\sqrt{T}$ and F/AP Methods: Figure 9 illustrates the most commonly used gas path methods for a mixed flow afterburning turbofan. The F/AP method uses nozzle throat area (A_8), nozzle pressure (P_{t8}), and gross thrust coefficient (Cg) to determine gross thrust. Nozzle throat area is measured directly, nozzle inlet pressure is calculated from measurement of turbine discharge pressure, and Cg is obtained from a correlation of nozzle pressure ratio and throat area.

The $F/W\sqrt{T}$ method uses nozzle gas flow (W_8), nozzle throat temperature (T_{t8}), and nozzle velocity coefficient (Cv) to determine gross thrust. Nozzle inlet temperature is determined from an energy balance using engine inlet temperature and fuel flow; nozzle gas flow is derived from engine inlet airflow, fuel flow, and bleed extraction; and Cv is obtained from a correlation of nozzle pressure ratio and area ratio.

SAENORM.COM : Click to view the full PDF of air5020a

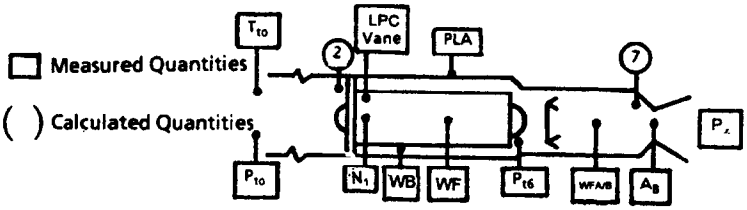

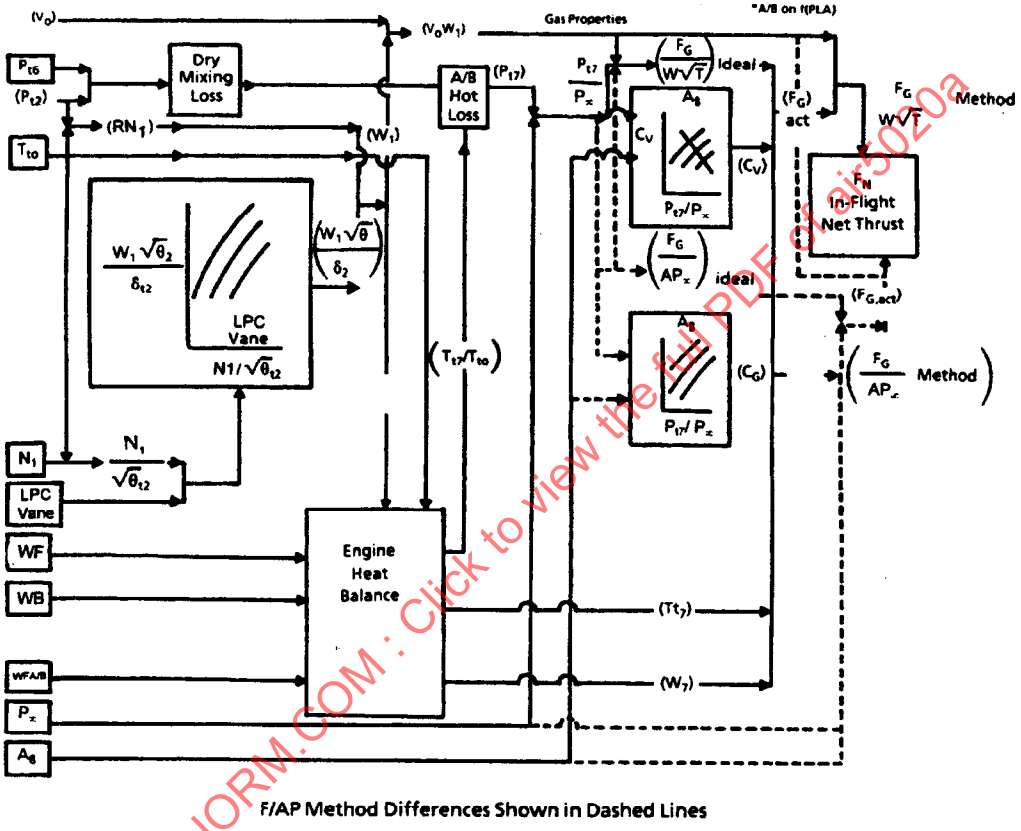

FIGURE 9 - Typical Gas-Path Nozzle Methods (F/W $\sqrt{T}$ and F/AP) for Mixed-Flow Afterburning Turbofan

SAENORM.COM : Click to view the full PDF of air5020a

4.1.1 (Continued):

Both of these techniques require the determination of engine inlet airflow for the calculation of ram drag. This airflow is usually obtained from a fan or compressor map as a function of rotor speed, pressure ratio, and variable vane position. Inlet distortion effects on airflow have been found to be negligible for steady-state operation, but may be more significant for time-variant distortion.

The selection of which gas path method to use should be based on the specific type of testing, since some methods are more sensitive to transient errors. For example, with variable nozzle turbofan engines, the $F/W\sqrt{T}$ method may have better steady-state uncertainty than the F/AP method, but may have worse uncertainty for throttle transients. This is caused by the temperature calculation using an energy balance that does not include the transient rotor acceleration and heat-transfer terms. The F/AP method is insensitive to these transient effects because both the pressure and area are measured directly and are not based on energy balance assumptions. This is true even considering that the measurement of absolute area may have reduced accuracy since the measurement in the change in nozzle area typically provides a better indication of transient thrust than that obtained using the steady-state energy balance assumption (refer to 6.2.4 for a disscussuon of factors affecting nozzle area measurement). For best overall uncertainty, a combined technique can be developed which uses the $F/W\sqrt{T}$ method to evaluate the stabilized end points, and the F/AP method to define the transient characteristic.

The steady-state gas path methods have been successfully used for quasi-steady maneuvers such as aircraft accelerations and dynamic maneuvers such as wind-up turns and push-over/pull-ups. Even during maximum afterburner accelerations, this has resulted in acceptable thrust calculation uncertainty for validation of the aircraft drag polar. Less success has been achieved using the steady-state gas path methods during variable throttle transients. Section 7 contains examples of the relative accuracy for the different types of gas path methods during transients.

4.1.2 Tailpipe Method: A specialized version of the F/AP method called the simplified gross thrust method (SGTM) has been developed to compute engine gross and net thrust in real time over the entire aircraft operating flight envelope. This has been developed and evaluated successfully for a variety of variable exhaust turbojet and turbofan fighter engines, including the J85, F100, and F404 engines (References 4.1 through 4.3).

For the determination of gross thrust, the SGTM requires a measurement or determination of free-stream static pressure, $P_{\_}$, and gas path pressure measurement at three locations in the engine afterburner duct as shown in Figure 10 for the F404 engine application. The three afterburner measurements are turbine discharge pressure (P_{t558}), flameholder exit static pressure (P_{S6}), and exhaust nozzle inlet static pressure (P_{S7}). The SGTM can have an additional benefit since engine degradation and inlet distortion are a second-order effect on gross thrust determination because all engine measurements are downstream of the rotating machinery. The second-order effect would be the effect of engine degradation and inlet distortion on the calibration coefficients used for the thrust determination.

SAENORM.COM : Click to view the full PDF of air5020a

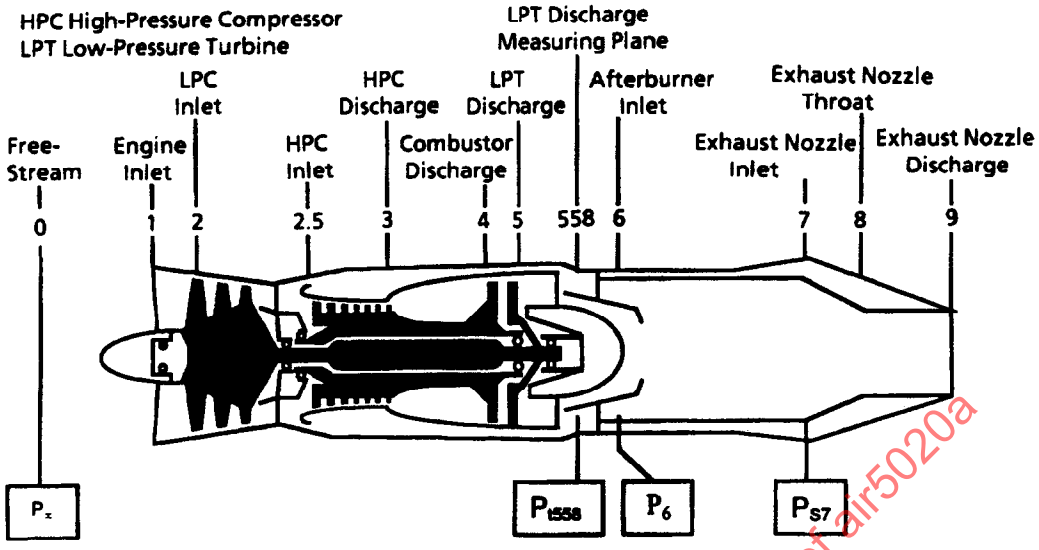

FIGURE 10A - F404 Engine Station and Sensor Locations

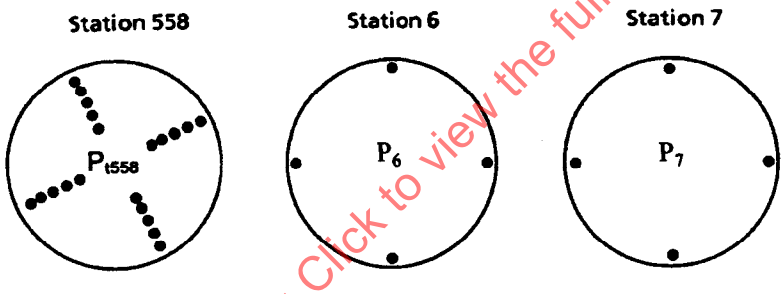

FIGURE 10B - Location of Engine Pressure Rakes Utilized by the SGTM

FIGURE 10 - Real-Time Thrust Method Engine Instrumentation System

SAENORM.COM : Click to view the full PDF of air5020a

4.1.2 (Continued):

The SGTM provides gross thrust based on a one-dimensional analysis of the flow in the engine afterburner and exhaust nozzle. Figure 11 shows a block diagram of the algorithm. The algorithm provides analysis of the flow in the afterburner duct from the turbine exit to the exhaust nozzle exit. It determines first the total pressure at the afterburner entrance, (P_{t6}) and then at the exhaust nozzle entrance (P_{t7}). The exhaust nozzle throat area (A_8) is also computed. Gross thrust is then computed from the calculated value of P_{t7} and A_8 and measured nozzle static pressure. This method is a specialized version of the F/AP method, but utilizing a calculated rather than measured nozzle area. A detailed derivation of the SGTM equations is presented in Reference 4.4.

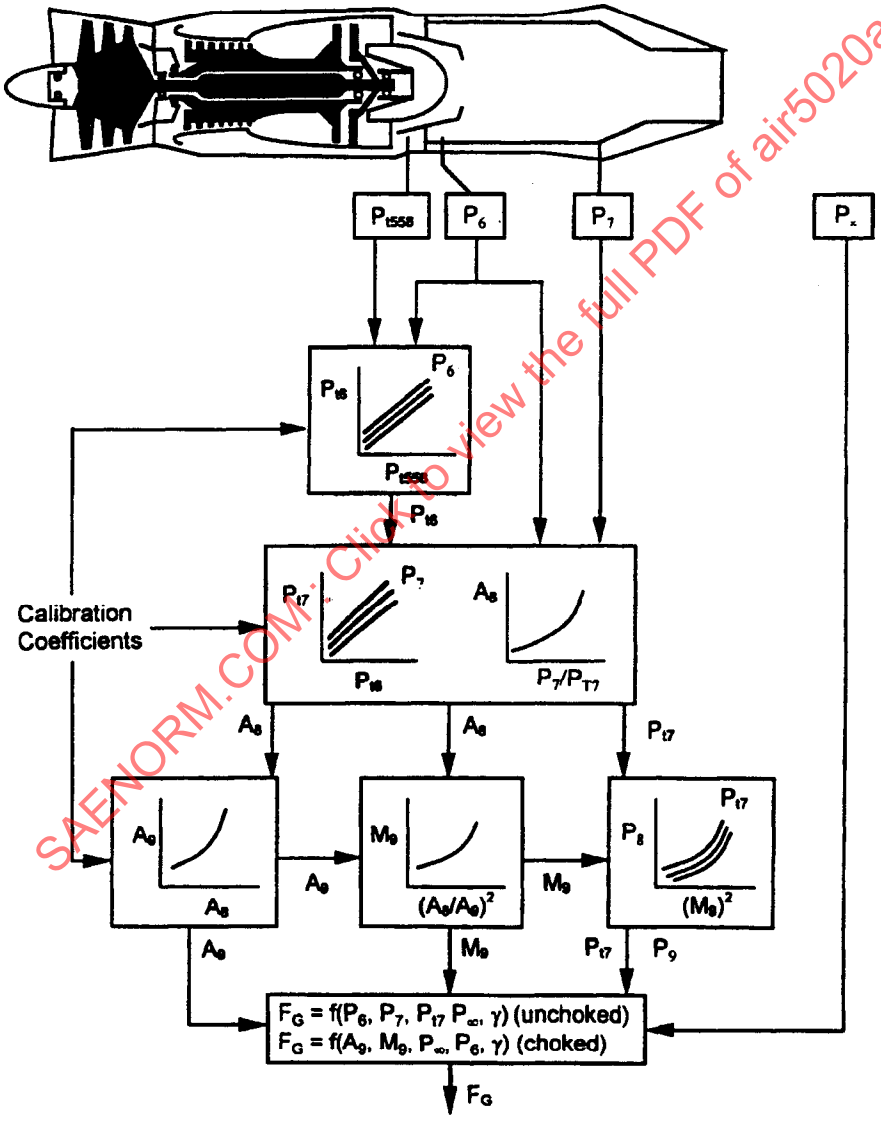

FIGURE 11 - Flow Chart of the SGTM

SAENORM.COM : Click to view the full PDF of air5020a

4.1.2 (Continued):

An expanded version of the SGTM has been developed to calculate net thrust (SNTM) (Reference 4.3). This algorithm was developed for real-time vehicle performance determination and uses the simplified approach demonstrated with the SGTM. Inlet mass flow is determined by calculating mass flow rate at the afterburner entrance using flow parameters determined in the SGTM gross thrust algorithm and the turbine discharge total temperature measured by existing engine instrumentation. This mass flow rate is used to compute the inlet mass flow rate after accounting for compressor bleed air extraction and fuel mass addition using an empirical model calibrated using altitude facility test data. Ram drag is computed using this airflow and the vehicle's measured true velocity. Because the mass flow is calculated in the engine afterburner section where the gas flow is well-mixed, inlet flow distortion effects are minimized.

Calibration coefficients for a particular engine are determined using data obtained during altitude and sea-level-thrust facility tests. The coefficients correct for the effects of internal friction, mass transfer (leakages), three-dimensional effects, and the effect of the simplifying assumptions used in the theory. Calibration coefficients obtained through calibration of an individual engine can typically be used for all engines of the same model (Reference 4.3) with only a second-order decrease in accuracy because of engine-to-engine variations (engine-to-engine variance is reflected in the measured tailpipe pressures). The uncertainty of the SGMT was determined during altitude facility testing to ±1.8% (2σ) which resulted in a net thrust uncertainty of ±2.7% (Reference 4.3).

The real-time thrust method described above was developed for quasi-steady-state applications. Its unique approach of evaluating only augmentor flow and its simplistic instrumentation requirements encourage further evaluation for dynamic applications. Section 7 contains examples of the real-time thrust method during throttle transients.

4.2 Engine Transient Simulations:

Transient engine characteristics can be modeled using modern computing techniques (References 3.7 and 4.5). These models are usually created to support the engine development process for prediction of transient engine operation, analysis of operability problems, and control system design. These models can also be used for determination of in-flight thrust during transient operation.

Two types of transient simulations are in general use. The most accurate is the nonlinear aerothermodynamic model. This is a comprehensive, high-fidelity representation of the engine which models the aerodynamic and thermodynamic components. The second type is the simplified model which is usually developed for real-time applications. This type is considerably faster and less expensive to execute, but may have increased uncertainty due to the less rigorous component representations. Both of these models have been used for the evaluation of in-flight thrust during engine throttle transients.

The simplified models are further divided into three methods. The piecewise linear (state-variable) method is the only known real-time application for calculating in-flight thrust, and is discussed further in 4.2.2. The transfer function and torque extraction methods are two other types of simplified real-time models employed to locate errors in engine control logic prior to incorporation into control hardware. All three of these simplified methods use a steady-state model as the starting point of the transient mode operation.

SAENORM.COM : Click to view the full PDF of air5020a

4.2.1 Aerothermodynamic Model: The nonlinear aerodynamic model is a comprehensive representation of the engine components (Reference 4.6). This includes the thermodynamic representation, heat transfer, volume dynamics, thermal clearance effects, turbine cooling air variation, and control sensor lags. The basic analytical model utilizes steady-state component maps and cycle analysis methods for calculating performance at each operating point. For transient operation, the additional calculations are as follows:

a. Rotor acceleration is determined by evaluating the torque output of each turbine relative to the torque requirement of the fan or compressor.

b. Heat-transfer calculations are performed in each engine component to accurately model the engine metal and gas temperatures, and the resultant transient engine match.

c. The dynamics of the major engine component volumes are incorporated to represent the time rates of change of pressure, temperature, and mass within each component.

d. Thermal clearance effects are modeled to represent the transient blade tip and seal clearance changes due to differential expansion of rotors and cases, resulting in changes in component efficiency and flow capacity.

e. Turbine cooling flow variation during transients is modeled by accounting for the effects of temperature on the flow capacity of the cooling passages.

f. Control sensor lags and actuator dynamics are included in the model to properly simulate their response to true gas temperatures, pressures, and geometry, and the resultant control system actions.

Figures 12 and 13 show typical examples of the calculation flow paths for steady-state and transient models, respectively. As indicated, the cycle analysis flow paths are similar with the addition of the "dynamics" representation for the transient model.

4.2.2 Simplified Linear Model: The second type of transient model commonly used is the simplified linear model. This type of model is usually developed for real-time applications such as flight simulators, but can also be used for transient in-flight thrust determination. This model consists of a simplified linear representation of the engine rather than the comprehensive representation of each component as in the nonlinear aerothermodynamic model. This results in less complex computer code, making it capable of real-time execution, but usually at the expense of increased uncertainty.

The piecewise linear model (or "state variable" model) consists of empirical relationships between engine parameters such as fuel flow versus rotor speed, and can be considered as a sophisticated "table look-up" procedure. In order to achieve acceptable accuracy, a matrix of partial derivatives is used to define sensitivities of all pertinent parameters to changing conditions during an engine transient.

SAENORM.COM : Click to view the full PDF of air5020a

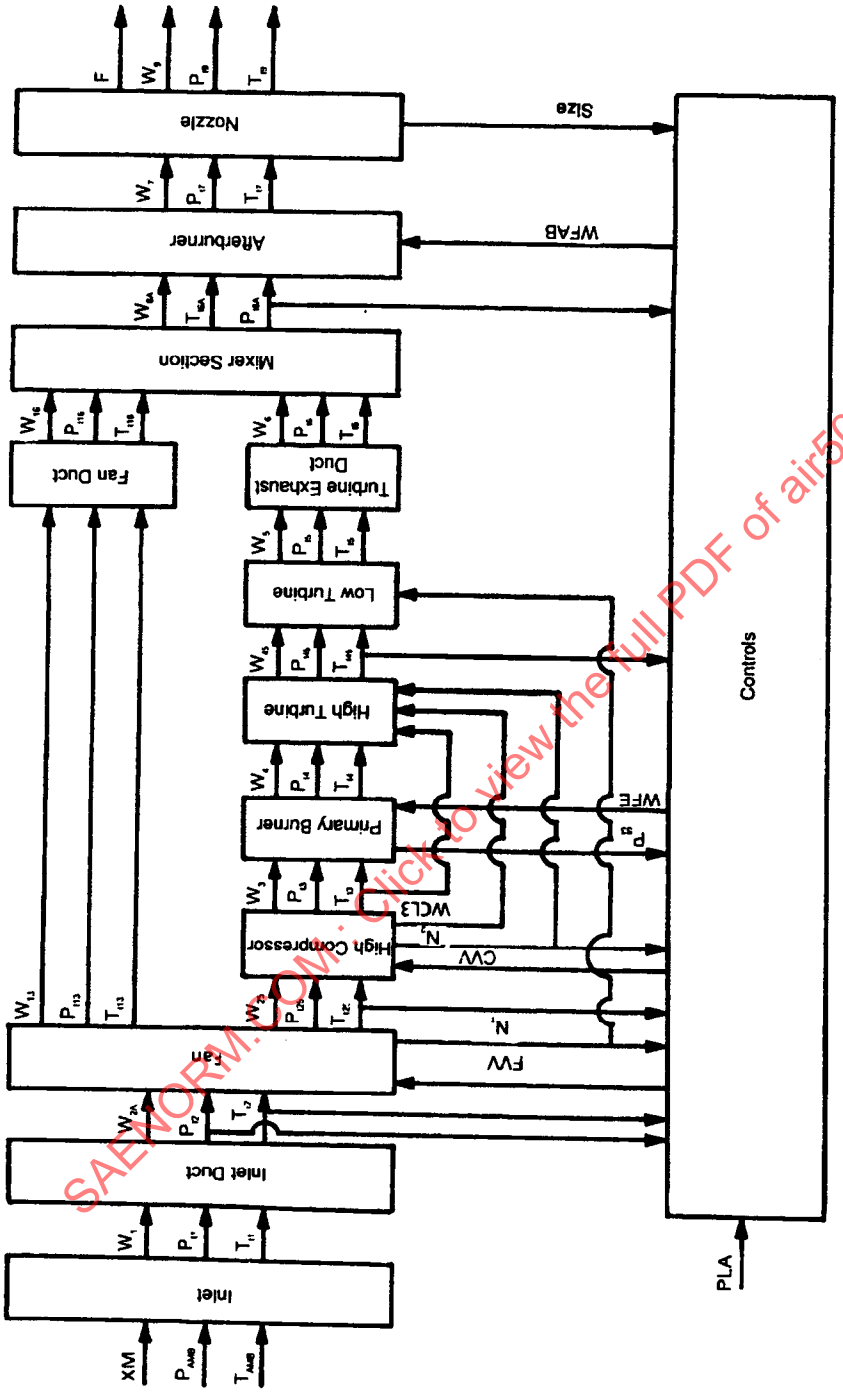

FIGURE 12 - Example of Calculation Flow Path for a Typical Turbofan Engine, Steady-State

SAENORM.COM : Click to view the full PDF of air5020a

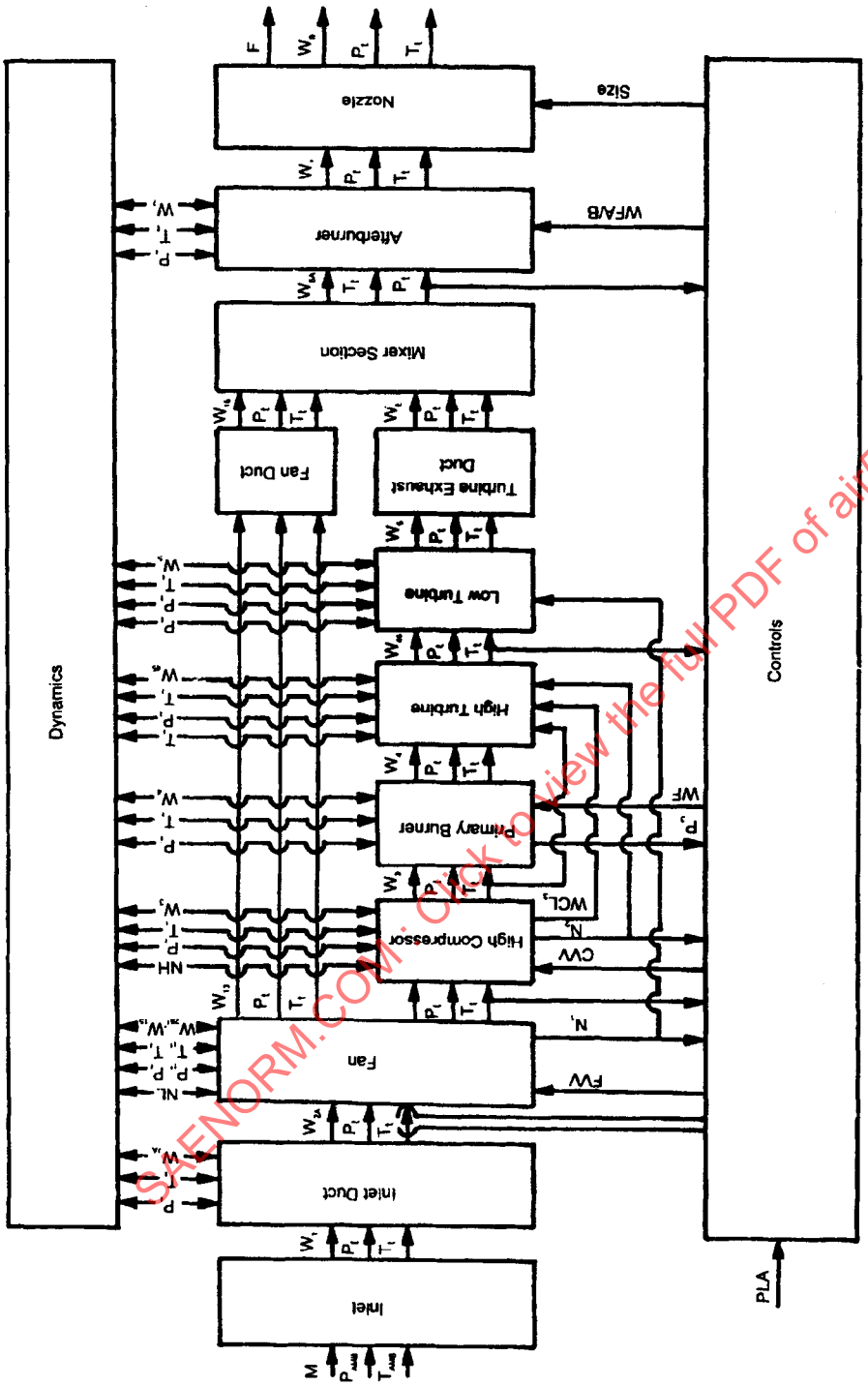

FIGURE 13 - Example of Calculation Flow Path for a Typical Turbofan Engine, Steady-State

SAENORM.COM : Click to view the full PDF of air5020a

4.2.2 (Continued):

For in-flight thrust, measured engine parameters such as rotor speeds and fuel flow can be used to drive the model. The model then determines through its partial derivative matrix the resulting effect on engine performance parameters such as airflow, temperatures, and pressure ratios. Thrust can then be calculated from the conventional gross thrust and ram drag equations.

Although simplified linear models have not had widespread use for in-flight thrust determination, they have been developed for many engine designs in support of other applications such as flight simulators, control benches, or "iron birds". These same models can be used for in-flight thrust determination if properly validated through comparison to engine test data or nonlinear aerothermodynamic models.

4.2.3 Model Validation: Validation of the transient model fidelity is accomplished through comparison to engine data from ground, altitude facility, and flight testing. This comparison is evaluated during steady-state and transient operation, and refinements are made to the model as necessary to match the measured rotor speeds, gas path temperatures and pressures, and performance. For example, realistic modeling of the heat sink distribution is necessary to simulate the proper engine match and correctly position the transient operating point. This validation process is conducted at selected points throughout the flight envelope for various throttle transients. Figure 14 compares an engine transient for IRT to Idle to IRT at 35,000-ft altitude, 0.8 M. Good agreement can be noted, thereby validating the modeling techniques.

Engine transient models can be calibrated in Altitude Test Facilities with the results that flight and propulsion system transients planned for flight tests can be reproduced to 1 to 2% of gross thrust during throttle transients (Reference 4.7). Figure 15A shows an example of transient math model validation for gross thrust where validation refers to the measure of the model fidelity to represents the engine hardware performance. Figure 15B shows an example of transient math model validation after refinement where refinement refers to the process of updating engine component maps and thermal and mechanical time constants with Altitude Test Facility test data.

4.2.4 Application of Transient Models for In-Flight Thrust: Once the fidelity of the transient model is assured, it can be used to evaluate transient in-flight thrust by forcing the simulation to run to the measured engine parameters such as fuel flow, variable geometry, and flight conditions (References 4.8 and 4.9). Figure 16 shows the results of an in-flight thrust analysis for an idle to military power transient at 40K ft, 0.5 M. The traces for afterburner inlet pressure (P_{t6}) and corrected fan speed (N_{1C}) show excellent agreement between the transient simulation and the test data. Since P_{t6} reflects nozzle pressure ratio and N_{1C} reflects total engine airflow, this provides confidence that the calculated thrust is correct. Also shown on this figure is a comparison between the transient simulation thrust and the quasi-steady $F/W\sqrt{T}$ gas path method. As expected, the gas path method results in an erroneously high thrust value due to not properly accounting for the transient terms. For this 5-s throttle transient, the transient thrust error is up to +8%. An additional feature of the transient model is the ability to calculate parameters which are not normally measured such as T_{t4} as shown on Figure 16.

SAENORM.COM : Click to view the full PDF of air5020a

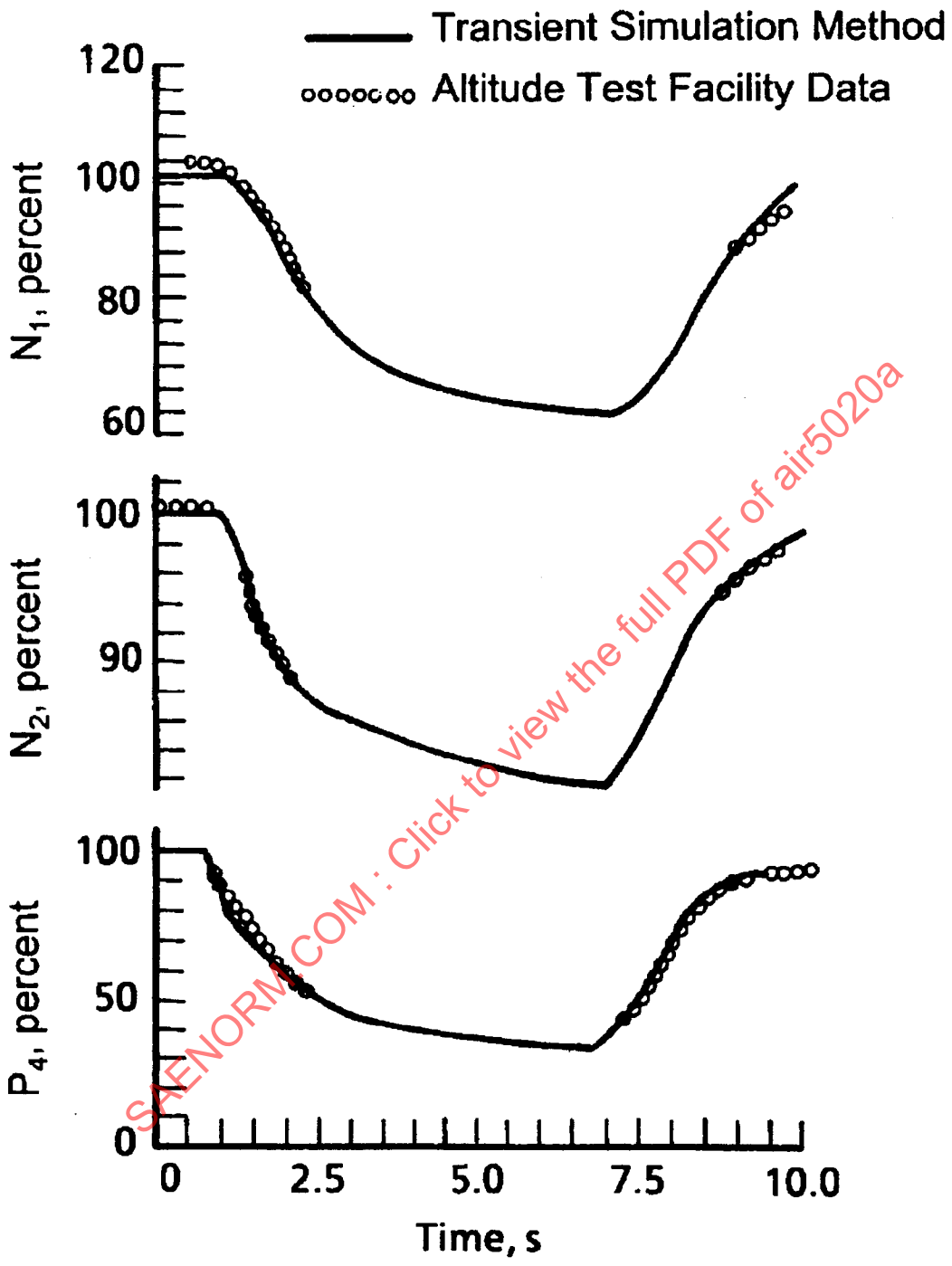

SAENORM.COM : Click to view the full PDF of air5020a

FIGURE 14 - Validation of Transient Modeling Terms Through Comparison to Test Data
(IRT to Idle to IRT Throttle Snap at 35 Kft/0.8 M)

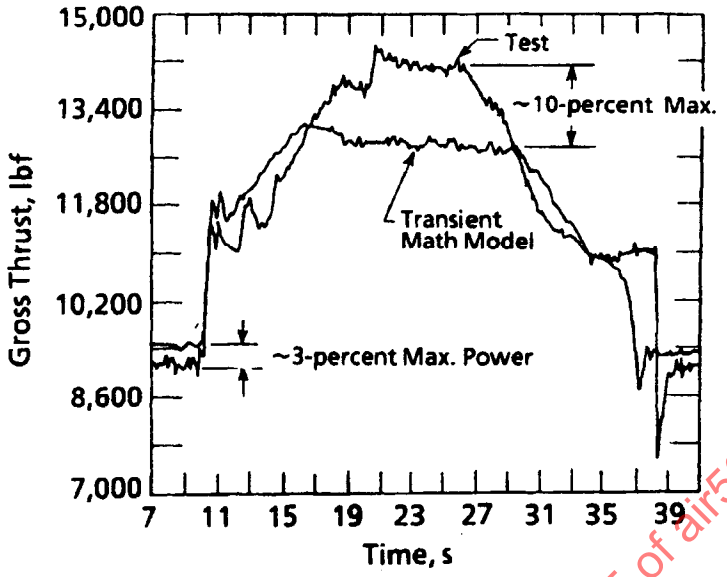

FIGURE 15A - Model Validation

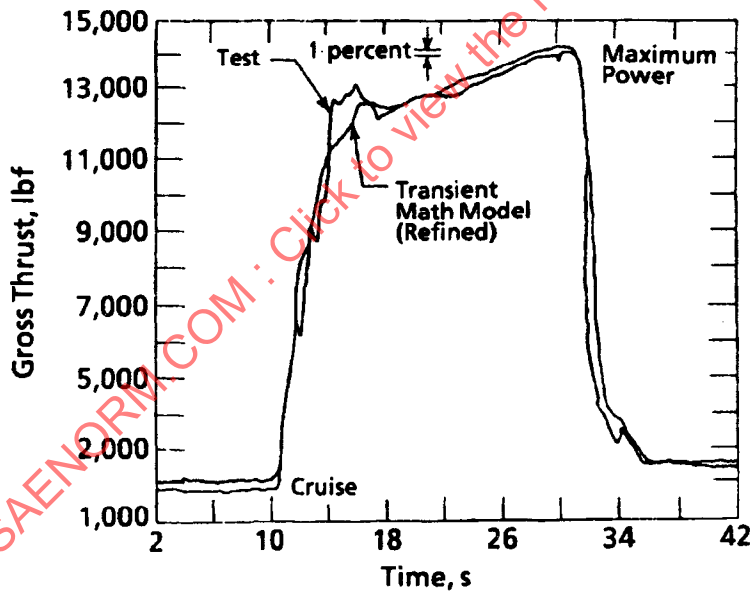

FIGURE 15B - Model Refinement

FIGURE 15 - Validation and Refinement of Transient Model Simulation With Altitude Facility Test Data

SAENORM.COM : Click to view the full PDF of air5020a

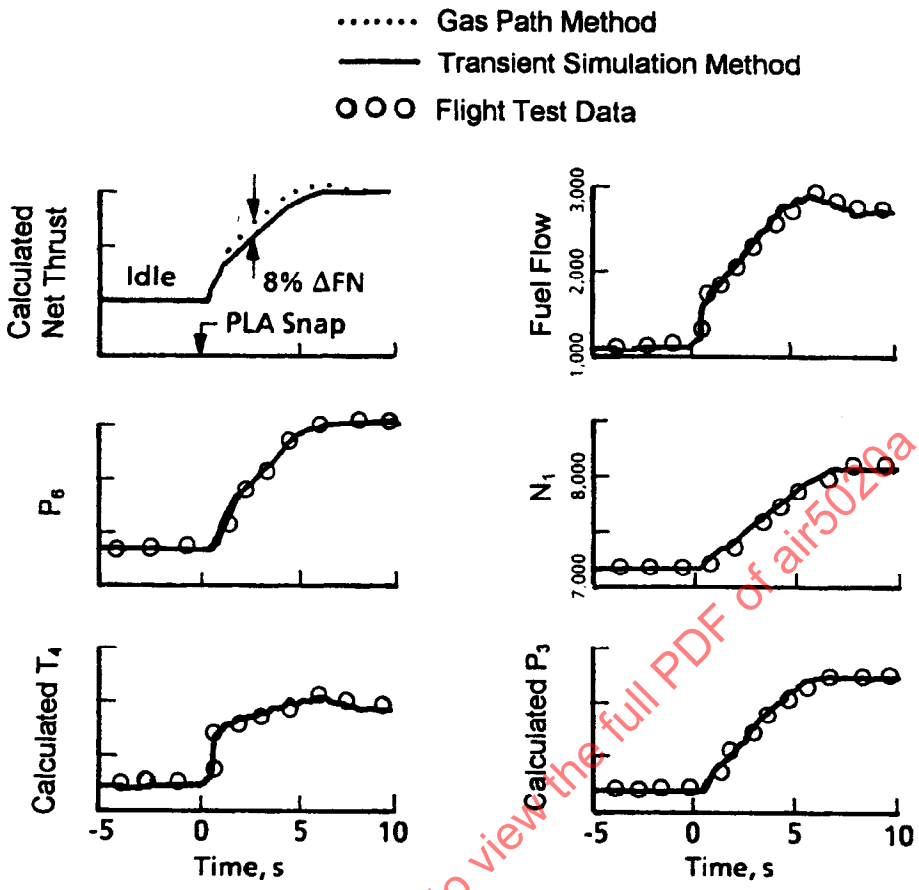

FIGURE 16 - Transient Simulation Comparison With Gas Path Method and Validation With Flight Data (Idle to IRT Snap Throttle Transient at 40 Kft/0.5 M)

SAENORM.COM : Click to view the full PDF of air5020a

4.2.4 (Continued):

Figure 17 is a second example showing calculated in-flight thrust during a transfer from maximum afterburner to secondary control at 30,000 ft, 1.2 M. During this process the afterburner flame is rapidly extinguished, resulting in a 60% thrust change in 0.1 s. The good agreement between measured and calculated augmentor pressure (P_{t6}) and the use of measured nozzle area gives confidence in the calculated thrust during the transient. Relative to the previous example, the quasi-steady $F/W\sqrt{T}$ method in this case results in a much larger error due to the faster timing of the event, with as much as a +40% error in the transient thrust value.

Figure 18 is a thrust analysis during an in-flight aerial refueling transient. In this maneuver, the pilot is continuously modulating the throttles to position the aircraft relative to the tanker. Input parameters were measured flight conditions, fuel flow, nozzle area, and variable geometry. The calculated net thrust, together with throttle position and airplane longitudinal acceleration, N_x, is shown. Note that the net thrust changes are in phase with measured airplane acceleration. This provides additional confidence that the thrust calculation is representative.

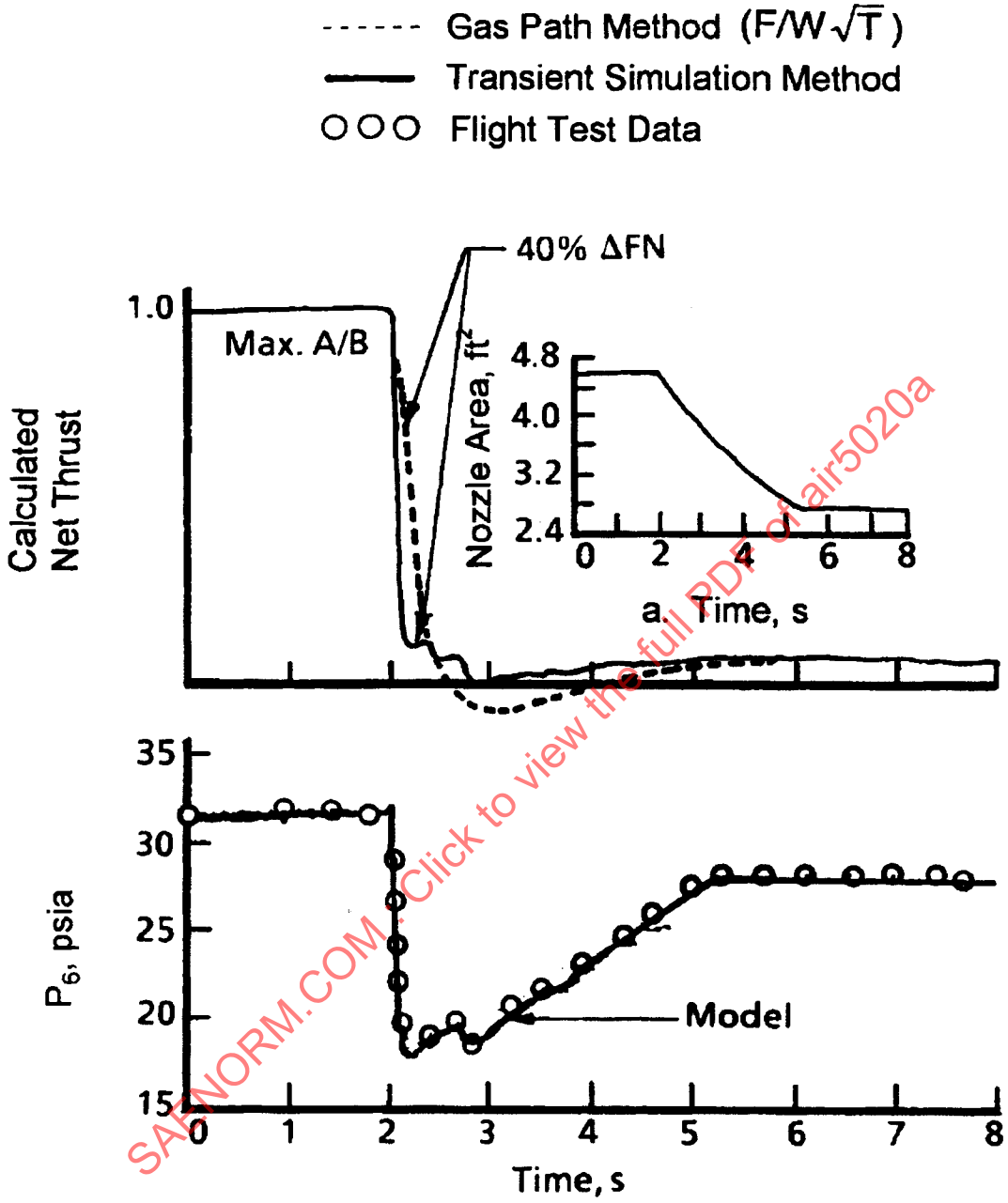

SAENORM.COM : Click to view the full PDF of air5020a

FIGURE 17 - Errors in Gas Path Method for Rapid Events Such as Control Mode Transfer From Primary to Secondary Mode (Maximum Power at 30 Kft/1.2 M)

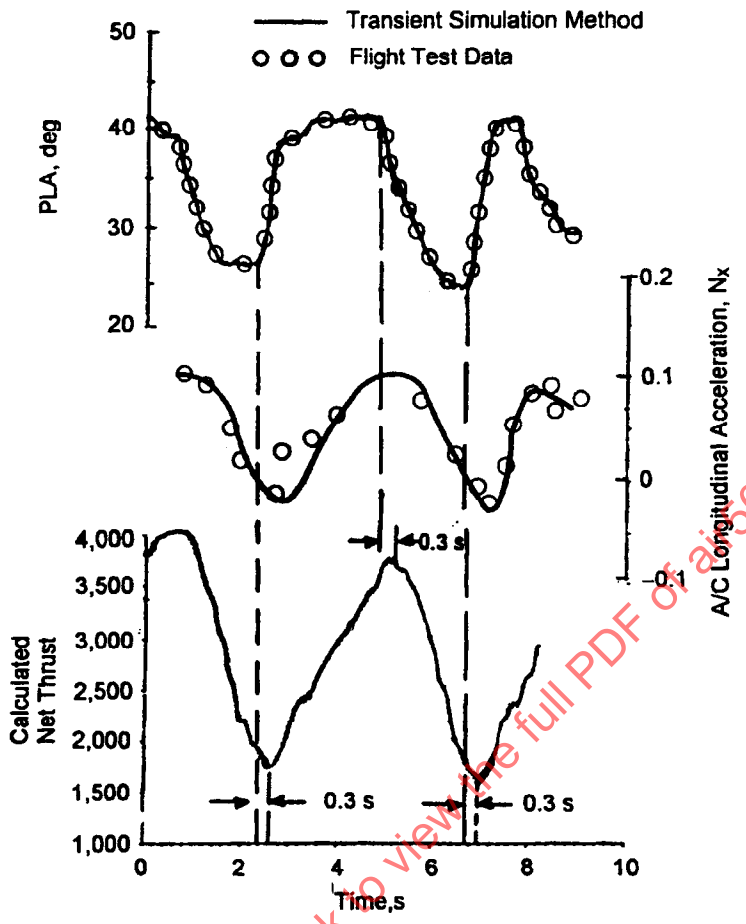

FIGURE 18 - Validation of Transient Simulation for In-Flight Thrust During Aerial Refueling (20 Kft/0.65 M)

4.3 Engine-Independent In-Flight Thrust Methods:

In the vast majority of in-flight thrust approaches, the use of ground-based testing to produce in-flight correlations has been necessary because of the general inability to directly measure the engine characteristic in question (i.e., inlet momentum, exit momentum, applied force). To a great extent, the success of in-flight thrust strongly depends upon the ability of test cell correlations to remain consistent during flight testing. The addition of time-dependence in thrust measurement invokes an additional dimension on correlation requirements, making the task of ground correlation more difficult. Three methods have been recognized which attempt to directly measure in-flight thrust: engine inlet/exhaust surveys, engine mount (trunnion) strain measurements, and excess thrust measurements.

SAENORM.COM : Click to view the full PDF of air5020a

4.3.1 Inlet/Exhaust Survey Method: Engine inlet and exhaust wake surveys can be used to measure the inlet and exit momentum of an engine under steady-state conditions, but have had limited application because of the relative complexity of installation, coupled with the difficulty of correlating associated installation effects. Since the traverse itself is time-dependent, it cannot be used for evaluation of transient thrust without some time lag correction methodology. Direct measurement of inlet and exhaust momentum may be possible in the future through the use of laser velocimeters. This is an emerging technology that, conceptually at least, has the potential capability to measure the flow velocity profile at both the engine inlet and exhaust planes. A distinct advantage of this technology is the possible ability to measure transient conditions without affecting the internal or external flow fields. The current capability of laser velocimeters and laser Doppler anemometers is discussed in, for example, References 4.10 through 4.14.

4.3.2 Trunnion Method: Strain measurements on engine mounts attempt to measure engine thrust loads directly but have met with limited success in the past. The primary difficulty is making essential corrections to these measurements to account for engine-to-nacelle bridge forces and inlet thrust. The trunnion thrust method is, in principle, self-compensating for engine thermal transients if all measurements are made with adequate transient fidelity. Possible transient problems include differential thermal growth in the engine supports and seals which cause extraneous tare forces in the force measuring system. Other mechanical interfaces such as the inlet seals, bleed ducting, power takeoff shaft, and fuel lines, for example, need to be taken into consideration. Additional transient considerations which complicate this approach are the acceleration forces on the system during aircraft maneuvers. This requires compensation for forces due to acceleration along the flight path axes. The technology for the trunnion thrust method is unproven for in-flight time-dependent thrust determination.

4.3.3 Excess Thrust Method: Although not adopted as a primary in-flight thrust method, excess thrust measurement can be used as a means to validate in-flight thrust procedures for aircraft that have previously established drag characteristics. For example, if the same aircraft has flown with two different engine models, the difference in excess thrust can be used to assess the relative engine performance change. This technique has been used to evaluate alternate engine options for current high-performance aircraft. Excess thrust is either measured by accelerometers or calculated from an energy method based on flight path versus time. These measurements are discussed in detail in 7.3.

4.4 Summary:

The determination of in-flight thrust can be obtained during transient operation using several methods. The conventional gas path techniques can be utilized for quasi-steady maneuvers with fixed throttle. For maneuvers including variable throttle, the transient engine simulation approach can reduce uncertainty by accounting for the transient energy and mass terms.

SAENORM.COM : Click to view the full PDF of air5020a

4.4 (Continued):

Gas path methods of in-flight thrust determination use measured flow properties throughout the engine to determine gross thrust and ram drag based on steady-state correlations from ground and altitude test facilities. Gas path methods in general are economical from both a development and implementation correlation because of the use of steady-state relationships and reduced computational data requirements. The two principal types of gas path method are the "flow-temperature" ($F/W\sqrt{T}$) and "pressure-area" (F/AP) methods. Successful application can be expected for dynamic aircraft maneuvers with fixed throttle, such as aircraft accelerations/decelerations, wind-up turns, and push-over/pull-ups. For variable throttle, a combination of the two methods can provide better uncertainty and confidence in the results.

For variable throttle or rapidly changing flight conditions, the uncertainty with gas path methods increases because of volume dynamics, transient energy terms, component performance changes, and instrumentation lags. The transient simulation approach can be utilized to account for these unsteady terms, but at the expense of cost and development time. The nonlinear aerothermodynamic model is the most accurate representation, and consists of a comprehensive, high-fidelity representation of the engine components which models all of the unsteady terms. An alternate approach is the simplified linear model which is derived from the aerothermodynamic model but utilizes transient correlations or a partial derivative matrix to determine the transient performance. Although fast enough to execute in real time, the simplified model has increased uncertainty due to less rigorous component representations.

Validation of the transient model fidelity is accomplished through comparison to engine data from ground, altitude facility, and flight testing. This comparison is evaluated during steady-state and transient operation, and refinements are made to the model as necessary to match the measured rotor speeds, gas path temperatures and pressures, and performance. Once the fidelity of the transient model is assured, it can be used to evaluate transient in-flight thrust by forcing the simulation to run to the measured engine parameters such as fuel flow, variable geometry, and flight conditions.

From a theoretical approach, engine-independent techniques could provide an attractive alternative for in-flight thrust by eliminating the need to account for internal engine characteristics. However, to date, none of the totally engine-independent methods have demonstrated measurement uncertainty capabilities typically required for flight test thrust evaluations. Techniques which are identified in this category are inlet/exhaust surveys using the laser velocimeter, the strain-gaged trunnion, and excess thrust methods.

SAENORM.COM : Click to view the full PDF of air5020a

5. TEST FACILITIES:

There are four principal types of test facilities used in the determination of aircraft and propulsion system performance:

a. Propulsion (Ground-Level and Altitude) Test Facilities
b. Aircraft Installed Facilities
c. Wind Tunnel (Aerodynamic Model Test) Facilities
d. Flight Test Facilities

5. (Continued):

Each of these test facilities plays a different but essential role in determining aircraft in-flight performance. In this section, test facility transient operating characteristics and general capabilities to support the determination of in-flight time-variant thrust are reviewed.

5.1 Propulsion (Ground-Level and Altitude) Test Facilities:

While flight test is the process of evaluating the integrated performance of full-scale airframe and propulsion hardware, the flight environment is not easily controlled for systematic test evaluations. The Ground-Level Test Facility and Altitude Test Facility provide a means for isolating the propulsion system in a controlled environment which enables systematic-type testing. Propulsion ground test facilities also have capabilities to simulate steady-state environmental conditions (as those encountered in steady-level flight), and to obtain propulsion system data during engine power transients at set environmental test conditions. In the case of the Altitude Test Facility, some capability to simulate environmental transients also exists.

5.1.1 Facility Configurations: A typical Ground-Level Test Facility is shown in Figure 19. Pertinent features of the facility include the atmospheric air intake system, the test cell and thrust stand, the exhaust collector, and exhaust stack. In a Ground-Level Test Facility, engine transient performance can be accomplished relatively easy and at moderate cost compared to an Altitude Test Facility. The Ground-Level Test Facility is generally limited to ambient inlet environmental test conditions; however, there are some ground-level facilities with main ram air capability.

SAENORM.COM : Click to view the full PDF of air5020a

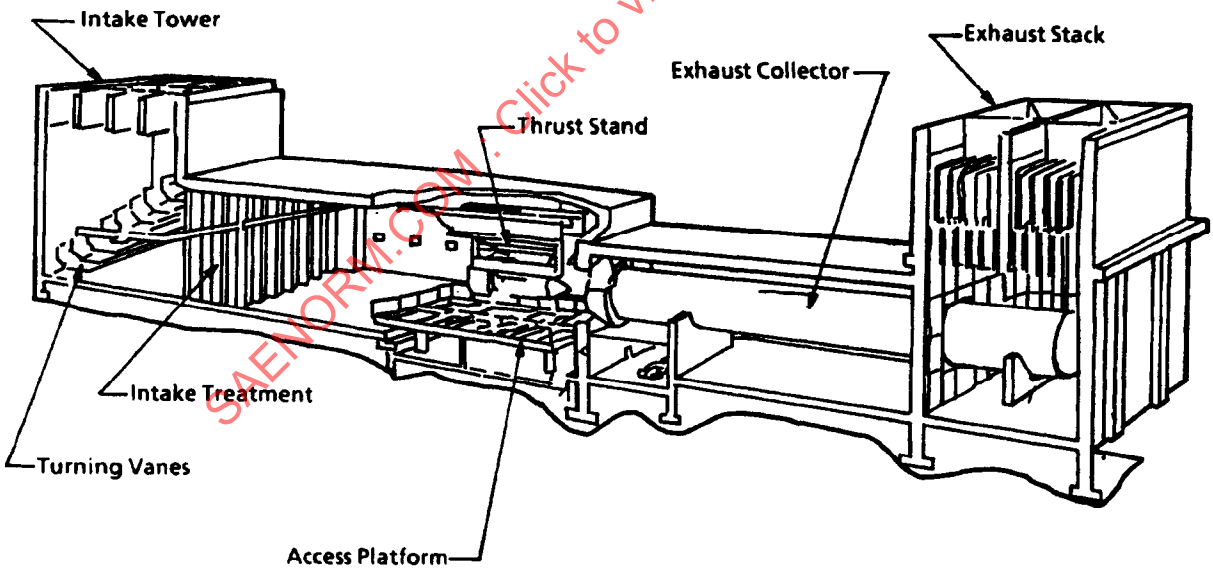

FIGURE 19 - Typical Ground-Level Engine Test Facility

5.1.1 (Continued):

A conventional altitude test facility configuration with capability to control environmental conditions during engine power transients is shown in Figure 20. In this installation, the turbine engine is installed on a thrust stand with the inlet directly connected to the facility air supply system. The installation employs a zero-leakage labyrinth air seal or a positive sealing plastic slip-ring assembly as a means to mechanically isolate the fixed inlet structure from the free-floating thrust stand. Air supplied to the engine inlet is conditioned to the pressure and temperature required to simulate the desired flight conditions. A bellmouth is employed to provide smooth airflow to the engine inlet. To control the engine discharge environment (corresponding to the ambient pressure at the simulated altitude), an exhaust collector duct is installed to remove the engine exhaust gases and provide pressure recovery to supplement the facility exhaust machinery. A test cell bypass air duct is provided to improve inlet pressure control during the engine transients. This latter installation arrangement provides the best means of measuring the performance of turbine engines and has been adapted to engine transient testing. Engine transient testing is generally conducted to verify engine operability characteristics during engine power transients at constant engine inlet and exhaust pressure and constant inlet temperature. In most altitude test facilities, the airflow control valves and exhaust control valves are remotely located from the engine test cell. This remoteness results in large, effective volumes which minimize the variance in set conditions during transient engine operations.

An Altitude Test Facility configuration for optimal control of environmental conditions during engine mission simulation testing is shown in Figure 21. Pertinent features of the facility include the close-coupled hot and cold air supply lines and control valves to accomplish rapid inlet air temperature and pressure changes. With this test configuration, the test article can be temperature-conditioned and subjected to simulated mission profiles of time-variant flight subsonic/supersonic Mach number and altitude with constant or variable ram recovery. The engine can also be concurrently subjected to inlet total pressure distortion, power extraction, and fuel temperature conditions. The test configuration depicted in Figure 21 is presently limited to engines up to the 10 to 20,000-lbf thrust class.

SAENORM.COM : Click to view the full PDF of air5020a

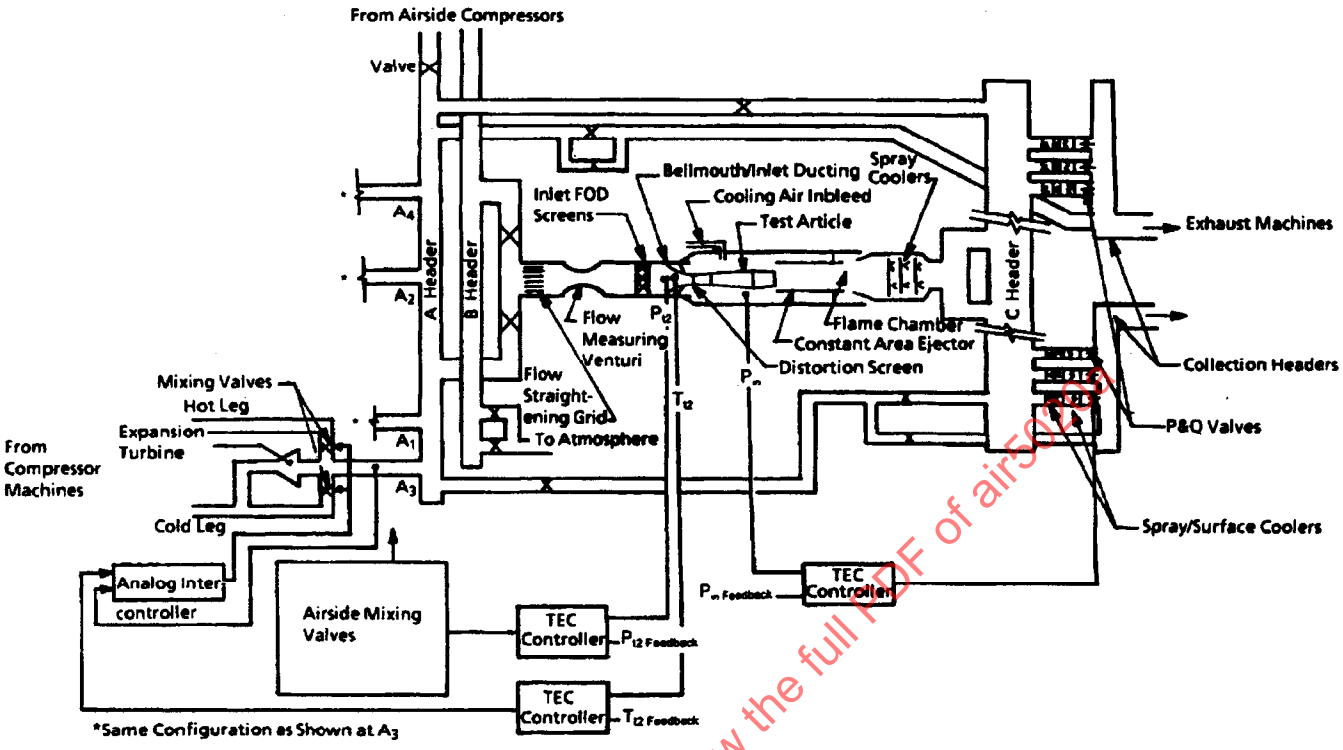

FIGURE 20 - Altitude Test Facility Configuration (Mission Simulation Testing)

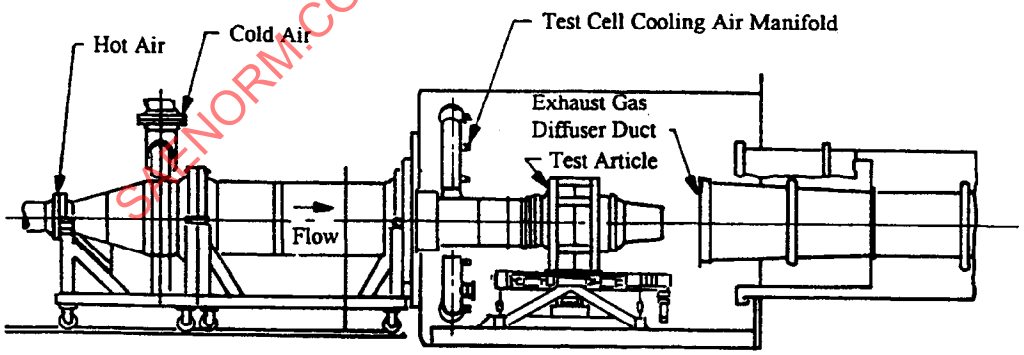

FIGURE 21 - Altitude Test Facility Configuration for Simulation of Flight Transients

SAENORM.COM : Click to view the full PDF of air5020a

5.1.2 Facility Operating Concepts: In the Ground-Level Test Facility the only mode of transient control is the engine power lever. In the altitude test cell, both the engine power and test environmental conditions can be controlled. The Altitude Test Facility (Figures 20 and 21) has three modes of control for flight and environmental conditions. The available modes are: manual control by operators, automatic control by analog controllers, and automatic control through use of a digital closed-loop control system.

To achieve optimal control of environmental flight conditions during power or flight condition transients requires integrated control of the facility inlet airflow mixing valves, bypass flow, and exhaust flow. Desired test conditions are programmed into the control system, either as set points, time-dependent paths, or combinations. The actual set conditions are measured and fed back to the test control system which commands valve positions for the inlet airflow, bypass flow, and exhaust flow valve to achieve the desired test conditions. Engine power setting can be controlled open-loop via a programmable throttle, if required.

The capability of modern altitude test facilities (test configuration, Figure 20) to maintain set conditions for rapid engine throttle movement (i.e., <5 s) from idle to intermediate power is dependent on the engine airflow rates and the particular test installation, but is nominally 1 to 5% for pressure and 0.5 to 2% for temperature. Transient change of environmental test conditions is also accomplished, but the degree of control of pressure and temperature is influenced by a wide range of factors. In major engine altitude test facilities, the rates of change in pressure to simulate aircraft in-flight maneuvers can usually be readily accomplished; the rate control of temperature is the limiting factor. Temperature ramp rates of 1 to 3 deg/s, depending on the test conditions and engine airflow rates, can normally be achieved using facility plant equipment. Special test installations using circumferential array of nozzles for injection of liquid or heated air have been employed, but this type installation is not considered standard practice for engine performance evaluations.

Typical deviations from programmed trajectories for environmental flight simulations (test configuration, Figure 21) are Mach number (±0.05) and pressure altitude (±100 ft). Environmental flight simulation is also conducted in the test configuration depicted in Figure 20, but with a higher deviation in Mach number. The magnitude of this deviation is primarily a function of the required rate of change in engine inlet temperature.

5.1.3 Engine Sweep Testing: Requirements to set and maintain simulated altitude flight conditions for slow (>1 min) power sweep testing are well within the Altitude Test Facility capabilities previously discussed. The airflow transients associated with this type of testing impose less severe requirements than during snap power transients; however, the objective of sweep testing is to extract equivalent steady-state performance from the transient sweep data. This objective necessitates that set condition variations be minimized to reduce the magnitude of adjustments to the data for deviations from desired test conditions.

SAENORM.COM : Click to view the full PDF of air5020a

5.1.3 (Continued):

Shown in Figure 22 are transient and steady-state data results from Reference 5.1 for a low-bypass turbofan engine during power sweeps of 1 and 5 min from idle-to-intermediate power settings at fixed environmental test conditions. Shown in Figure 23 are transient and steady-state thrust comparisons at four power sweeps of less than 1 min. The results in Figure 23 are for a low-bypass turbofan engine at fixed flight conditions and illustrate that significant deviations can be obtained in transient and steady-state thrust for the same energy (fuel flow) input condition. Test results of the type shown in Figures 22 and 23 can be used to quantify the magnitude of the time-dependent terms on engine performance and to evaluate the accuracy of transient performance prediction methods. As engine transient simulation modeling techniques are improved, sweep testing will become more attractive because of the potential for test cost savings.

5.1.4 Aircraft Inlet Flow Simulators: Currently, three methods are generally used for the simulation of inlet flow-field distortion generated by an aircraft inlet system during maneuver conditions. These methods are distortion screens, the Airjet Distortion Generator, AJDG, (Reference 5.2), and the Free-jet Test concept (Reference 5.3). The three methods for simulating inlet generated flow-field distortion are used for steady-state engine testing, but each method can be conceptually considered for limited transient engine testing.

For instance, the AJDG (Figure 24) is basically a fast-acting air injection and control system and is described in detail in Reference 5.2. The AJDG has the advantage over fixed geometry screens because many patterns can be set in a single test period (which reduces test cost); this theoretically offers the capability to simulate transient distortion (i.e., changes in distortion patterns and intensity) to represent changing aircraft attitude. At present, the absolute level of distortion intensity attained with the AJDG is about half that provided by screens. There are also ongoing efforts to evaluate the use of variable blockage-type screens which also could have some level of transient and dynamic distortion simulation capability. The Free-jet Test concept is dependent upon developing transient free-jet test methods for simulating aircraft maneuvers.

5.1.5 Power and Thrust Vector Transient Evaluation: This section discusses the methodology used in the Altitude Test Facility to characterize engine transient thrust performance, which is the basis for developing in-flight thrust methods. The information herein is based on material contained in Reference 5.4.

A major turbine engine operability consideration and specification requirement is the need for a propulsion system to respond to the selection of the power lever in a required time period with no engine/component instabilities. This requirement often necessitates comprehensive tests at many flight conditions with installation effects and can involve testing with inlet pressure distortion representative of specific aircraft/inlet maneuver conditions. New technology systems such as the two-dimensional convergent-divergent (2D/CD) vectoring exhaust systems add an additional dimension to this aspect of operability, i.e., thrust vector transients.

SAENORM.COM : Click to view the full PDF of air5020a

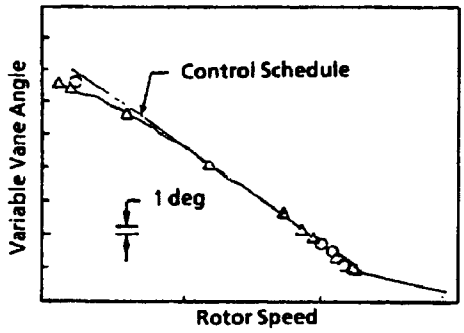

FIGURE 22A-1 - Variable Vane Tracking

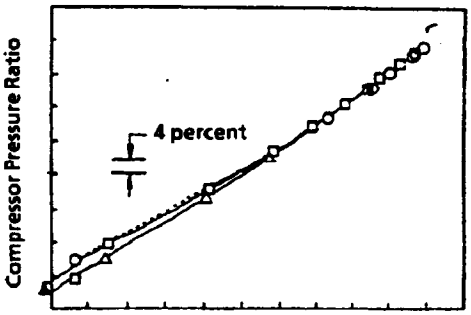

FIGURE 22A-2 - Compressor Operating Line

Legend
□ Transient Adjusted
△ Transient/Unadjusted
○ Steady-State Data

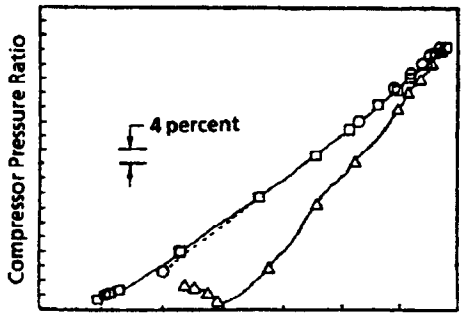

FIGURE 22A-3 - Engine Compressor Efficiency

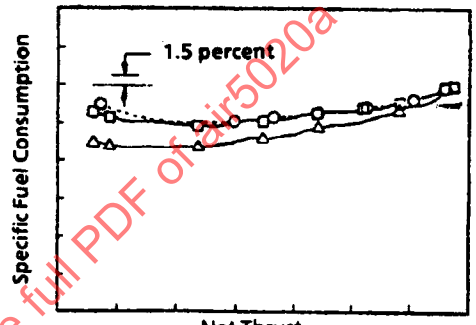

FIGURE 22A-4 - Fuel Efficiency

FIGURE 22A - Results for 1-min Sweep

SAENORM.COM : Click to view the full PDF of air5020a

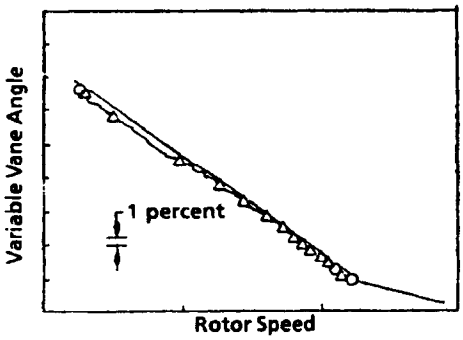

FIGURE 22B-1 - Variable Vane Tracking

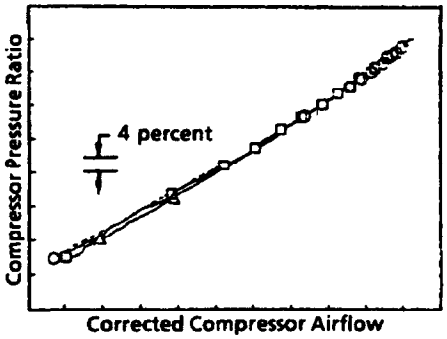

FIGURE 22B-2 - Compressor Operating Line

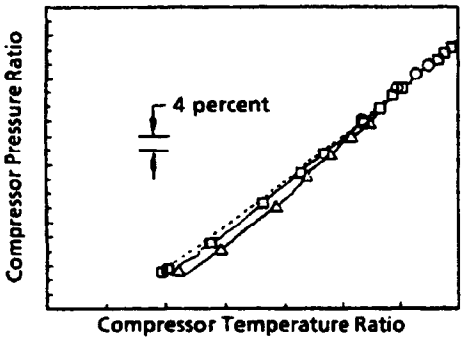

FIGURE 22B-3 - Compressor Efficiency

Legend
□ Transient Decel/Adjusted
△ Transient Decel/Unadjusted
○ Steady-State Data

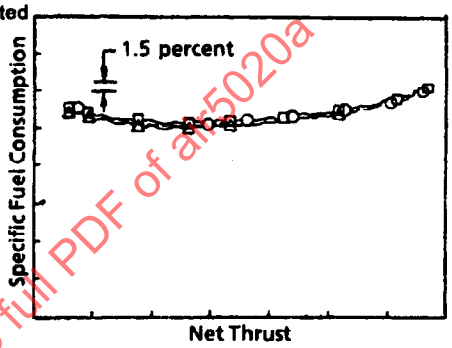

FIGURE 22B-4 - Fuel Efficiency

FIGURE 22B - Results for 5-min Sweep

FIGURE 22 - Comparison of Engine Transient and Steady-State Operation
(Turbofan Engine from Idle to Intermediate Power)

SAENORM.COM : Click to view the full PDF of air5020a

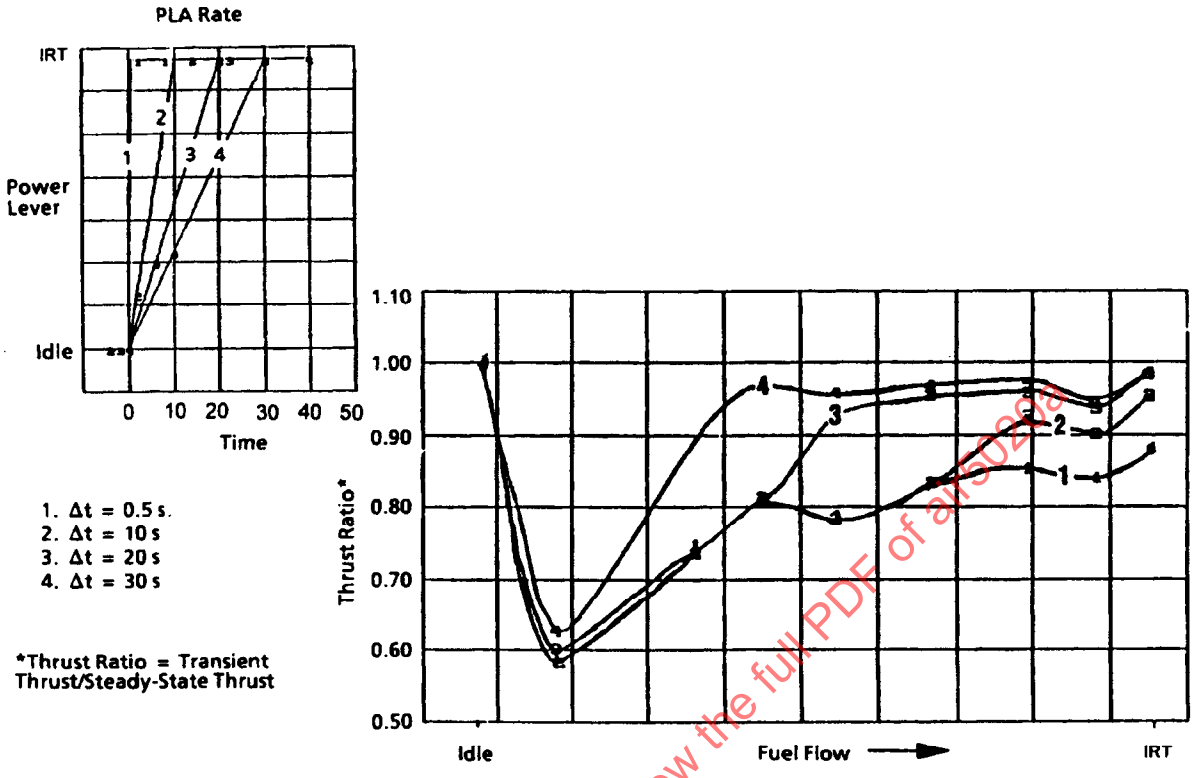

FIGURE 23 - Transient Effects on Engine Net Thrust (Accel at Fixed Flight Conditions)

SAENORM.COM : Click to view the full PDF of air5020a

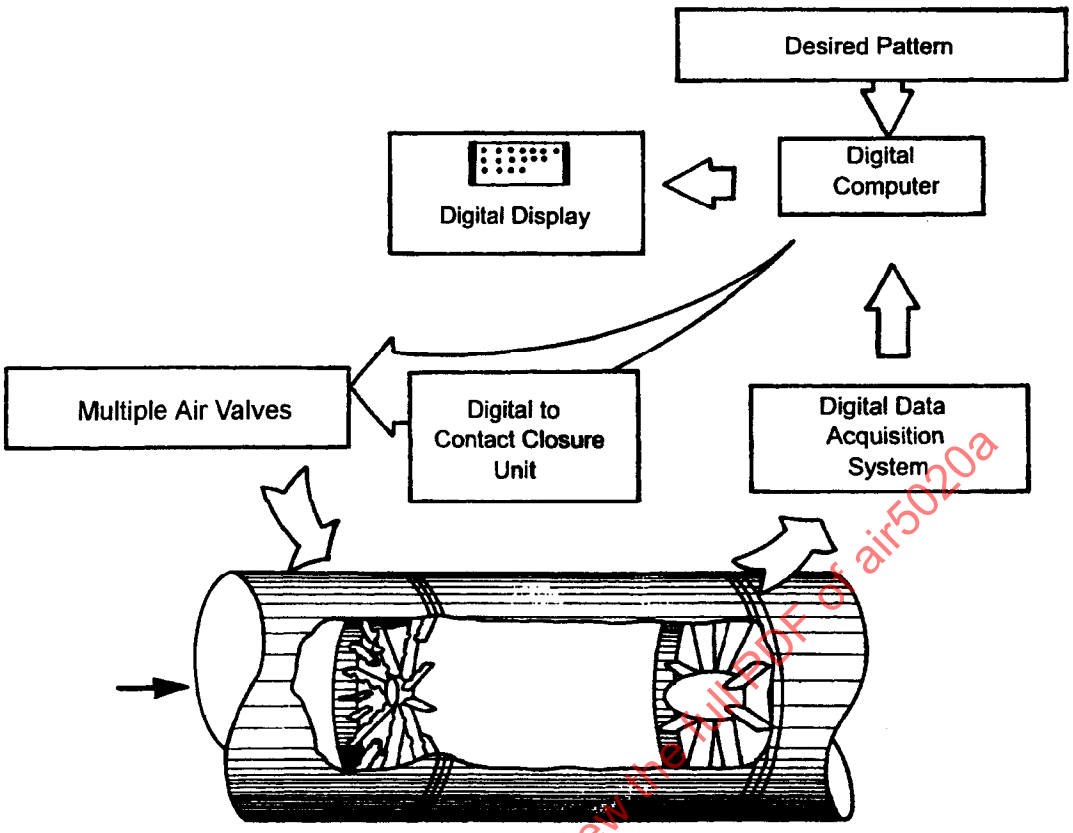

FIGURE 24 - Airjet Distortion Generator

5.1.5 (Continued):

Power transients are simulated by setting engine inlet total pressure and total temperature to the levels corresponding to the desired altitude and flight Mach number, and test cell ambient pressure is set to the level corresponding to the ambient pressure at the desired altitude. Installation effects such as bleed and horsepower extraction are generally set at the desired levels at intermediate rated thrust, and the power or thrust vector transient (or profile) of interest is then performed. Satisfactory or unsatisfactory (instabilities experienced) completion of the transients is an obvious indication of engine/component stability or instability.

A figure of merit derived from snap power transients and used as a measure of engine responsiveness is time to thrust. Time to thrust is determined from power lever advance to the attainment of the required thrust level (generally 90 to 95% of the change in gross or net thrust). The transient calculation of gross and net thrust most often utilizes a calibrated bellmouth to determine engine airflow for reasons previously discussed in 5.1.2. Force measurements are taken directly from thrust stand load cells and do not require response compensation. Idle-to-intermediate rated thrust response of a low-bypass-ratio augmented turbofan engine is shown in Figure 25. The time to achieve 95% of the thrust change is also indicated. A typical format for comparing thrust response to specification requirement is shown in Figure 26.

SAENORM.COM : Click to view the full PDF of air5020a

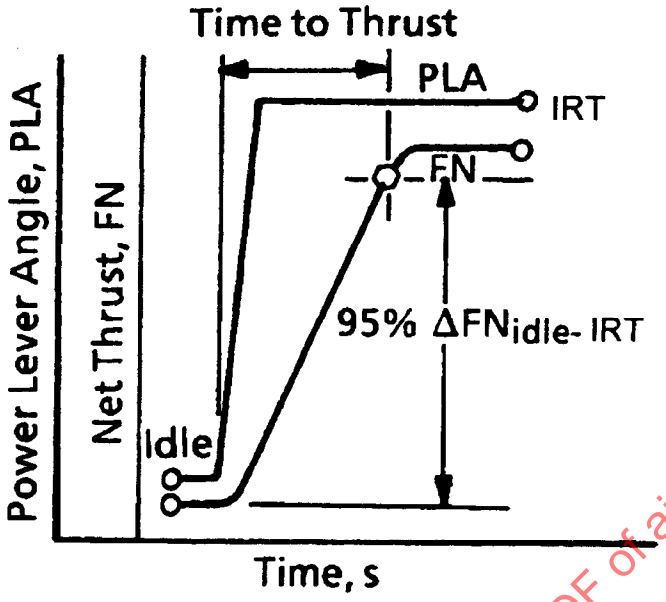

FIGURE 25 - IRT Thrust Response

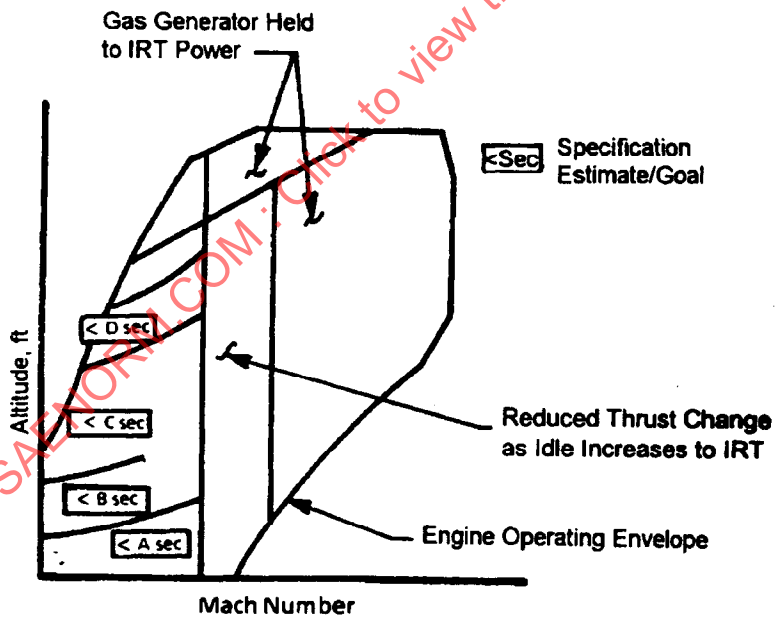

FIGURE 26 - Thrust Response Compared to Requirements

SAENORM.COM : Click to view the full PDF of air5020a

5.1.5 (Continued):

Alternate methods for determining thrust response time have been used in the past which relate thrust to other more directly measurable parameters such as engine pressure ratio or corrected speed. The relationship of thrust to speed or engine pressure ratio was developed from steady-state data. These early methods have, for the most part, been abandoned in favor of thrust determined directly from force measurements because of differences in steady-state and transient variable geometry scheduling and the need to directly observe thrust response as a function of time.

Other aspects of transient engine operation evaluated during snap power transients include thrust overshoot and thrust droop. Thrust overshoot, illustrated in Figure 27, may be caused by an overly aggressive control accel schedule and can lead to turbine rotor inlet temperature overshoot and an undesirable thermal cycle on engine hot parts.

SAENORM.COM : Click to view the full PDF of air5020a

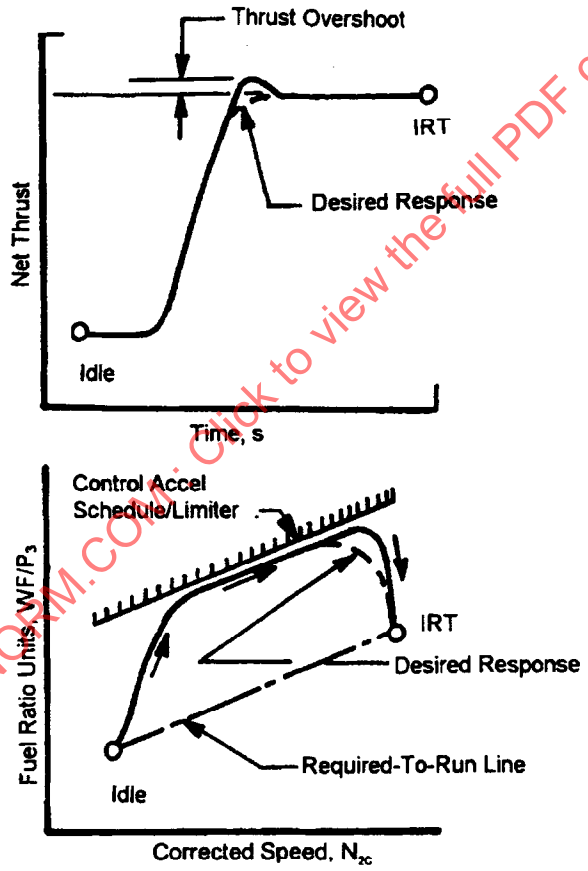

FIGURE 27 - Thrust Overshoot

5.1.5 (Continued):

Thrust droop (Figure 28) can be caused by transient engine rematch leading to engine operation being overridden by control limits. The steady-state match is eventually established and thrust reaches the thermally stable level.

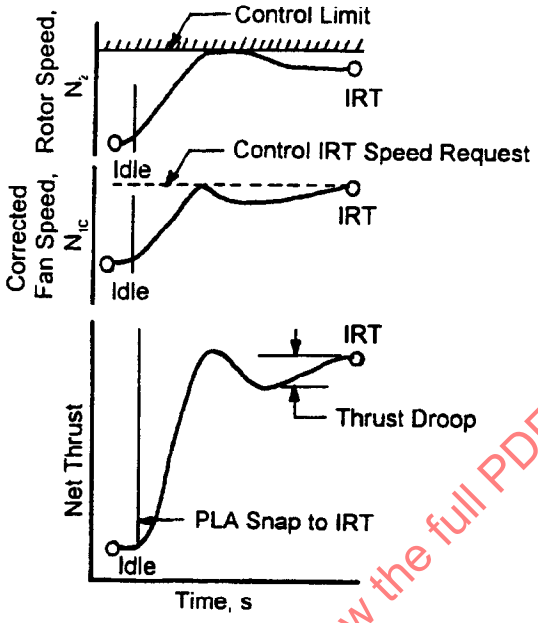

FIGURE 28 - Thrust Droop

New applications of thrust vectoring to military aircraft propulsion systems, although not addressed for in-flight thrust determination in this report, are emerging and, as such, test and evaluation methodologies are being developed. One aspect of thrust vector operability currently being evaluated in ground tests is the response relationship of the control vector request, Θ_{cr} (or nozzle flap metal angles) to the vector angle resolved from thrust stand force measurements, Θ_{eff} (Figure 29).

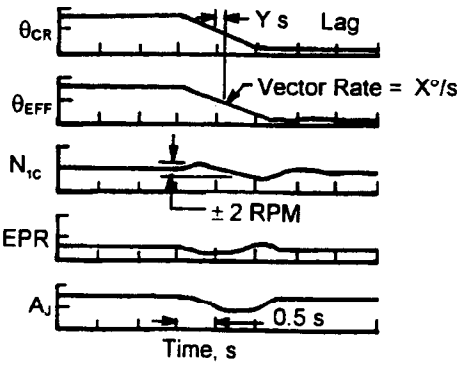

FIGURE 29 - Thrust Vector Response

SAENORM.COM : Click to view the full PDF of air5020a

5.1.5 (Continued):

Another consideration of engine power transient testing is that facility test conditions can deviate from the desired set point. Variations in inlet pressure and temperature and ambient pressure contribute additional uncertainty to the results obtained. Currently, much attention is focused on developing methods to analytically adjust engine thrust response times to account for these set condition variations. One method employed is the use of corrected net thrust, F_N/γ, as a means for quantifying time to thrust. This simple nondimensional adjustment satisfactorily accounts for inlet pressure variations, but does not address temperature or ambient pressure set condition variations. Recently, another method of correcting for inlet pressure and temperature and ambient pressure has been investigated. The method utilizes fundamental turbine engine cycle relationships to adjust transient data for set condition variations. This new method offers a more comprehensive adjustment methodology, and the limits for its application are explored and discussed in Reference 5.5.

5.2 Aircraft Installed Facilities:

Installed static thrust can be evaluated in aircraft tie-down facilities such as the one shown in Figure 30. Although thrust cannot be determined at flight operating conditions, the device can provide useful information in evaluating the modified net thrust term (F_N^*) in Equation 2 (incorporating the installation effects of inlet internal performance, bleed air extractions, and horsepower extractions) for comparison with simulation models at both steady-state and transient engine operating conditions.

Tie-down facilities are designed around "floating" platforms which are instrumented with high-precision load cells to measure thrust. The platform can be designed with the additional capability of weighing the aircraft and locating the center-of-gravity position, but these additional functions require modifications to the thrust stand design. Specifically, each of the landing gear requires its own scale. For aircraft equipped with a tricycle landing gear, the main landing gear is positioned on the platform, and the tires are chocked. Bicycle landing gear would require a different mounting installation; however, it could be accomplished in much the same manner as for the tricycle landing gear. The nose gear is free to move, ensuring that all thrust forces are transmitted through the main landing gear chocks. For center-of-gravity determination and thrust vector alignment with the platform, the nose gear requires an elevator for raising and lowering the nose. The "floating" of the platform is achieved by simple and/or pinned joints such that only axial forces are measured. The axial forces are focused to single or multiple supports through the use of framing networks. Load cells are normally positioned on the positive longitudinal axis focal points for thrust measurements. Each focal point incorporates one or more high-precision load cells. The use of multiple load cells improves the statistical population of the measurement which provides for improved accuracy.

The physical boundaries attendant to the platform housing may induce forces on the aircraft and thrust measurement structure that are included in the load cell measurements. Isolation and correction of the load cell measurements for these items is accomplished in much the same manner as for the ground level engine test cell as discussed in Section 5.1.2.2 of AIR1703 (Reference 1.1).

SAENORM.COM : Click to view the full PDF of air5020a

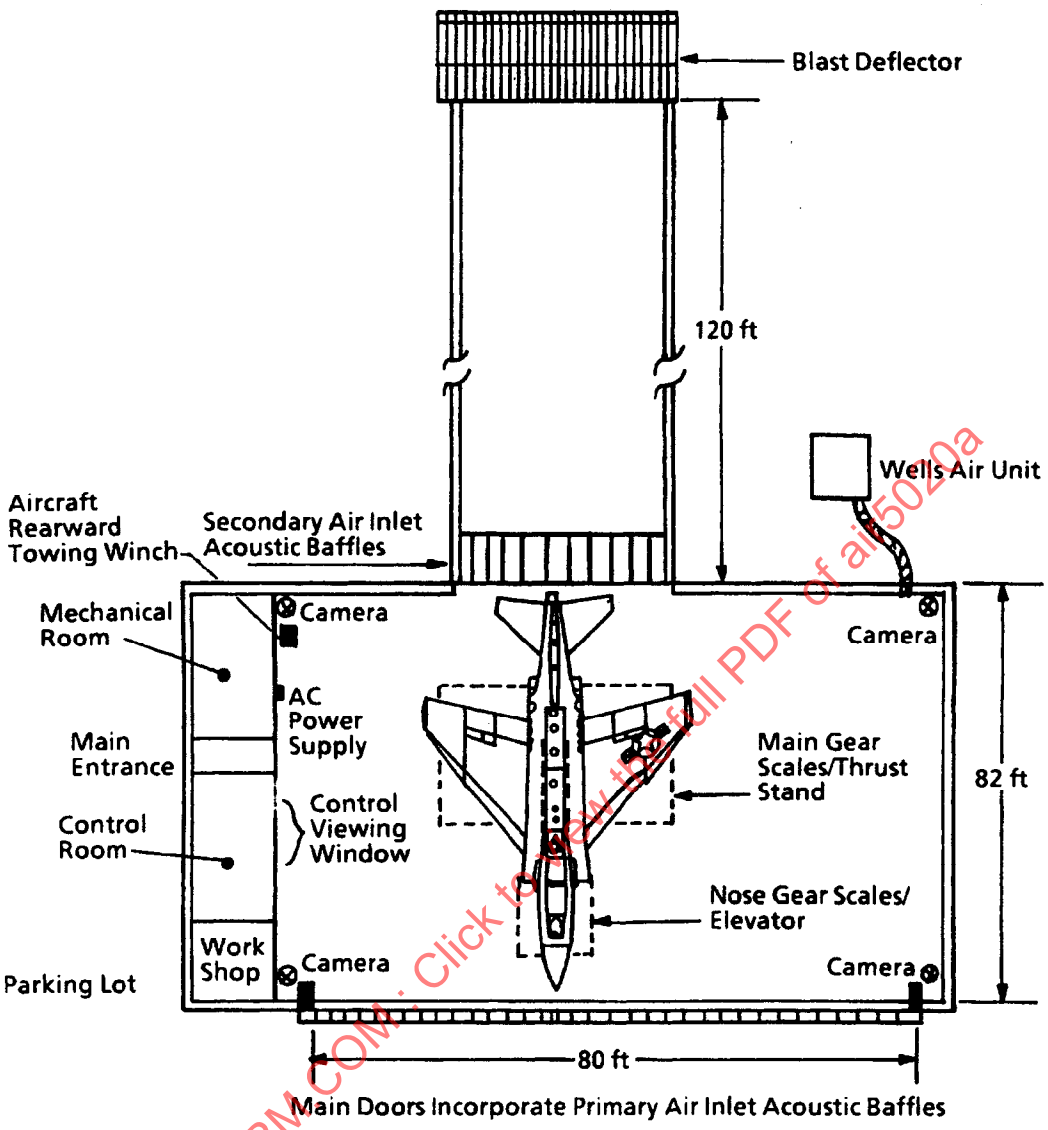

FIGURE 30 - Typical Aircraft Tie-Down Facility

SAENORM.COM : Click to view the full PDF of air5020a

5.3 Aerodynamic Model Test (Wind Tunnel) Facilities:

The throttle-dependent aerodynamic forces that are accounted as a part of the net propulsive force are determined in the aircraft development program. As such, the value of these forces is part of the initial aerodynamic database that comes directly from wind tunnel test data and analytical modifications thereto. In flight testing it is impossible to treat the airframe and engine as separate entities; they are both parts of an integrated system. Thus, when addressing any differences between flight test data and predicted air vehicle system performance (as is the topic of Section 7), as well as determining whether any transient effects would affect either data set, knowledge of the capabilities and characteristics of not only the engine Altitude Test Facility, but also the wind tunnel, must be considered.

5.3.1 Wind Tunnel Capabilities: The air vehicle configuration development process is long and arduous (approaching, but not quite as long as the engine development). The initial configuration resulting from mission requirements, manufacturer's databases, and computational fluid dynamics (CFD) is refined and incrementally improved as the result of test data obtained in fairly small, comparatively inexpensive wind tunnels. As the configuration matures, higher quality and absolute (rather than incremental) data are required to more accurately define the configuration aerodynamic performance, the throttle-dependent effects, inlet performance characteristics, and to predict full-scale integrated system performance. This requires larger scale models to improve model fidelity, as well as to maximize Reynolds number (which could also be achieved at higher operating pressure and/or lower temperature as in the NTF at NASA Langley Research Center). Naturally, larger models require larger wind tunnels to minimize wind tunnel blockage and wall effects. Typical examples and operating envelopes of large, state-of-the-art, wind tunnels, where the Engineering and Manufacturing Development (EMD) wind tunnel testing has been done for many modern weapon systems, are presented in Reference 5.6 (a catalog of Wind Tunnel Facilities). The uncertainty in free-stream test conditions at steady-state operating conditions for one typical facility is given in Figure 31. These uncertainties are quite low and are the result of (extremely accurate) instrumentation and tunnel calibration uncertainty, including the scatter in data due solely to the wind tunnel dynamics at "steady" conditions. Not included are any model configuration-dependent effects resulting from model/wall mutual interference which may become significant (particularly in the transonic speed range) when the model cross-section area exceeds 0.2 to 0.5% of the tunnel cross-section area.

5.3.2 Wind Tunnel Operating Characteristics: Except for a very few special cases, wind tunnels are designed to operate at steady-state conditions. In closed-circuit wind tunnels, any perturbation to the flow anywhere in the circuit has the potential for changing the test section free-stream conditions. (An exception would be to a solid wall supersonic tunnel where for sufficient pressure ratio across the nozzle the Mach number is a function only of the nozzle area ratio. An additional consideration is that the free-stream gas properties are also a function of the supply, or stagnation conditions.) For example, changing the test model attitude changes the flow over the model which changes the total test section drag (which is reflected as test section pressure loss) which, in turn, can change the tunnel pressure ratio and, therefore, the free-stream Mach number and/or pressure altitude. Thus, wind tunnel data typically are acquired only when the set tunnel conditions are within a fairly small, predefined band about the nominal desired conditions, and the rate of change in conditions is quite low.

SAENORM.COM : Click to view the full PDF of air5020a

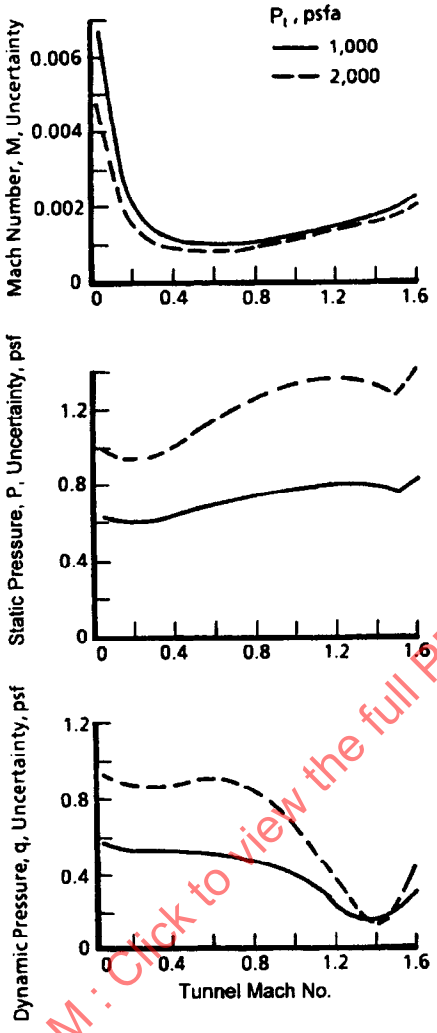

FIGURE 31 - AEDC Tunnel 16T Uncertainty in Free-Stream Test Conditions

5.3.2 (Continued):

Operation of each wind tunnel is a unique function of that respective facility. The mode of control of test conditions varies with the range of condition, e.g., in the AEDC Tunnel 16T there are four uniquely different methods of setting Mach number. The method used depends upon the desired Mach number. Test condition rate of change in Tunnel 16T (which is fairly slow because of the tunnel size) varies, depending upon the specific condition, but is on the order of 0.05 to 0.1 M per min, 1 psi per min for total pressure, and 0.5 to 3 °F per min for stagnation temperature. During a Mach number change, it is almost impossible to maintain pressure altitude, and during a pressure altitude transient, Mach number will vary. Even recognizing that the rate of change of conditions is a strong function of the size (or inertia) of a tunnel, one can see that real-time transient operation of a wind tunnel is not a practical method to obtain the effects of transients on the vehicle aerodynamics or throttle-dependent forces.

SAENORM.COM : Click to view the full PDF of air5020a

5.3.2 (Continued):

In addition to the above, another complicating factor in obtaining usable transient data in wind tunnels is the fact of the subscale wind tunnel models and the rate of change required for a model transient to simulate a full-scale vehicle transient. For any given transient event, the scaled model time (t_{Mod}) increment is related to the full-scale time (t_{FS}) increment by:

$$t_{Mod} = K_S * t_{FS} \quad \text{(Eq.13)}$$

where:

K_s = (model scale) x (flight temperature/wind tunnel temperature)$^{1/2}$

Thus, assuming the temperature ratio to be near 1.0, a wind tunnel-simulated transient must be accomplished in the flight transient time multiplied by the model scale (a value which, for large wind tunnels, is typically in the 0.05 to 0.20 range for manned air vehicles, and 0.2 to 1.0 for air-breathing missiles). Thus, while wind tunnel model attitude variations occur at maximum rates of only about 0.1 to a maximum of 5 deg/s, depending upon the specific support system and model mass, an air vehicle pitch rate of 20 deg/s would require a 10% model pitch rate of 200 deg/s to simulate the transient. Also, to simulate an attitude change in the wind tunnel would require that the model center of rotation be at the simulated vehicle center-of gravity location, which presently is extremely difficult and would be quite expensive for most test installations. Clearly, simulating a transient like this would be impractical, if not physically impossible. (It might be possible to determine the approximate magnitude of the effects of a pitch transient on performance data using dynamic stability testing techniques, but that has not yet been demonstrated for performance data where the uncertainty requirements are much stricter.)

5.4 Flight Test Facilities:

Flight test facilities provide the final integration of airframe and engine for evaluation of overall system performance. The objective is to combine the thrust and drag characteristics measured from gound-based facilities with in-flight measurements of system operating conditions to verify that the engine and airframe meet performance requirements throughout the envelope. Although the flight environment is not easily controlled for systematic test evaluations, the atmospheric and operational disturbances experienced in flight cannot be readily simulated in ground or wind tunnel facilities. This is a particularly important factor for evaluations at dynamic flight conditions where external forces and the inlet flow field are continually changing.

Full-scale evaluations of new propulsion systems are also conducted using flight test aircraft. These aircraft may be production vehicles for engine upgrade programs, or prototype of new aircraft (Figure 32). Because most dedicated propulsion flight test aircraft are multi-engine platforms, little risk is involved when exploring new concepts. Their complexity and cost vary, based on the goals and requirements of the experiment. The primary advantage of flight test aircraft is that they provide a real environment to evaluate new propulsion concepts, modifications, or improvements.

SAENORM.COM : Click to view the full PDF of air5020a

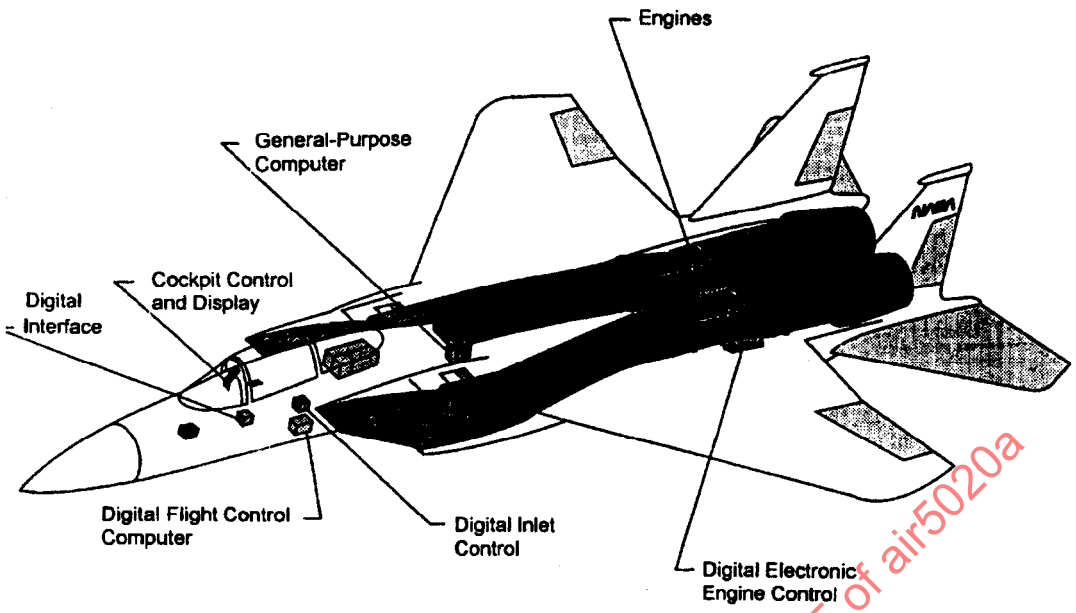

FIGURE 32 - Features of a Flight Research Facility

5.4 (Continued):

A separate class of flight test aircraft is the "flying test bed." This consists of specially modified aircraft to conduct propulsion research experiments. In particular, they provide a means for evaluating installed thrust during actual flight. The gas path thrust determination methods (see 4.1) are commonly used to determine F_{IPF} during quasi-steady flight conditions. If the vehicle drag characteristic is well known for the test bed, it can be used at stabilized flight conditions to verify F_{IPF} values. Excess thrust methods can also be utilized in flight if the aircraft is equipped with accelerometers. Essentially, the change in thrust due to a throttle change is directly measurable with the determination of excess thrust. Detailed examples of this flight test technique are presented in Section 7.

5.5 Summary:

Ground-level propulsion test facilities have established measurement systems and practices to quantify engine time-variant performance and to provide the most accurate means for correlation of engine operational parameters to time-variant measured thrust which include snap power transients to determine engine time-to-thrust, thrust droop, and thrust overshoot. Sea-level test facilities are typically limited to engine power time-variant performance evaluations at ambient test conditions, while altitude test facilities provide this capability over the entire engine operational envelope with some additional capability for environmental transient engine testing. For environmental testing, altitude facilities can track pressure altitudes for most aircraft flight scenarios within 100 ft. Altitude facility airflow temperature rate change capability is typically on the order of 1/2 to 3 deg/s. There are, however, test techniques that use liquid air or heated air injection which enable higher temperature ramp rates to be obtained for smaller thrust class engines.

SAENORM.COM : Click to view the full PDF of air5020a

5.5 (Continued):

Aircraft sea-level tie-down facilities offer the opportunity to rapidly and inexpensively track the behavior of an in-flight thrust measurement system as well as the opportunity to check various engine installation sensitivities such as aircraft bleed and power extraction. Absolute levels of installed thrust, however, are normally questionable due to unquantifiable induced aircraft and cell forces. Tie-down facilities are useful for the validation of installed thrust transients where the absolute level of thrust is not critical to the evaluation. In general, differences between the in-flight thrust measurement system prediction and cell measured force is considered to be "cell factor."

Aerodynamic model test (wind tunnel) facilities use reduced-scale airframes and engine propulsion simulators to bookkeep both drag and throttle-dependent aerodynamic forces required to determine net propulsive force. Except for a very few special cases, aerodynamic test facilities are designed to operate at steady-state test conditions. With the exception of high "g" aircraft maneuvers (which are considered impractical for simulation in wind tunnels), transient environmental simulation was not determined to be required to quantify conventional aircraft external aerodynamic performance.

Flight test facilities provide the capability to evaluate overall airframe and engine system performance operating in the real flight environment, or near-real flight environment in the case of flight test beds. With today's hardware and software technology advances, flight test beds are capable of acquiring and processing aircraft and engine time-variant operational measurements to provide near real-time net propulsive time-variant thrust.

The general capabilities of test facilities to support time-dependent in-flight thrust determinations are summarized in Table 3.

SAENORM.COM : Click to view the full PDF of air5020a

TABLE 3 - Summary of Test Facility Simulation and Transient Capabilities

Simulation Parameter	Facility Capability Propulsion Ground Stand	Facility Capability Propulsion Altitude	Facility Capability Aerodynamic Wind Tunnel	Facility Capability Aircraft Ground Stand	Facility Capability Aircraft Flight
Aircraft Configuration	Inlet Flow Simulators	Inlet Flow Simulators	Scale Models	Full Scale	Full Scale
Aircraft Attitude, α, β	Inlet Distortion ($d\alpha$, $\beta/dt = 0$)	Inlet Distortion ($d\alpha$, $\beta/dt = 0$)	Flight Envelope ($d\alpha$, $\beta/dt = 0$)	α, $\beta = 0$ ($d\alpha$, $\beta/dt = 0$	Flight Envelope ($d\alpha$, β/dt = Duplicated)
Flight Mach No, M	Sea-Level Static ($dM/dt = 0$)	Engine Envelope (dM/dt = Limited)	Flight Envelope ($dM/dt = 0$)	Sea-Level Static ($dM/dt = 0$)	Flight Envelope (dM/dt = Duplicated)
Flight Altitude, H	Ambient ($dH/dt = 0$)	Engine Envelope (dH/dt = Simulated)	Flight Envelope ($dH/dt = 0$)	Ambient ($dH/dt = 0$)	Flight Envelope (dH/dt = Duplicated)
Engine Configuration	Full Scale	Full Scale	Inlet/Exhaust Simulators	Full Scale (Installed)	Full Scale (Installed)
Engine Power Lever Angle, PLA	Duplicated ($dPLA/dt$ = Duplicated)	Duplicated ($dPLA/dt$ = Duplicated)	Inlet/Exhaust Simulation ($dPLA/dt = 0$)	Duplicated ($dPLA/dt$ = Duplicated)	Duplicated ($dPLA/dt$ = Duplicated)

SAENORM.COM : Click to view the full PDF of air5020a

6. TEST DATA ACQUISITION SYSTEMS:

For the purpose of acquiring test data, measurement systems are classified as steady-state, transient, or high-response in accordance with the frequency response requirements.

A steady-state measurement system is one in which the measurement signal can be time averaged, whereas a transient measurement system signal can be averaged only over increments of time sufficiently small to define the time-variant behavior characteristics. A dynamic measurement system is one in which the spectral characteristics of the measurement system signal are required. In discussing the material in this report, the general frequency guidelines used to characterize measurement systems are typically:

a. Steady-State System - 0 to 0.2 Hz
   Based on multiplex pressure valve settling times with minimal (50 ft of 1/8-in) line volume.
b. Transient System - 0 to 40 Hz
   Based on 5 samples/s (sps) requirement for accurate reconstruction of periodic (sinusoidal) signals and general practice of acquiring data at 200 sps. Measurement probe/ device response may limit this bandwidth to lower frequencies.
c. High-Response System - 0 to 20,000 Hz

These different operating frequency ranges have a significant influence on the measurement sensor, transducer, and data acquisition system design. For in-flight thrust determination, measurement of the higher frequencies associated with high-response systems is not required; therefore, measurement system discussions in this section are limited to transient systems (i.e., < 40 Hz).

6.1 In-Flight Thrust Measurement:

Flight test aircraft are unique because of the special instrumentation installed to evaluate the propulsion and inlet systems. In each case, the aircraft are modified to incorporate flight test instrumentation, data processing, recording, and telemetry systems. Current flight test data systems have the capability to handle in excess of 3,000 parameters from a combination of Frequency Modulation (FM), Pulse Code Modulation (PCM), 1553 Mux (Reference 6.1), and digital control sources.

Engine instrumentation typically includes gas path pressures, temperatures, rotor speeds, fuel flows, variable geometry, and control system parameters. These are routinely processed at sampling rates up to 20 sps but for dynamic events are increased up to 500 sps . Figure 33 illustrates the typical engine instrumentation for flight test.

The airborne instrumentation system is shown in Figure 34. This usually includes a PCM system which provides a high-speed digital stream of the engine and airframe parameters. The PCM signal is then recorded on the airborne tape recorder and transmitted via telemetry to the ground station. A separate FM data system is frequently used for high-response instrumentation.

SAENORM.COM : Click to view the full PDF of air5020a

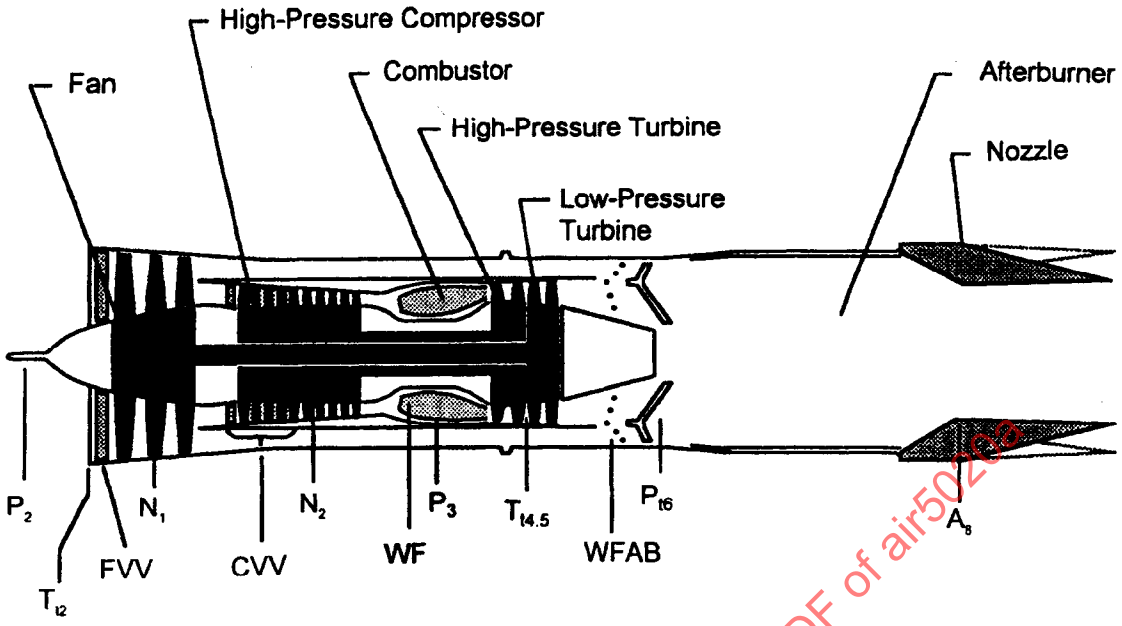

FIGURE 33 - Typical Flight Instrumentation Measurements on a Turbofan Engine

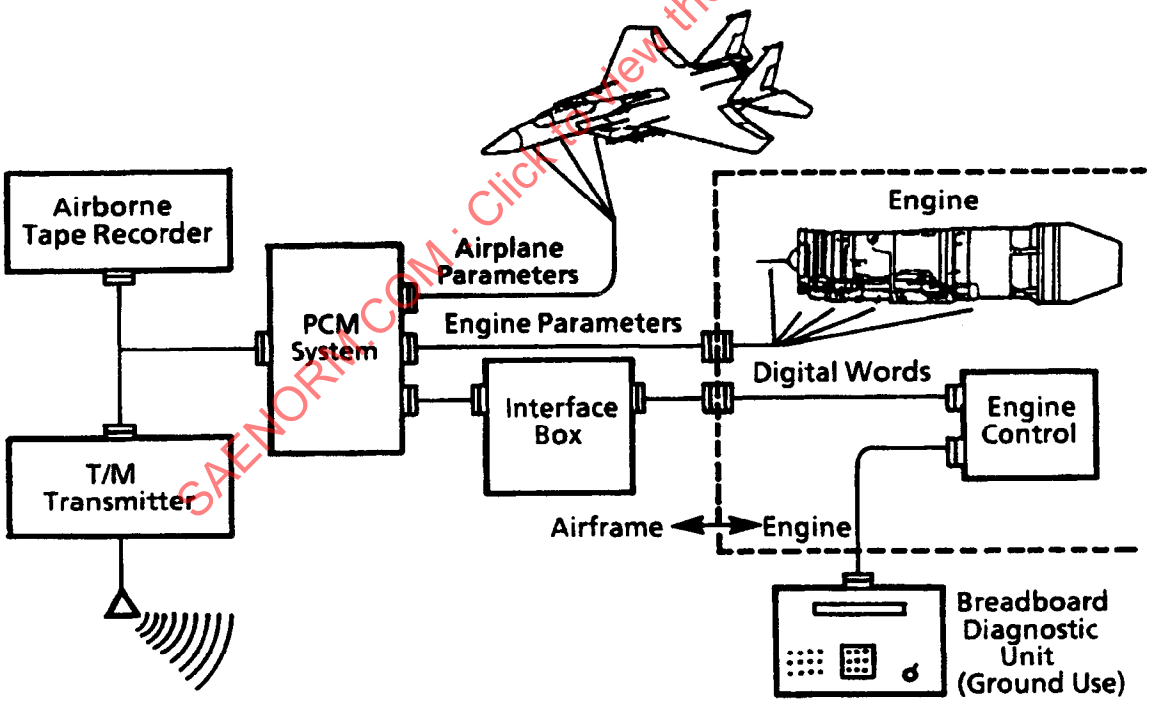

FIGURE 34 - Instrumentation System

SAENORM.COM : Click to view the full PDF of air5020a

6.1 (Continued):

Figure 35 shows the real-time data system, including the ground station. The ground station receives the aircraft telemetry signal, processes the PCM signal into engineering units, and drives the real-time displays in the mission control room. These displays typically consist of cathode ray tubes, stripcharts, X-Y plotters, and digital listings. Similar ground stations are used for posttest processing of the airborne data tape for generation of the final test data.

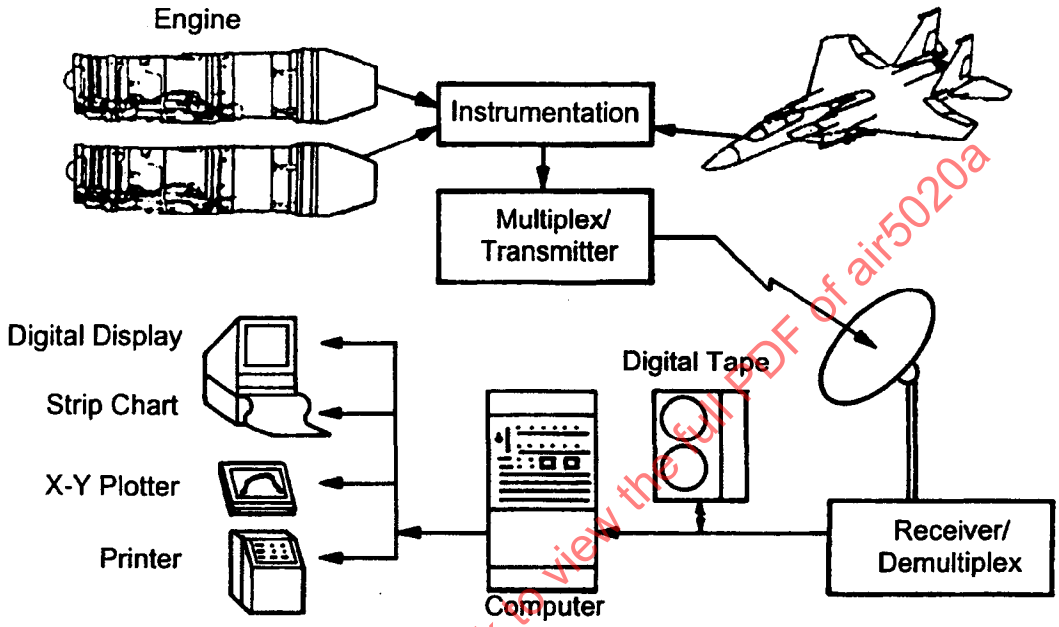

FIGURE 35 - Example of a Real-Time Data System

In this section the instrumentation required for the In-Flight Transient Thrust Methods of Section 4 are specified. For instance, the Gas Path Method requires a different set of engine instrumentation in flight to maximize the data accuracy than the instrumentation required for the transient simulations. In either case, the flight test instrumentation should be installed on the engine during ground tests to calibrate the methods for flight test.

6.1.1 Gas Path Methods: Instrumentation requirements for in-flight thrust determination depend on the flight test analysis method chosen. Each engine has its own unique set of parameters that should be measured or inferred in flight in order to provide the information necessary to calculate net thrust. For instance, nozzle throat area is constant on some engine configurations, whereas other configurations have variable areas. In another case, fan inlet pressure is often inferred from inlet rig data correlation to other measured parameters. The fundamental parameters required for each method must be measured or inferred through correlation. Instrumentation that increases data validation or accuracy of the in-flight thrust is optional. The sensitivity of the methods to the optional instrumentation will vary for each engine configuration.

SAENORM.COM : Click to view the full PDF of air5020a

6.1.1 (Continued):

Table 4 summarizes the typical instrumentation installed on the engine and aircraft for analysis with the gas path methods. The thrust parameter (F/AP) and specific thrust parameter ($F/W\sqrt{T}$) methods are the same gas path methods discussed in AIR1703 (Reference 1.1). The Simplified Net Thrust Method (SNTM) in Table 4 is described in more detail in 4.1.2.

TABLE 4A - Typical Gas Path Methods Instrumentation
(Nonafterburning Engine with Constant Area Exhaust Nozzle)

Parameter Name	F/AP	$F/W\sqrt{T}$	SNTM
Aircraft:			
Altitude	X	X	X
Mach No	X	X	X
Fan Inlet Pressure	X	X	--
Free-Stream Total Temperature	X	X	--
Engine Bleed Extraction	(optional)	X	--
Engine Power Extraction	(optional)	(optional)	--
Power Lever Angle	X	X	--
Time	X	X	X
Engine:			
Fan Speed	X	X	--
Fan Variable Vane Position	(optional)	(optional)	--
Main Burner Fuel Flow	--	X	--
Turbine Discharge Total Pressure[1]	X	X	X
Nozzle Exit Static Pressure	(optional)	(optional)	--
Nozzle Inlet Static Pressure	--	--	X
Exhaust Gas Temperature	--	--	X

[1] Required to acquire nozzle entrance pressure, utilizing upstream measurements of core and/or duct pressure at the mixing plane location.

TABLE 4B - Typical Gas Path Methods Instrumentation
(Nonafterburning Engine with Variable Area Exhaust Nozzle)

Parameter Name	F/AP	$F/W\sqrt{T}$	SNTM
Aircraft:			
Altitude	X	X	X
Mach No	X	X	X
Fan Inlet Pressure	X	X	--
Free-Stream Total Temperature	X	X	--
Engine Bleed Extraction	(optional)	X	--
Engine Power Extraction	(optional)	(optional)	--
Power Lever Angle	X	X	--
Time	X	X	X
Engine:			
Fan Speed	X	X	--
Fan Variable Vane Position	(optional)	(optional)	--
Main Burner Fuel Flow	--	X	--
Turbine Discharge Total Pressure[1]	X	X	X
Nozzle Throat Area	X	--	--
Nozzle Area Ratio	(optional)	--	--
Nozzle Exit Static Pressure	--	--	--
Nozzle Inlet Static Pressure	--	--	X
Exhaust Gas Temperature	--	--	X

[1] Required to acquire nozzle entrance pressure, utilizing upstream measurements of core and/or duct pressure at the mixing plane location.

SAENORM.COM : Click to view the full PDF of air5020a

TABLE 4C - Typical Gas Path Methods Instrumentation
(Afterburning Engine with Variable Area Exhaust Nozzle)

Parameter Name	F/AP	$F/W\sqrt{T}$	SNTM
Aircraft:			
Altitude	X	X	X
Mach No	X	X	X
Fan Inlet Pressure	X	X	--
Free-Stream Total Temperature	X	X	--
Engine Bleed Extraction	(optional)	X	--
Engine Power Extraction	(optional)	(optional)	--
Power Lever Angle	X	X	--
Time	X	X	X
Engine:			
Fan Speed	X	X	--
Fan Variable Vane Position	(optional)	(optional)	--
Main Burner Fuel Flow	--	X	--
Augmentor Inlet Total Pressure	X	X	X
Augmentor Inlet Static Pressure	--	--	X
Augmentor Fuel Flow	--	X	--
Exhaust Nozzle Inlet Static Pressure[1]	--	--	X
Nozzle Throat Area	X	--	--
Nozzle Area Ratio	(optional)	(optional)	--
Nozzle Exit Static Pressure	(optional)	(optional)	--
Turbine Exit Gas Temperature	--	--	X

[1] Required to acquire nozzle entrance pressure, utilizing upstream measurements of core and/or duct pressure at the mixing plane location.

6.1.2 Transient Simulation Methods: In transient simulations, the flight test data are evaluated as a function of time, rather than the instantaneous point-by-point basis with the conventional gas path methods. The advantage of the simulation is the ability to account for time-variant effects such as rotor acceleration and thermal effects on component performance. The result is that secondary effects on nozzle gas flow and entrance temperatures are addressed in the thrust estimate.

There are two different approaches to estimate in-flight thrust with an aerothermodynamic transient simulation during postflight data processing. The basic approach determines nozzle gas flow, nozzle entrance temperature, and nozzle coefficients based on similar instrumentation requirements to the Gas Path Methods (see Table 5, Aero Model Input Type 1). An alternative approach is to rely on the accuracy of the simulation thermodynamics to estimate thrust based on measured engine control actuator and valve positions (see Table 5, Aero Model Input Type 2). The difference between the two approaches is the degree to which the simulation thermodynamics are relied upon to estimate in-flight thrust.

Real-time analysis during the flight test can be accomplished with the Simplified Linear Model (SLM). Table 5 summarizes the typical instrumentation installed on the engine and aircraft for analysis with the transient simulation methods.

SAENORM.COM : Click to view the full PDF of air5020a

TABLE 5A - Transient Simulation Method Instrumentation
(Nonafterburning Engine with Constant Area Exhaust Nozzle)

Parameter Name	Aero Thermo Model (Type 1)	Aero Thermo Model (Type 2)	SLM
Aircraft:			
Altitude	X	X	X
Mach No	X	X	X
Fan Inlet Pressure	X	X	X
Free-Stream Total Temperature	X	X	X
Engine Bleed Extraction	(optional)	X	(optional)
Engine Power Extraction	(optional)	(optional)	(optional)
Power Lever Angle	--	X	--
Time	X	X	X
Engine:			
Fan Speed	X	--	X
Fan Variable Vane Position	(optional)	--	(optional)
High Pressure Compressor Speed	--	--	X
HPC Variable Vane Position	--	--	(optional)
Main Burner Fuel Flow	X	X	X
Turbine Discharge Total Pressure[1]	X	--	--
Nozzle Exit Static Pressure	(optional)	(optional)	(optional)

[1] Required to acquire nozzle entrance pressure, utilizing upstream measurements of core and/or duct pressure at the mixing plane location.

TABLE 5B - Transient Simulation Method Instrumentation
(Nonafterburning Engine with Variable Area Exhaust Nozzle)

Parameter Name	Aero Thermo Model (Type 1)	Aero Thermo Model (Type 2)	SLM
Aircraft:			
Altitude	X	X	X
Mach No	X	X	X
Fan Inlet Pressure	X	X	X
Free-Stream Total Temperature	X	X	(optional)
Engine Bleed Extraction	(optional)	X	(optional)
Engine Power Extraction	(optional)	(optional)	(optional)
Power Lever Angle	--	X	X
Time	X	X	X
Engine:			
Fan Speed	X	--	X
Fan Variable Vane Position	(optional)	X	(optional)
High Pressure Compressor Speed	--	X	X
HPC Variable Vane Position	--	--	(optional)
Main Burner Fuel Flow	--	X	--
Turbine Discharge Total Pressure[1]	X	--	--
Nozzle Throat Area	X	X	X
Nozzle Area Ratio	(optional)	X	X
Nozzle Exit Static Pressure	(optional)	(optional)	(optional)

[1] Required to acquire nozzle entrance pressure, utilizing upstream measurements of core and/or duct pressure at the mixing plane location.

SAENORM.COM : Click to view the full PDF of air5020a

TABLE 5C - Transient Simulation Method Instrumentation
(Afterburning Engine)

Parameter Name	Aero Thermo Model (Type 1)	Aero Thermo Model (Type 2)	SLM
Aircraft:			
Altitude	X	X	X
Mach No	X	X	X
Fan Inlet Pressure	X	X	X
Free-Stream Total Temperature	X	X	(optional)
Engine Bleed Extraction	(optional)	X	(optional)
Engine Power Extraction	(optional)	(optional)	(optional)
Power Lever Angle	--	X	X
Time	X	X	X
Engine:			
Fan Speed	X	--	X
Fan Variable Vane Position	(optional)	--	(optional)
High Pressure Compressor Speed	--	--	X
HPC Variable Vane Position	--	--	(optional)
Main Burner Fuel Flow	--	X	--
Augmentor Inlet Total Pressure[1]	X	--	--
Augmentor Fuel Flow	--	X	--
Nozzle Throat Area	X	X	X
Nozzle Area Ratio (optional)	X	X	
Nozzle Exit Static Pressure	(optional)	(optional)	(optional)

[1] Required to acquire nozzle entrance pressure, utilizing upstream measurements of core and/or duct pressure at the mixing plane location.

6.1.3 Excess Thrust Measurement Methods: The excess thrust method of in-flight thrust determination does not rely on any engine instrumentation, but on the measurement of excess thrust via methods described in 7.3 and lift coefficient. These data are then used with a predefined drag polar to infer changes in net propulsive force. Table 6 gives typical instrumentation required for the application of this thrust determination method.

TABLE 6 - Excess Thrust Measurement Method Instrumentation

Parameter	Flight Path Accelerometer, FPA Method	Body Axis Accelerometer, BAA Method	Energy Method
Longitudinal Acceleration	X	X	--
Lateral Acceleration	--	X	--
Normal Acceleration	X	X	--
Angle of Attack	--	X	--
Angle of Sideslip	--	X	--
Angular Rates	X	X	--
Angular Accelerations	--	X	--
Aircraft Weight	X	X	X
Altitude	X	X	X
Airspeed/Mach Number	X	X	X
Ambient Temperature	--	--	X
Time	X	X	X

SAENORM.COM : Click to view the full PDF of air5020a

6.2 Ground and Flight Test Facility Measurements:

This section presents the approaches used in ground propulsion test facilities and flight test beds to measure engine transient performance, and is based on material contained in Reference 5.1.

The current practice for transient test and evaluation is to use quasi-steady relationships (and where possible, measurements) for most parameters of interest, i.e., airflow and thrust. The same measurement principles used to acquire steady-state performance data are used to acquire transient data for operability analysis. To avoid or compensate for unnecessary instrument lags, some special practices or steps are taken.

The second-order or time-dependent effects are considered for each individual measurement or relationship. Some of the more common considerations and methods for measurement response compensation are discussed in the following subsections.

6.2.1 Engine Thrust/Force Measurement: With the direct-connect installation used in propulsion altitude test facilities, engine thrust is most often determined using an external force balance technique (Figure 36).

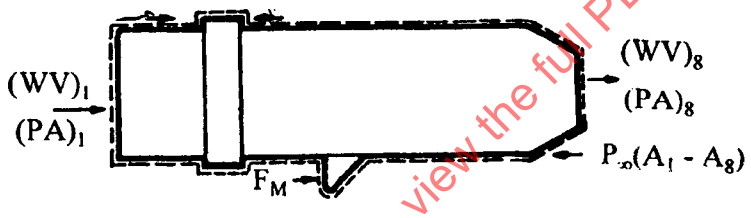

FIGURE 36 - Thrust Stand Force Balance for a Planar Nozzle Engine

$$W_1V_1 + P_1A_1 = W_8V_8 + P_8A_8 + P_\infty(A_1 - A_8) - F_M \qquad \text{(Eq.14a)}$$

and the definition of gross thrust (F_G) is

$$F_G = W_8V_8 + A_8(P_8 - P_\infty) \qquad \text{(Eq.14b)}$$

With this technique, the determination of gross thrust,

$$F_G = W_1V_1 + F_M + A_1(P_1 - P_\infty) \qquad \text{(Eq.14c)}$$

requires measurement of all body forces acting through the engine mounts. The measurement of a portion of these body forces, F_M, is accomplished with the thrust stand. For axisymmetric exhaust nozzles, a conventional, single-component thrust stand is adequate for the measurement of forces generated along the engine centerline. The quasi-steady expression for gross thrust, (Equation 14c), and the corresponding quasi-steady assumptions of steady, level, nonaccelerating flight are used to determine transient gross thrust.

SAENORM.COM : Click to view the full PDF of air5020a

6.2.1 (Continued):

The application of thrust vectoring to military aircraft propulsion systems necessitates the measurement of multiple force components and requires special consideration be given to the thrust stand. A multicomponent thrust measurement system is illustrated in Figure 37.

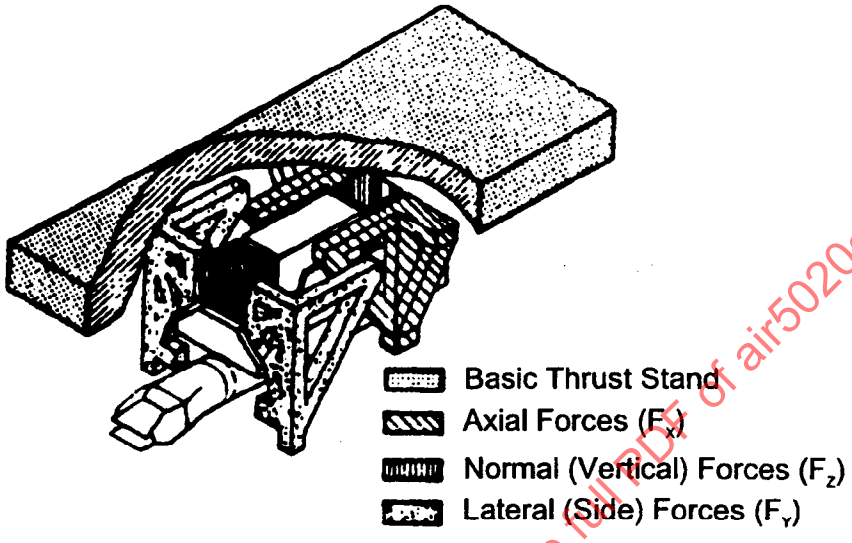

FIGURE 37 - Multi-Axis Thrust Stand

Measurement of transient forces in the vertical and side axes, F_Z and F_Y, respectively, allows the effective vertical vector angle, α_{eff} and effective side vector angle, β_{eff} to be determined using

$$\alpha_{eff} = TAN^{-1} F_z / F_G \quad \text{(Eq.15)}$$

$$\beta_{eff} = TAN^{-1} F_y / F_G \quad \text{(Eq.16)}$$

Transient thrust stand response and force measurement capabilities have been evaluated and found to require no transient response compensation. However, thrust stand force measurements are usually low-pass filtered at 10 Hz to eliminate stand natural frequencies from the data. The response and acquisition of the pressure measurements used to quantify the airflow and pressure area terms of Equation 14 should be consistent with the force measurement system response and data acquisition in order to obtain matched response characteristics.

6.2.2 Engine Total Airflow Measurement: Three methods for transient engine total airflow are generally used for operability testing in the Altitude Test Facility. Any method employed must consider the change of mass within the control volumes from the point of measurement to the engine inlet, referred here as duct capacitance, and described by Equation 17.

$$dW_{cv} / dt = (d\rho / dt)(v_{cv}) \quad \text{(Eq.17)}$$

SAENORM.COM : Click to view the full PDF of air5020a

6.2.2 (Continued):

The time-dependent effects resulting from the mass storage or duct capacitance for a direct-connect altitude facility installation are most often minimized by using a calibrated bellmouth calculation. The bellmouth measurement eliminates the contribution of plenum capacitance, leaving only the effect of inlet duct capacitance. The capacitance of the inlet ducting is directly related to the installation configuration, but current practice generally limits the length of the inlet ducting to about 3 times the duct diameter. Based on representative idle-to-intermediate snaps in typical regions of maximum airflow changes, the time-dependent effects are of a second-order nature (Figure 38) and are therefore typically not accounted for in transient total engine airflow and transient thrust calculations.

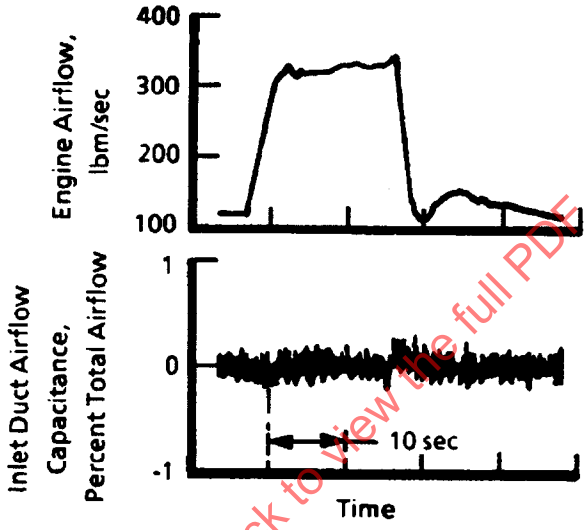

FIGURE 38 - Inlet Duct Mass Capacitance

There are basically two airflow measurement techniques available in flight to determine engine transient airflow rates: engine inlet duct/engine face measurements, and engine fan or low-pressure compressor flow mapping.

1. Engine flow measurements can be made indirectly by using inlet/engine face pressure rakes. This is the most difficult method of determining airflow in flight and has the advantage of accounting for inlet distortion and pressure recovery variations.

2. Fan rotor speeds and airflow relationships (maps) can be used to estimate airflow. For transient use, modified fan speed-airflow characteristics must be determined that account for the transient operating line effects of blade clearance of the fan blades and vanes. The slope of the corrected fan speed lines on the map must be considered. In addition, correction factors to account for varying bypass airflow during the transient must be accounted for, as well as the effects of accelerating versus decelerating fuel-air ratio schedules.

SAENORM.COM : Click to view the full PDF of air5020a

6.2.3 Engine Local Airflow Measurement: The concept of determining local Mach number, and thereby local airflow was explored during the late 70's as part of the Air Force-sponsored "Non-Recoverable Stall" program and during the early 80's as part of a NASA Energy Efficient Engine program. These efforts led to the development of Mach probes which have seen increasing use during altitude test programs. The Mach probes also provide a means for determining compressor post-stall performance and operating characteristics, as well as a method for quantifying compressor operating conditions at stall onset, i.e., stall line definition.

The Mach probe (Figure 39) operates on a relationship of forward and aft facing total pressure taps to local flow conditions. The operating principle is that the forward probe measures free-stream total pressure, and the aft probe measures a pressure which is indicative of free-stream static pressure.

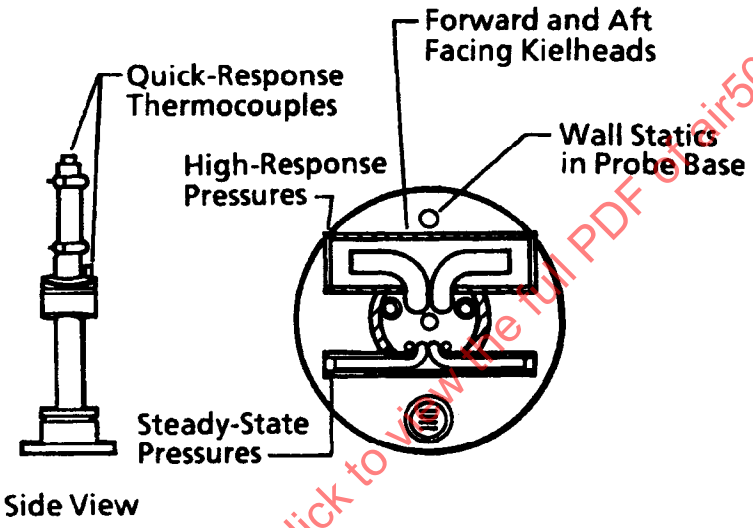

FIGURE 39 - Mach Probe

Mach number is related to the measured pressures through isentropic relationships,

$$M = \sqrt{\frac{2}{\gamma - 1}\left\{\left[1 - \frac{1}{C_D}\left(\frac{P_{t,fwd} - P_{t,aft}}{P_{t,aft}}\right)\right]^{\frac{1-\gamma}{\gamma}} - 1\right\}} \qquad \text{(Eq.18)}$$

$$\frac{W\sqrt{\theta}}{\delta} = C_f\sqrt{\frac{\gamma}{R}}\left[\frac{M}{1 + \frac{\gamma - 1}{2}M^2}\right]\frac{P_{t,STD}}{\sqrt{T_{t,STD}}} \qquad \text{(Eq.19)}$$

SAENORM.COM : Click to view the full PDF of air5020a

.2.3 (Continued):

Data uncertainties associated with Mach probe measurements are partially reduced by using a more accurate steady-state airflow measurement to provide calibration relationships for the airflows indicated by a Mach probe. In the case of the high-pressure compressor of a twin-spool turbofan engine, a choked turbine method of airflow determination often determines the calibration standard. The calibration procedure involves the use of steady-state compressor operating line data. A probe-derived airflow is developed and applied to Mach probe-indicated airflow during the compressor transient of interest. This "calibration" procedure is illustrated in Figure 40.

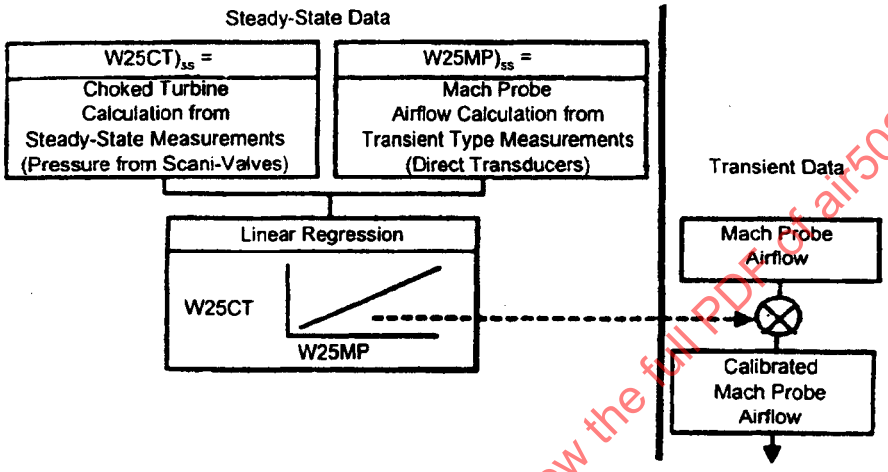

FIGURE 40 - Mach Probe Calibration Procedure

.2.4 Engine Rotor Speeds and Variable Geometry Positions: Engine rotor speeds, compressor variable geometry and power lever positions, and engine exhaust nozzle area are measured with the same devices used to obtain steady-state data and typically require no correction for transient response in the bandwidth of interest.

Engine rotor speed measurements are usually made by measuring the frequency of a magnetic pickup on the rotor or engine generator/alternator. This method is considered highly accurate and requires no time phase shift.

Variable geometry includes fan and compressor guide vanes, nozzle area, and inlet ramp/area. In most cases, a linear variable differential transducer (LVDT) is used to measure variable geometry positions. The accuracy of LVDT measurements can vary, depending on mechanical slippage and the magnitude and nature of the nozzle forcing functions. Nozzle area, for instance, is difficult to measure because of thermal effects, hysteresis, and the complication of error magnification caused by converting a linear measurement to an area measurement.

SAENORM.COM : Click to view the full PDF of air5020a

6.2.5 Engine Fuel Flow: Highly responsive fuel flow meters should be used in transient performance testing. Conventional axial-flow turbine-type volumetric flowmeters are normally used for measurements of transient fuel flow rates. Flowmeters must be sized to the flow rate range of interest to obtain best accuracy. Also, the flowmeter should have adequate signal conditioning to provide a clean signal and still maintain adequate frequency response characteristics and be located as close as possible to the engine to eliminate time phase problems. These type measurements typically do not require corrections for transient response.

6.2.6 Pressure Measurements: Pressure measurements made to track transient engine behavior/operation, whether facility or engine internal, are typically close-coupled to the sense point to reduce attenuation, and to avoid inducing pneumatic lag. The practice of close-coupling measurements generally eliminates the need for signal response compensation. For those cases where this cannot be accomplished, methods for compensating pressure measurements with inadequate response are available. One method commonly used is to conduct pretest checks with known pressure inputs and determine appropriate correction factors. Increased data uncertainties accompany close-coupled pressure measurements because they are generally substitute calibrated as opposed to multiplex pressure valves (steady-state system) which are in-place calibrated against an accurate, traceable standard.

The primary difficulty in obtaining high-frequency pressure measurement is the pressure loss owing to the friction attenuation within the sensing system. Typically, most of the friction loss comes from within the pneumatic tubing used to transmit pressure impulses from the internal engine sensor to the measurement transducer. This characteristic can be minimized by careful design of the pressure tube length and volume. Short line lengths (small volumes) are desirable to reduce attenuation and obtain higher-frequency response characteristics. In some cases it is not practical to close-couple the transducer and sensor due to physical constraints. In this case, the attenuation can be measured by laboratory test or estimated by mathematical models. Whitmore discusses the development and validation of a generic technique derived from the Navier-Stokes equations to accurately predict pneumatic attenuation errors (Reference 6.2).

Because transient engine performance is associated with variable pressure at a given engine station, the use of pressure rakes may be required to achieve desired accuracy. In this case, special attention should be given to line lengths to assure all pressures are of the same time phase. This is particularly important if the sensors are manifolded together.

To provide the best accuracy during transients, high-response transducers are often paired together with steady-state pressure transducers. The steady-state transducer is more accurate during steady-state operation and provides a good reference for the high-response transducer. Because pressure transducers (not sensors) are extremely sensitive to temperature variations, they must be isolated with thermal blankets and/or heaters to maintain a constant thermal environment. In addition, the transducer should be calibrated at its operating temperature.

SAENORM.COM : Click to view the full PDF of air5020a

6.2.7 Temperature Measurements: Internal engine temperatures are critical to the measurement of engine performance. Thermocouples have been, and remain at this time, the most-used temperature technology in the gas turbine engine for the following reasons (Reference 6.3):

a. It is a well understood technology,
b. It is widely available,
c. It is a relatively inexpensive product,
d. The accuracy, while not the highest, is generally acceptable, and
e. The thermocouple ranges can be broad, depending upon the type of thermo-elements chosen.

Generally, aerodynamic and metal temperatures are sensed using the same type thermocouples used in the steady-state testing. In some cases, quick response thermocouples comprised of smaller gauge wire are used.

For either case of isothermal floating reference junctions, universal temperature references are mounted inside the test cell or, if test cell temperatures require, outside the test cell. The signals are then routed out of the cell through ports on the copper conductor. Corrections to the temperature data are made in the same manner as for steady-state data; the reference junction temperature is measured with a resistance temperature device, and the indicated temperature is adjusted to account for the reference temperature.

Corrections for transient lag in the gas path measurements are accomplished using the first-order differential equation

$$T_{t_g} = T_{t_M} + (T_{tc})\left(\frac{dT_{tM}}{dt}\right) \qquad \text{(Eq.20)}$$

where:

T_{tg} = the gas temperature corrected for the thermocouple response
T_{tM} = the measured temperature
T_{tc} = the thermocouple time constant

Thermocouple time constants are available for the most commonly used gauges of thermocouple wire and have been estimated based on NACA TN-3455. It should be noted, however, that temperature measurements are frequently not compensated, i.e., the time-dependent aspects are assumed negligible.

In addition to thermocouples, Resistance Temperature Devices (RTDs) are increasingly being used in the compressor section of the engine because of their high accuracy. RTDs operate on the principle that the electrical resistance of the material is temperature-dependent. The resistance of the metals used as sensing elements usually increases with increasing temperature, whereas commonly used semiconductor materials (such as thermistors) decrease in resistance. RTDs are more accurate than thermocouples but are typically limited to +500 °C, depending upon the materials used to fabricate the transducer.

SAENORM.COM : Click to view the full PDF of air5020a

6.2.8 Aircraft Aerodynamic Forces: The aircraft aerodynamic forces and moment data are obtained from six-component force and/or moment balances installed in the wind tunnel aircraft model(s). Typically, these data are obtained in the vehicle body axis system and are mathematically transformed into the vehicle stability axis system. The direct force and moment measurements are adjusted for tares such as model weight, flow through inlet air momentum, and model base/cavity pressure effects. These data are then modified for the effects of the model support system, model test afterbody geometry and nozzle pressure ratio, model test inlet geometry and mass flow ratio, vehicle center of gravity and trim effects, vehicle excresences and protuberances not modeled, model-to-flight Reynolds number differences, etc. as described in AIR1703.

6.2.9 Accelerometer Measurements: Modern aero-performance analysis methods often rely on highly accurate accelerometer measurements to obtain excess thrust as described in 7.3. A typical body-mounted accelerometer package is co-located with rate gyro and angular accelerometer packages near the aircraft center of gravity. An inertial system combines all of these in one unit while the flight path accelerometer package is mounted on a boom forward of the aircraft away from the angular rate and acceleration measurement locations.

A linear accelerometer package normally consists of three accelerometers configured to independently measure vehicle lateral, longitudinal, and normal accelerations. In the flight path accelerometer package, only longitudinal and normal accelerations are measured. Sensor alignment is critical to sensor accuracy. A special ("fine" ranged) linear accelerometer package is often installed to provide more accurate acceleration measurements over a limited measurement range instead of the full range capability of the aircraft. Table 7 presents ranges and uncertainties for both "coarse" and "fine" measurements used during a typical flight test program (Reference 6.4).

SAENORM.COM : Click to view the full PDF of air5020a

TABLE 7 - Typical Accelerometer Ranges and Uncertainties

Axis	Coarse Range (g's)	Coarse Uncertainty (g's)	Fine Range (g's)	Fine Uncertainty (g's)
Lateral (N_Y)	-1 to +1	±0.11	-0.65 to + 0.65	±0.001
Longitudinal (N_X)	-1 to +1	±0.11	-0.65 to + 0.65	±0.001
Normal (N_Z)	-3 to +8	±0.11	-1 to +3	±0.003

6.3 Data Processing:

Data processing requirements are primarily a function of the thrust measurement methodology selected, the response characteristics of the instrument measurement system, sampling rate capabilities of the data acquistion system, and measurement uncertainty goals. This section contains some of the data processing considerations employed in propulsion test facilities, wind tunnels, and flight test facilities.

6.3.1 Propulsion Test Facility: Digital data acquisition systems are most commonly used in the Altitude Test Facility for acquisition of low-bandwidth data (less than 20 Hz) such as for steady-state performance testing and power and flight condition transient testing. Analog data systems are used in the Altitude Test Facility but are utilized for the acquisition of more dynamic data/phenomena (high frequency/bandwidth) such as time-variant inlet total pressure distortion, investigation of compression system post-stall operating characteristics, and combustion (acoustic) instabilities.

State-of-the-art digital data systems currently in use in the Altitude Test Facility are configured/capable of acquiring an aggregate of 40,000 sps of data. To obtain data with sufficient samples to characterize nonperiodic or random processes in the 20 Hz range requires sample rates as high as 200 sps for each channel of data (i.e., measurement). This will typically allow the acquisition of 200 channels of data for the analysis of engine performance or operating characteristics. Another practice in use is to selectively sample measurements at a rate commensurate with the measurement device's response characteristics. This use of selective sampling requires that data fill techniques be used when calculations are to be made with parameters of different sample rates.

The most critical feature in using transient measurement systems is the selection of an appropriate bandwidth or low-pass cutoff frequency compatible with the test objectives. This selection necessitates that the acquired data has dynamic characteristics which fall below the cutoff frequency and that all data above that frequency can be rejected. One of the more common data filters used in ground tests to filter digital transient data is an auto-regressive software filter of the form:

$$Y_k = CY_{k-1} + (1-C)X_k \qquad \text{(Eq.21)}$$

where:

Y_k = filtered data at the current time step
Y_{k-1} = filtered data from previous time step
X_k = unfiltered data at the current time step
C = filter constant

This filter is frequently employed for transient data processing because of its simplicity and ease of use. A more detailed description of filters, including mathematical derivations and guidelines for proper selection of filter constant, is provided in Reference 6.5.

SAENORM.COM : Click to view the full PDF of air5020a

6.3.2 Wind Tunnel: Because of the fairly rigid wind tunnel balance and model-to-balance attachment coupled with the often noisy and turbulent wind tunnel environment, there is usually a high dynamic component in the model balance (force and moment) analog signals. As a result of this, the balance signals are heavily low-pass filtered to a low, approximately 2 Hz, cutoff frequency. Further filtering may be done on the digitized signal so that virtually all of the dynamic component of a low-frequency (4 to 10 Hz) signal is removed from the data, and considerably more at higher frequencies. It is possible to eliminate this filtering and record the raw signal, but in the past this has resulted in such extreme data scatter, even at steady-state conditions, as to be impractical. Eliminating the analog filtering (or setting a low-pass analog filter cutoff frequency to some value slightly above the maximum frequency of interest) and designing a "notch" digital filter to the specific frequency of interest is a method of acquiring data to determine the time-dependent nature of the model transient aerodynamic performance. However, most large wind tunnel force and moment data have large dynamic components in the 5 to 200 Hz range, and with a 10% scale model, 10 Hz simulates only a 1 Hz full-scale frequency.

Thus, it is apparent that air vehicle transients of interest (for performance measurements) cannot be simulated adequately in wind tunnels (see 5.3.2), and even if they could be simulated, it is doubtful that meaningful measurements could be obtained.

6.3.3 Flight Test Facility: Data processing as defined in this document includes, but is not limited to, signal conditioning, analog and/or digital processing, recording, telemetry, and final data computations. Current, generally acceptable practices of data processing, hardware capacities, data acquisition designs, and the recommendations made in AIR1703 for steady-state thrust are also suitable for transient thrust measurement. For transient thrust measurement, fully digital data acquisition systems may be used; however, special attention should be applied to those time-critical parameters of the thrust calculation. Certain time-critical data will require instrumentation of increased dynamic range and response and associated increased sample rates. Processing of time-critical data will require special hardware and software considerations for accuracy and time correlation.

6.3.3.1 Signal Conditioning: Signal conditioning is herein defined as a series of operations including amplification, filtering, sampling, digitizing, and formatting and is the most important part of data processing for the time-critical data of transient thrust measurement. Sampling method is the most important part of signal conditioning if time correlation is required. Twenty samples per second for engine data and 5 sps for flight condition data are typical rates for steady-state thrust determination. Time-critical data involving transient thrust measurement or flight condition measurement may require sample rates exceeding 200 sps. Sampling rates should be ten times the expected data frequency to ensure accurate signal reconstruction. Presample filtering for noise and antialiasing is a usual practice and may be especially necessary for measurements that contain high-frequency data or noise. Time-critical data are sensitive to the "filtering effects" of signal conditioning and will require careful accounting of overall frequency response to determine change in signal spectral distribution, i.e., phase shifts. (Reference 6.3).

SAENORM.COM : Click to view the full PDF of air5020a

6.3.3.2 Time Correlation: As noted, time correlation problems result from the normal process of signal conditioning. Time correlation problems or phase shifts are minimized by careful design of signal reconstruction methods using filters and sampling techniques. Also, careful design of frame structure by locating individual words (time-critical data) as close together as possible within a frame minimizes phase differences during sampling. Time correlation problems are eliminated or minimized by sample methods such as simultaneous sampling and by signal reconstruction methods using low-pass filters or linear interpolation. Simultaneous sampling is hardware intensive, usually expensive, and represents a significant departure from conventional systems, but is the most ideal for time correlation. Theoretical ideal signal reconstruction is accomplished with a low-pass filter, allowing reasonable interpolation, but requires very careful design to avoid additional phase shifting. Linear interpolation between samples is the most-common method that may only be suitable for transient data if sample rates are sufficiently high. Another option, time tagging, is a software solution for time correlation but is not common and may add to computational lag. Post processing of data to achieve time correlation is a common procedure. This requires estimates of the varying time delays introduced by components of the various data acquisition systems.

6.3.3.3 Final Data Computations: Computational lag or time delay can result from computer hardware limitations and algorithm complexity. Algorithm iteration rate should match the highest input frequency data desired for real-time correlation. Estimates of time delay can be determined and, in some cases, corrected either online or postflight. State-of-the-art systems designed for steady-state thrust determination can accommodate modest growth in input requirements and algorithm complexity. But the added complexity of transient math models or increased instrumentation requirements commonly require that time-delay corrections be applied postflight.

6.4 Measurement Uncertainties:

Measurement uncertainty analysis is the means to identify error sources, their relative magnitude, and limits which then provides a basis for selecting measurement systems and measurement operational procedures. An added advantage of uncertainty analysis is the capability to generate error sensitivity charts. Error sensitivity is the uncertainty propagated to the final result because of a unit uncertainty in the parameter. Error sensitivity charts can be generated by making finite increments in an element, usually through the data reduction program, and determining the percent change in the final parameter (refer to References 6.6 and 6.7 for details). Error sensitivity charts provide two major benefits: they enable the tester: (1) to make pretest estimates of measurement accuracies for a specified level of effort, and (2) to identify the measurement system error sources that can most effectively be worked to improve the test results. Other benefits which can be realized include test matrix optimization and development of automated data quality verification tools tailored to critical parameters. Generation of in-flight thrust error sensitivity charts can be accomplished once the data reduction program, the measurement inputs, and the data presentation format are specified. An example of an error sensitivity chart used in an altitude test facility (Reference 6.8) net thrust determination is shown in Figure 41. The chart abscissa lists the error sources that influence the measurement of the performance parameter and the chart ordinate specifies the level of influence.

SAENORM.COM : Click to view the full PDF of air5020a

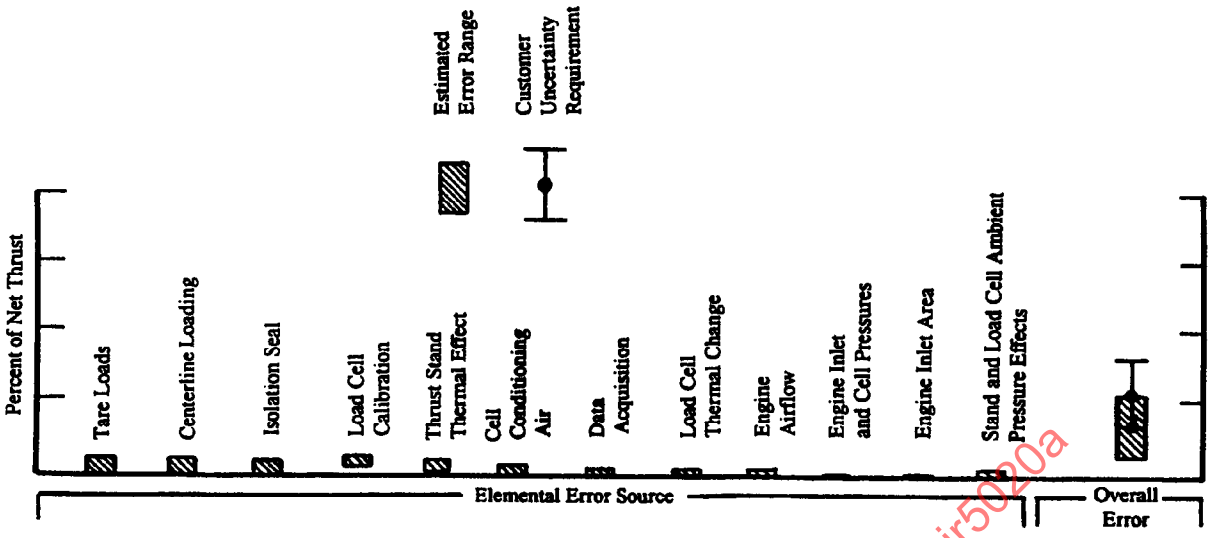

FIGURE 41 - Example of a Thrust Error Sensitivity Chart

6.4 (Continued):

A preflight measurement uncertainty analysis and generation of error charts is essential to programs with limited resources since it reduces the risk of making erroneous decisions. The methodology for estimating steady-state measurement uncertainties is reported in several documents published by major technical organizations (e.g., References 6.6 and 6.7); and the measurement uncertainty considerations for determining steady-state in-flight thrust are reviewed in AIR1678. The methodology for estimating time-variant measurement uncertainties, however, is not established and requires development of an industry-accepted methodology for comparing the measured value in time with the true value in time. A transient uncertainty methodology which uses a transient adder to the steady-state uncertainty value has recently been reported in Reference 6.4. The concept of using an adder to the steady-state value is ideal from an engineering application standpoint. Establishing error analysis techniques for time-variant functions can be a complex issue and requires some means of evaluating measurement system factors such as frequency response, amplitude, phase position, roll-off characteristics, mechanical backlash, thermal and mechanical inertia, spatial distribution, and other phenomena. Pressure and temperature measurement system time constants and damped response fidelity can be evaluated by applying known signal input pulses or varying frequency sinusoidal waves. Since absolute, (as opposed to differential) time-variant measured parameters involve both steady-state and time-variant measurement errors, transient measurement uncertainties will be greater than corresponding steady-state values.

SAENORM.COM : Click to view the full PDF of air5020a

6.4 (Continued):

If a time-variant measurement uncertainty methodology is not available, the tester must use steady-state measurement methodology and his experience to predict the additional uncertainties for time-variant effects. However, if the flight test techniques and measurement methods fall within the quasi-steady assumption, as put forth in this document, then application of steady-state measurement uncertainty methodology will provide an accurate first-order estimate of the measurement errors, and the steady-state error sensitivity charts can be used to analyze and evaluate the proposed in-flight thrust determination methods.

The following paragraphs in this section provide an overview of general measurement uncertainty expectations for ground and flight testing.

6.4.1 Propulsion Test Facility: Because of resource and time constraints and the lack of industry accepted transient measurement uncertainty standards, transient measurement uncertainty requirements are not typically specified by test users. Instead, it is assumed that good transient measurement system design and application practices are employed. To quantify an uncertainty level, several altitude engine test programs were reviewed to provide an estimate of both steady-state and transient measurement uncertainties. The transient measurement uncertainty levels identified in this survey were primarily based on measurement frequency response requirements and generally range from 1-1/2 to 2 times the level obtained for steady-state measurements (Table 8).

SAENORM.COM : Click to view the full PDF of ars5002

TABLE 8 - Typical Altitude Facility Instrumentation Uncertainty

Parameter	Uncertainty (U_{95}), percent U = (B +2S) Steady State	Uncertainty (U_{95}), percent U = (B + 2S) Transient <10 Hz
Pressure	±0.1	±0.5
Temperature	(±0.25% Rd + 1.1 °F)	(±0.5% Rd +3.2 °F)
Fuel Flow	±0.5	±1-1.5
Speeds	±0.02	±0.3
Geometry Positions	±1.0	±2.0
Force	±0.4	±0.7
Engine Nozzle Area	±0.7	±1.4

6.4.2 Wind Tunnel: Typically, the wind tunnel environment allows much closer control of independent variables than in flight testing. Also, being a permanent installation permits environmental control of the instrumentation. This combination in turn allows acquisition of extremely accurate data. In the Mach number range from about 0.3 to 1.5, Mach number is known to within 0.003 for most wind tunnels, and the free-stream pressures are accurate to within approximately 0.1% of value (see 5.3.1). Model pressures routinely are measured with accuracies of 0.1% of the instrument full-scale range, and model forces are measured to within 0.25% of full scale. Confidence in data quality is provided by repeat measurements and redundant methods. Consequently, a high-fidelity database of the aircraft model aerodynamic characteristics is acquired before the first flight.

6.4.3 Flight Test Facility: Transient measurement uncertainties are not typically specified for flight tests. Representative measurement uncertainties quoted for steady-state flight testing are presented in Table 9.

TABLE 9 - Typical Flight Test Instrumentation Uncertainty for Steady-State Data

Measurement Type	Uncertainty (U_{95})
Pressure	±0.5%
Temperature	±0.5%
Fuel Flow	±1.0%
Speeds	±0.5%
Control Surface Positions	±2.2 deg or 0.66%
Angular Rate	±1.3%
Angle of Attack	±0.2%
Linear Acceleration	±0.5%
Airspeed	±2 knots
Altitude	±10 ft at sea level
	±40 ft at 40 kft
Engine Nozzle Area	±3.0%

SAENORM.COM : Click to view the full PDF of air5020a

6.5 Summary:

Aircraft and engine instrumentation should be selected to insure adequate acquistion of test data to analyze and validate aircraft in-flight thrust. For instance, the various gas path methods are quite similar in instrument requirements and by adding engine customer bleed airflow, engine fuel flow, and tailpipe static pressure, three gas path methods are available for the independent evaluation of in-flight thrust. The benefit of multiple methods is the added confidence in the results. Also, should instrumentation for either the nozzle area or the engine customer bleed airflow gather erratic data, analysis of the other methods along with aircraft instrumentation can help locate the faulty data. This type of measurement redundancy enables the affected method to be discarded while the unaffected methods can be used for analysis of aircraft characteristics. Redundancy, therefore, should always be added to increase the chances of obtaining adequate data to analyze the aircraft drag polar.

6.5 (Continued):

There is also much commonality in aircraft and engine instrument requirements for gas path and transient simulation methods. The major difference between gas path and transient simulation methods is the time-dependency measurement requirement of the simulation methods (gas path methods require data only at specified times). Time-dependency means that the data acquisition and process requirements for transient simulation methods are significantly greater than gas path methods. Another consideration is that while transient simulations provide more detailed information and account for engine thermal and inertial time effects, these methods are also more expensive to develop and maintain. Therefore, use of aerothermodynamic transient simulation models also requires "cost-effective" considerations.

With respect to the measurement systems, the same measurement practices used to acquire steady-state performance data can generally be used to acquire time-variant data, providing second-order time-dependent effects are accounted. Examples of second-order time-dependent effects include thermocouple time constants and pressure mass storage or duct capacitance corrections.

Careful consideration should be given to the sample rates and response characteristics of the measurement system. The response characteristic of the instrumentation system limits the rate at which the data can be acquired accurately and may limit the methods that can be considered to analyze flight test data. Engine test facilities acquire transient engine performance-type data using low-bandwidth data systems (i.e., less than 20 Hz) with a sampling rate of 200 samples/s. Digital data systems with this capability are well within today's flight test technology and, therefore, data acquistion for in-flight time-variant thrust determinations should not pose a problem. When processing time-dependent data, care is required in the selection of an appropriate bandwidth or low-pass cutoff frequency to ensure compatibility with the thrust measurement system requirements. For this reason, final data filtering may best be accomplished off-line or posttest, thereby ensuring that critical information is recorded.

A time-variant measurement uncertainty methodology has not yet been adopted by industry, but one has recently been proposed in AGARD report AR-320. A steady-state measurement uncertainty analysis will provide a first-order estimate of time-dependent in-flight thrust and will be nearly correct for elemental measurements if the data are obtained within the quasi-steady guidelines specified in this document. Redundancy of in-flight thrust determination methods is also an accuracy issue. It is through closure between different methods that diagnosis and quantification of interaction of factors which influence the determination of time-dependent flight thrust can be resolved, and confidence can be obtained in the aircraft measured drag polars.

Finally, early definition of how in-flight data are to be acquired, processed, reduced, and presented is essential to obtaining an accurate value of in-flight thrust. Through early definition, in-flight thrust methods can be defined, engines can be properly instrumented, measurement error sensitivity charts can be developed, and thrust databases can be compiled as part of the engine and airframe preflight development testing.

SAENORM.COM : Click to view the full PDF of air5020a

7. FLIGHT TESTING:

Flight test in-flight thrust determination procedures were developed in AIR1703 for the quasi-steady-state assumption. As discussed in Appendix C to AIR1703, the flight test methods and procedures used to evaluate in-flight thrust are not limited to steady-state conditions and include quasi-steady-state and aircraft dynamic motion. This section reviews the basic equations, the elements of these equations, and the types of aircraft maneuvers employed for determination of engine thrust and aircraft drag during time-dependent operating conditions. An additional consideration of this section is discussion of the preflight and postflight consistency checks and validation data checks that are done to enhance confidence in air vehicle thrust measurements.

Procedures for investigating and quantifying the uncertainty of in-flight thrust determinations are presented in AIR1678 and discussed in 6.4. Additional confidence in measurement uncertainty values is accomplished through improvement in procedures and equipment, and correction, if possible, of errors which may be identified through analysis of all available information. The potential error sources that may be isolated by test data analysis include those which are caused by: (examples of these error sources are included in AIR1703).

a. Unanticipated instrumentation problems
b. Uncertainty analysis error propagation items that are erroneously excluded, improperly modeled, or inaccurately bounded
c. Ground test facility limitations or test techniques
d. Unplanned changes in engine operating characteristics
e. "Mistakes"

Any potential error sources in the prediction analysis or the flight test results should be identified and resolved. Data confidence is enhanced when two or more methods with relatively weak coupling between input and output are employed and their results compare within expectations. Failure of the predicted uncertainty bands to overlap indicates an error source that must be investigated and resolved.

Most elements of the transient thrust validation process are identical to those discussed in Section 7 of AIR1703 for steady-state in-flight thrust determination. These validation procedures include preflight engine consistency checks, in-flight engine performance analysis, and definition of air vehicle aerodynamic characteristics (drag polar).

Additional procedures applicable to the nonsteady thrust determination include correlation between flight-measured engine transient characteristics and predictions, correlation between thrust and excess thrust measurements for transient throttle maneuvers, and checks against the validity of the quasi-steady assumption.

The following sections illustrate the data validation process using examples that are representative of actual programs.

SAENORM.COM : Click to view the full PDF of air5020a

7.1 Aircraft Performance:

Section 3.1.1 developed the thrust-drag accounting system and basic equations for the fully integrated aerodynamic/propulsion configuration and time-variant aircraft conditions. Assuming the chosen thrust-drag bookkeeping meets the suitability and consistency characteristics for tracking of the integrated propulsion airframe performance throughout the total development program (see 3.1 and Reference 3.1) the ΔD_{INL} and ΔD_{EXH} terms in Equation 3 can be incorporated into the reference drag at the flight stage of aircraft development.

$$D_{REFOP} = D_{REF} + \Delta D_{EXH} + \Delta D_{INL} \quad \text{(Eq.22)}$$

where:

D_{REFOP} is defined as the air vehicle reference drag at full-scale operating reference conditions.

Therefore, Equation 3 may be rewritten:

$$D_{AFS} = D_{REFOP} + \Delta D_{TRIM} + \Delta D_{RN} \quad \text{(Eq.23)}$$

Substitution of Equations 2 and 23 into Equation 1 results in the following simplified force accounting equation applicable at the flight test stage of air vehicle development:

$$F_{EX} = (F_N{}^* - \Delta F_{INL} - \Delta F_{EXH} - \Delta F_{TRIM}) - (D_{REFOP} + \Delta D_{TRIM} + \Delta D_{RN}) \quad \text{(Eq.24)}$$

The F_{EX} (excess thrust) term in Equation 24 is evaluated through either aircraft accelerometer measurements or energy considerations. A discussion of the equations associated with excess thrust measurement is deferred to 7.3 because an expansion of the simplifying assumptions used up to this point is required.

A discussion of the (modified net thrust) options available for in-flight thrust determination for time-dependent aircraft and/or engine operating conditions is contained in Section 4.

The flight test values for the incremental forces due to the inlet, exhaust, and vehicle trim (ΔF_{INL}, ΔF_{EXH}, ΔF_{TRIM} and ΔD_{TRIM}) are derived from wind tunnel scale model tests and incorporated into the flight test data correction procedures. The rationale for applying these steady-state derived increments to time-dependent aircraft and engine operating conditions is discussed in Section 3.

The incremental effect of Reynolds number (ΔD_{RN}) on vehicle drag is determined analytically from aerodynamic flat-plate skin friction theory and may include the effects of surface roughness, if required.

Section 7.2 derives the aircraft lift and drag force balance equations for flight test evaluation of the remaining term, D_{REFOP}, in Equation 24.

SAENORM.COM : Click to view the full PDF of air5020a

7.2 Aircraft Lift and Drag Force Balance Equations:

Section 7.1 developed the thrust and drag relations for an air vehicle operating under level (flight path angle equals zero), time-variant conditions. Expansion of these conditions to the cases where the vehicle flight path angle is not zero and the thrust vector is not aligned with the vehicle longitudinal reference axis is discussed in this section. AIR1703, Appendix C develops air vehicle lift and drag equations based on the force balance diagram shown in Figure 42. The force balance diagram has been simplified through the following assumptions: (1) all forces pass through the aircraft center of gravity; (2) no lateral inclination of the gross thrust vector exists; and (3) the aircraft is in symmetrical flight (i.e., the angle of sideslip for the steady-state, quasi-steady-state, and dynamic maneuvers described in 7.4 is maintained at or near zero).

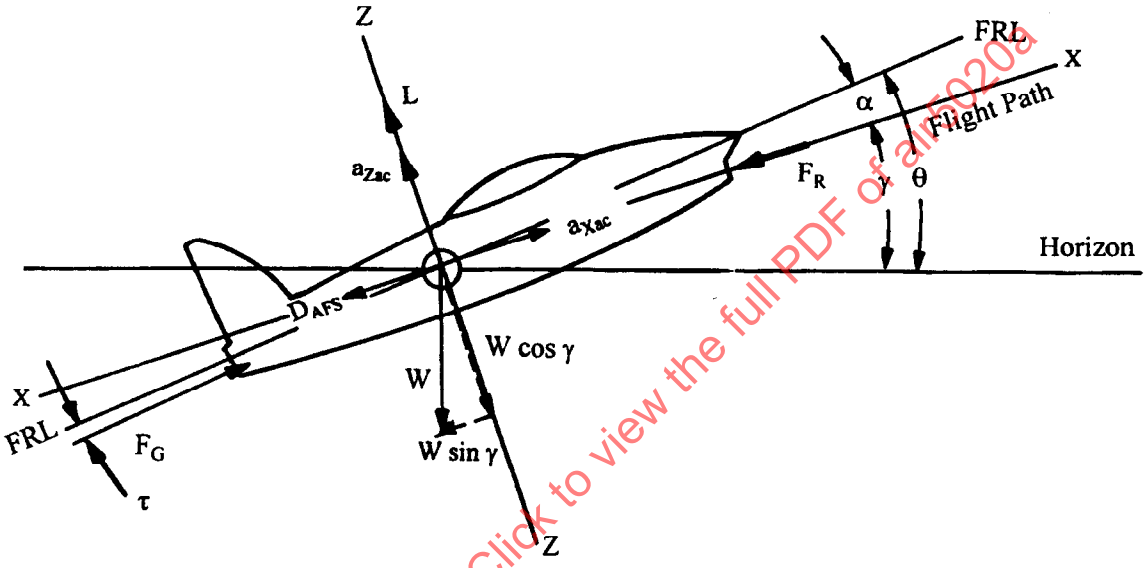

FIGURE 42 - Aircraft Force Balance Diagram

For ease of calculation, the forces are resolved parallel (x-axis) and perpendicular (z-axis) to the direction of flight (wind axes system). Resolving the forces along the flight path and assuming the mass change to be instantaneously zero, the excess thrust will result in an acceleration

$$\Sigma F_X = (W/g)a_{X_{AC}} \qquad \text{(Eq.25)}$$

$$F_G Cos(\alpha+\tau) - F_R - \Delta F_{INL} - \Delta F_{EXH} - \Delta F_{trim} - D_{AFS} - WSin\gamma = (W/g)a_{X_{AC}} \qquad \text{(Eq.26)}$$

Installed propulsive force along the flight path is defined as

$$F_{IPF_X} - F_G Cos(\alpha+\tau) - F_R = \Delta F_{INL} - \Delta F_{EXH} - \Delta F_{trim} \qquad \text{(Eq.27)}$$

SAENORM.COM : Click to view the full PDF of air5020a

7.2 (Continued):

Therefore, Equation 26 can be rewritten

$$D_{AFS} = F_{IPF_x} - W\mathrm{Sin}\gamma - (W/g)a_{x_{AC}} \quad \text{(Eq.28)}$$

For the forces perpendicular to the flight path

$$\Sigma F_z = (W/g)a_{Z_{AC}} \quad \text{(Eq.29)}$$

$$L - W\mathrm{Cos}\gamma + F_G\mathrm{Sin}(\alpha+\tau) = (W/g)a_{Z_{AC}} \quad \text{(Eq.30)}$$

$$L = W(\mathrm{Cos}\gamma + (W/g)a_{Z_{AC}} - F_G\mathrm{Sin}(\alpha+\tau) \quad \text{(Eq.31)}$$

Equations 28 and 31 are the drag and lift force-balance equations for an aircraft in symmetrical flight in the two-dimensional wind axis coordinate system. With Equation 27, aircraft lift and drag can be obtained through evaluation of engine gross thrust and ram drag, the α, γ, and τ geometric relations, and aircraft acceleration along and normal to the flight path.

Finally, combining Equations 27 and 28 and incorporation of the incremental forces associated with the F_{IPF} and D_{AFS} terms in Equation 24, results in definition of an air vehicle drag polar based on D_{REFOP}, which is independent of engine and airframe operating conditions.

$$D_{REFOP} = F_G\mathrm{Cos}(\alpha+\tau) - F_R - \Delta F_{INL} - \Delta F_{EXH} - \Delta F_{TRIM} - \Delta D_{TRIM} - \Delta D_{RN} - W\mathrm{Sin}\gamma - (W/g)a_{x_{AC}} \quad \text{(Eq.32)}$$

NOTE: Except where indicated, D_{REFOP} is the basis for the drag coefficient (C_D) data presented in this section.

7.3 Excess Thrust Measurement Options:

Air vehicle lift and drag may be determined through direct measurement of the acceleration terms, a_{xAC} and a_{zAC}, in Equations 28 and 31, or from the total energy change of the aircraft. Accelerometer methods employ highly accurate accelerometers to obtain an instantaneous measurement of inertial accelerations along and perpendicular to the flight path. To obtain a direct measurement of excess thrust, the accelerometer must be aligned to the aircraft flight path, either mechanically, as is the case with the Flight Path Accelerometer (FPA) method, or mathematically, as is the case with the Body Axes Accelerometer (BAA) method.

7.3.1 Flight Path Accelerometer (FPA): The FPA is mounted internal to a boom extending into the flow field ahead of the aircraft and is mechanically connected to an external angle-of-attack vane where it is free (theoretically) to align itself with the flight path of the aircraft. The true accelerations parallel and perpendicular to the flight path for the FPA are: (References 7.1 and 7.2)

$$a_{x_{FPA}} = a_{x_{AC}} + g\mathrm{Sin}\gamma \quad \text{(Eq.33)}$$

SAENORM.COM : Click to view the full PDF of air5020a

7.3.1 (Continued):

$$a_{z_{FPA}} = a_{z_{AC}} + g\text{Cos}\gamma \quad \text{(Eq.34)}$$

Substitution of Equations 33 and 34 into Equations 28 and 31 results in:

$$D_{AFS} = F_{IPF_x} - (W/g)a_{x_{FPA}} \quad \text{(Eq.35)}$$

$$L = (W/g)a_{z_{FPA}} - F_G\text{Sin}(\alpha + \tau) \quad \text{(Eq.36)}$$

where the wind axes longitudinal and normal accelerations are related to the measurement of aircraft lift and drag. Although theoretical application of the FPA is quite simple, in actual practice detailed attention must be given to the items which might cause misalignment of the FPA with the actual flight path of the aircraft, such as boom misalignment, bending of the boom and fuselage, aircraft pitch rates, and the local flow field in the vicinity of the FPA angle-of-attack vanes.

7.3.2 Body Axes Accelerometers (BAA): The BAA is not aligned with the aircraft flight path because it is fixed to the aircraft structure. Therefore, the aircraft angle of attack must be included in the resolution of the accelerometer vectors. Assuming the BAA is mounted along the fuselage reference line, FRL, the aircraft acceleration along the x and z axes is (Reference 7.1):

$$a_{x_{AC}} = a_{x_{FRL}}\text{Cos}\alpha - a_{z_{FRL}}\text{Sin}\alpha - g\text{Sin}\gamma \quad \text{(Eq.37)}$$

$$a_{z_{AC}} = a_{x_{FRL}}\text{Sin}\alpha + a_{z_{FRL}}\text{Cos}\alpha - g\text{Cos}\gamma \quad \text{(Eq.38)}$$

Substitution of Equations 37 and 38 into Equations 28 and 31 results in:

$$D_{AFS} = F_{IPF_x} - W/g[a_{x_{FRL}}\text{Cos}\alpha - a_{z_{FRL}}\text{Sin}\alpha] \quad \text{(Eq.39)}$$

$$L = W/g[a_{x_{FRL}}\text{Sin}\alpha + a_{z_{FRL}}\text{Cos}\alpha] - F_G\text{Sin}(\alpha + \tau) \quad \text{(Eq.40)}$$

7.3.3 Energy Method: If accelerometers are not available in the test aircraft, excess thrust may still be determined from energy considerations. Also, correlation of the energy method with accelerometer method results can aid in the isolation and correction of any bias errors that may exist in initial accelerometer measurement results. The total energy possessed by an air vehicle may be expressed instantaneously as the sum of its potential and kinetic energies:

$$E = PE + KE = WH + WV^2/2g \quad \text{(Eq.41)}$$

The energy per pound of aircraft weight or "specific energy" is

$$E/W = H + V^2/2g \quad \text{(Eq.42)}$$

SAENORM.COM : Click to view the full PDF of air5020a

7.3.3 (Continued):

The rate of change of specific energy is obtained by differentiation of Equation 42:

$$P_S = \frac{d(E/W)}{dt} = \frac{d(H + V^2/2g)}{dt} = \frac{dH}{dt} + \frac{V}{g}\frac{dV}{dt} \qquad \text{(Eq.43)}$$

Where P_S is defined as specific excess power, the aircraft performance parameter commonly used as a measure of an aircraft's ability to climb and/or accelerate. The relationship between excess thrust and the rate of change of specific energy is (References 3.4 and 7.2):

$$F_{EX} = F_{IFP} - D_{AFS} = \frac{W}{V}\frac{d(E/W)}{dt} = \frac{W}{V}\frac{d(H + V^2/2g)}{dt} = \frac{W}{V}\left[\frac{dH}{dt} + \frac{V}{g}\frac{dV}{dt}\right] \qquad \text{(Eq.44)}$$

Therefore, evaluation of excess thrust may be obtained from either a time history of the $[H + V^2/2g]$ term in Equation 44 or the summation of $[dH/dt + V/g\ (dV/dt)]$ from separate altitude and airspeed time histories.

Several methods are available for obtaining the requisite time-history information. Techniques and combinations of techniques which have been employed include radar space positioning, Askania camera space positioning, pitot-static pressure measurements, inertial space positioning, inertial velocity measurements from an inertial navigation system, and global positioning system.

Radar and camera data do not require aircraft instrumentation but restrict aircraft operation to a radar or theodolite range. The accuracy in both cases depends primarily on the quality of the tracking data, which depends on such factors as number of recording stations, range, and elevation angle.

Pitot-static pressure measurement approaches require onboard aircraft instrumentation and stable atmospheric conditions. If wind shears, gusts, or changing static pressure/geometric altitude relationships exist in the test air mass, erroneous apparent energy fluctuations will exist, and the resulting data scatter will increase significantly. Incorporation of inertial velocity measurements into the energy method equations will alleviate the problems associated with wind shears and gusts, but requires velocity measurements from a highly accurate onboard inertial guidance system.

SAENORM.COM : Click to view the full PDF of air5020a

7.4 Flight Test Maneuvers:

Various maneuvers are employed during flight test programs for evaluation of engine and air vehicle performance. These maneuvers range from steady-state (equilibrium conditions) to quasi-steady-state and dynamic operating conditions. The characteristics of the most commonly used fixed and variable throttle nonsteady maneuvers are outlined in Table 10. A brief description of these maneuvers is contained in the following paragraphs.

TABLE 10 - Flight Test Maneuvers

Maneuver	Nominally Constant	Primary Variables	Residual Variable
STEADY-STATE			
1-g Cruise	• Mach/Altitude	• None	• Note[1]
Sustained g Turn	• Mach/Altitude	• None	• Note[1]
QUASI STEADY-STATE			
Accel/Decel	• Altitude	• Mach	• Angle-of-Attack • Net Thrust • Excess Thrust
Climb/Descent	• Mach	• Altitude	• Angle-of-Attack • Net Thrust • Excess Thrust
DYNAMIC			
Push-Over/Pull-up	• Mach • Net Thrust	• Angle-of-Attack	• Excess Thrust • Altitude
Windup/Down Turn	• Mach	• Angle-of-Attack	• Net Thrust • Excess Thrust • Altitude

[1] Although excess thrust is targeted to be zero, any residual must be evaluated.

7.4.1 Quasi-Steady-State Maneuvers: Quasi-steady maneuvers are those flown near 1-g normal acceleration with a fixed throttle position (i.e., climbs, descents, level-flight accelerations, and decelerations). Figure 43 is an example of a level flight aircraft acceleration. Altitude is nominally held constant while Mach number is the primary variable. Net thrust varies as a result of the change in flight conditions and vehicle excess thrust varies as the difference between the propulsion and aerodynamic forces. The drag coverage for these types of maneuvers is limited to that obtainable within the near 1-g altitude and airspeed envelope of the vehicle, as indicated in Figure 43 (see AIR1703, Appendix C or Reference 7.3 for a discussion of the development of aircraft drag polars).

7.4.2 Dynamic Maneuvers: Dynamic maneuvers are characterized by transient variations in aircraft longitudinal and normal acceleration while the engine throttle is either fixed or varied. These maneuvers allow evaluation of the vehicle propulsion and aerodynamic characteristics covering a range of angles of attack beyond that which can be achieved through employment of either steady-state or quasi-steady-state maneuvers. The two types of dynamic maneuvers typically used are the push-over/pull-up and wind-up/down turns.

SAENORM.COM : Click to view the full PDF of air5020a

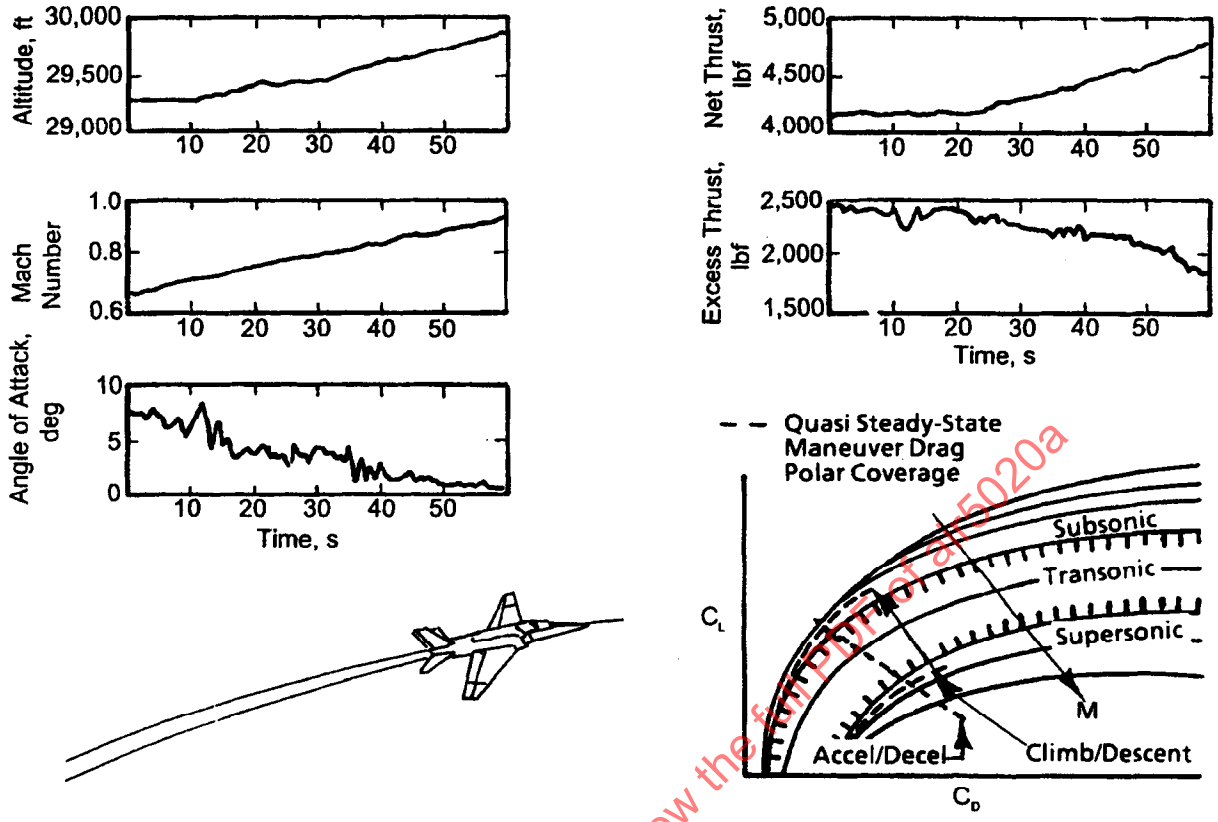

FIGURE 43 - Example Aircraft Acceleration Maneuver

7.4.2.1 Push-over/Pull-up Dynamic Maneuver: The characteristics of the push-over/pull-up maneuver are illustrated in Figure 44. The maneuver is performed after stabilizing at specified test conditions (altitude, Mach, and thrust required for equilibrium). Without a change in throttle setting, a push-over to approximately 0 g is performed, followed by a pull-up to approximately 2 g's (observing aircraft angle-of-attack and/or buffet limitations). The maneuver should be performed with aircraft pitch changes in a smooth, steady manner over a duration of not less than 20 s. Since Mach number will vary from the nominal test conditions, this maneuver is usually performed in the flight regime where the Mach variations do not materially affect evaluation of the vehicle aerodynamic characteristics (below drag divergence Mach number and angle of attack). Above drag divergence Mach number, this maneuver may be performed over a limited angle-of-attack range to mitigate the effect of Mach number variations on drag characteristics. Therefore, extensive drag polar coverage can be obtained along the left boundary, as indicated in Figure 44, but is somewhat limited at higher Mach numbers.

SAENORM.COM : Click to view the full PDF of air5020a

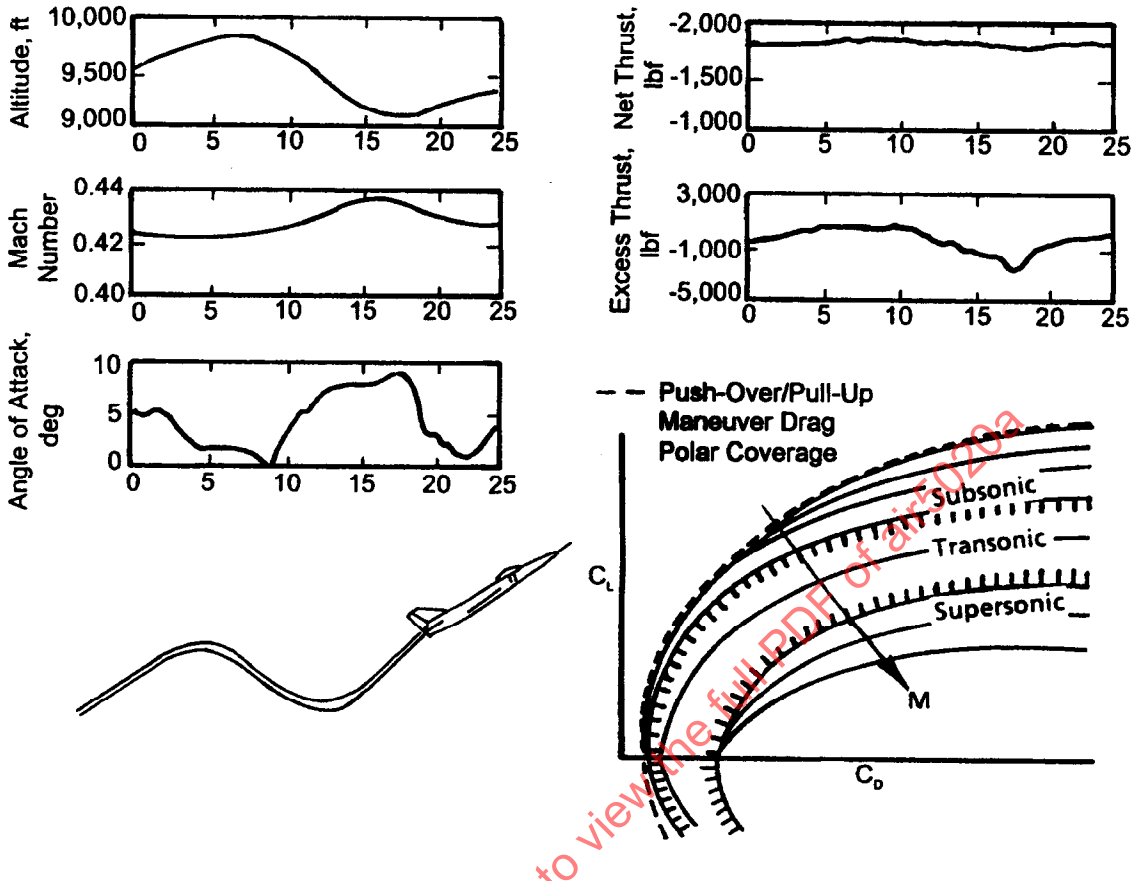

FIGURE 44 - Example Push-Over/Pull-Up Maneuver

7.4.2.2 Wind-Up/Down Turn Dynamic Maneuvers: The wind-up/down turn may be performed with the engine throttle either fixed or varied. The aircraft is stabilized at the target Mach number and altitude, after which a coordinated turn is initiated to either a target level of normal acceleration or angle of attack. In a wind-up turn, Mach number is nominally held constant, while during a wind-down turn, Mach number is allowed to fall off as altitude is nominally held constant. Wind-up turns are typically employed to evaluate the elevated angle of attack and Mach divergence flight regimes where control of Mach variations is critical to the evaluation of the vehicle aerodynamics. Wind-down turns are employed to evaluate a particular elevated angle of attack or normal load factor across a range of Mach numbers.

Figure 45 is an example of a fixed throttle wind-up turn. Mach number is nominally held constant. As angle of attack is increased, altitude is traded in an attempt to maintain the target Mach number. Drag polar coverage is along constant Mach lines, as indicated in Figure 45.

SAENORM.COM : Click to view the full PDF of air5020a

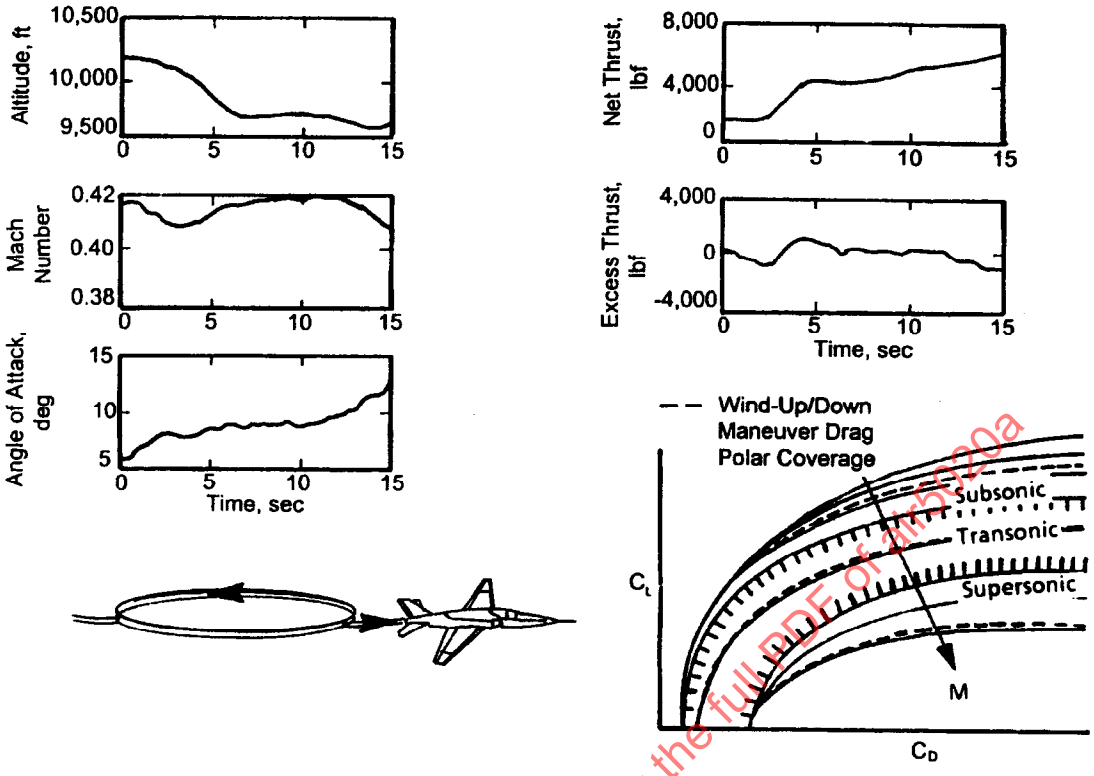

FIGURE 45 - Example Fixed-Throttle Wind-Up Turn Maneuver

7.4.2.2 (Continued):

Figure 46 is an example of a variable throttle wind-up turn maneuver. The maneuver is similiar to the fixed-throttle wind-up turn except that, in addition to Mach number, altitude is nominally held constant through modulation of thrust as normal acceleration is increased during the coordinated turn. Vehicle excess thrust will vary as a result of the changes in the aerodynamic and propulsion forces. As with the fixed-throttle wind-up turn, drag polar coverage is along lines of constant Mach number.

7.5 Data Consistency Checks:

As stated previously, most elements of the transient thrust validation process are identical to those discussed in Section 7 of AIR1703 for steady-state thrust determination. The transient validation process includes:

a. Preflight Engine Consistency Checks: All performance data should be included in the preflight engine consistency checks. Individual parameters, coefficients, and overall performance are compared between model and full-scale tests and with simulation models. Inconsistencies should be investigated prior to the flight test portion of the program. When satisfactorily completed, these consistency checks improve the overall confidence in the test program.

SAENORM.COM : Click to view the full PDF of air5020a

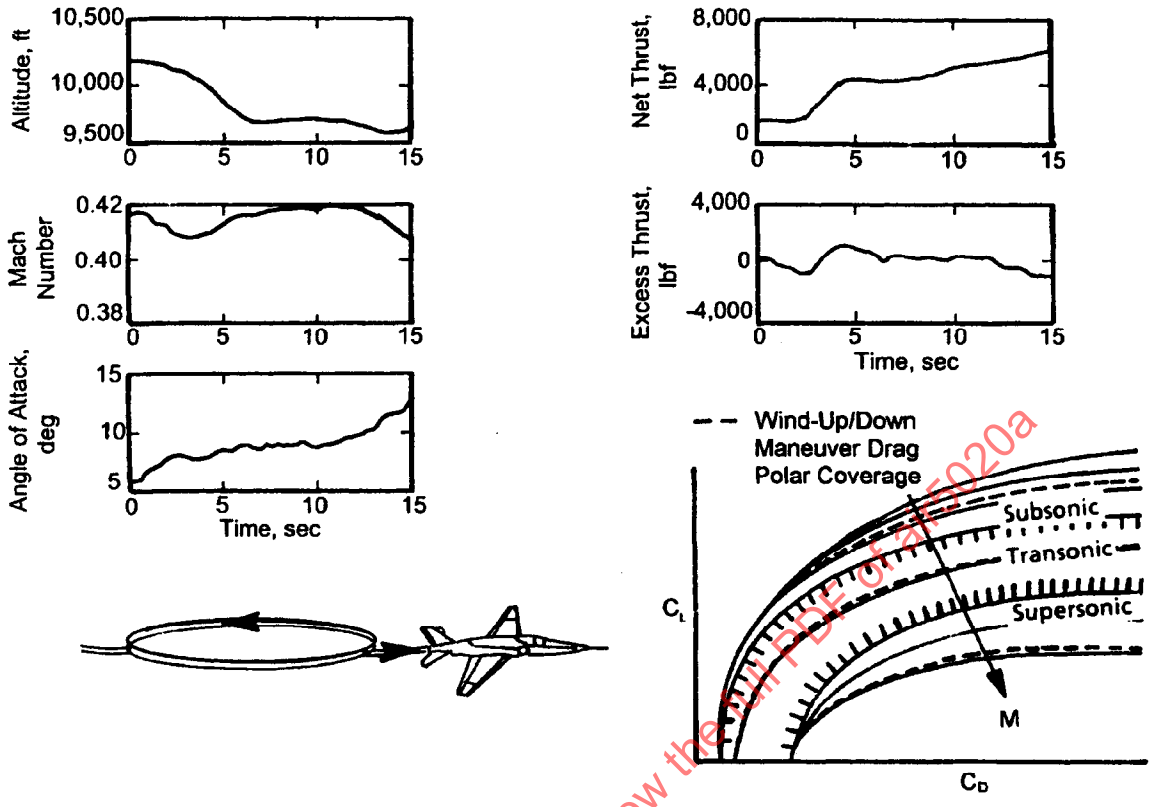

FIGURE 46 - Example Variable-Throttle Wind-Up Turn Maneuver

7.5 (Continued):

b. Postflight Engine Performance: Specific flight tests, as outlined in AIR1703 Chapter 7, are performed to determine and validate installed engine operating characteristics, i.e., thrust, fuel flow, and measured gas generator parameters as functions of engine power setting and flight operating conditions. The types of flight tests and data correlation techniques are those required to verify and validate engine calibration information. This information includes Mach number effects, Reynolds number and installation effects, and the effects of varying inlet and engine control schedules.

c. Aerodynamic Characteristics: The thrust measurement process, incorporating proper accountability for thrust and drag bookkeeping, Mach and Reynolds number effects, should result in a "unique" drag polar for a given aerodynamic and propulsion configuration. Analysis of the flight test aerodynamic data is useful, therefore, in identifying trends that are symptomatic of errors or inaccuracies within the various elements of the thrust/drag measurement process. These errors may be evidenced by a disagreement in the level of total air vehicle drag between one or more types of maneuvers or flights of the same aerodynamic configuration, or through erratic representation of the air vehicle induced drag and/or compressibility (Mach) characteristics. Appendix C to AIR1703 contains an overview of these items.

SAENORM.COM : Click to view the full PDF of air5020a

7.5 (Continued):

Additional procedures discussed in the following subsections applicable to time-dependent thrust determination include correlation between flight-measured engine transient characteristics and predictions, correlation of the calculated change in thrust with that measured with an onboard accelerometer for transient throttle flight maneuvers, and checks against the validity of the quasi-steady assumption.

7.6 Evaluation of the Quasi Steady-State Assumption:

The Quasi Steady-State Assumption implies that the steady-state thrust equations and relationships developed in AIR1703 are applicable to aircraft and engine conditions involving some level of time-dependency. Validation of the Quasi Steady-State Assumption can be accomplished through comparison of data obtained from quasi-steady and/or dynamic maneuvers with that obtained from corresponding steady-state maneuvers. However, detailed attention must be made to the various corrections that are required in order that these comparisons are made based on a common set of reference conditions. Adjustments for the effects of center of gravity, Reynolds number (skin friction drag), and engine thrust are required for all maneuvers. Acceleration-deceleration maneuvers may require correction to a constant normal load factor, normally 1 g. Dynamic maneuvers, e.g., push-over-pull-ups and wind-up turns, require correction to 1-g trimmed conditions to account for the additional control surface deflections (above that for 1-g flight) required to generate the maneuver. Subsequent to completion of these corrections and the data consistency checks described in 7.5, any remaining differences (or lack thereof) in the comparisons with the steady-state drag polar data may be used in assessing the validity of the Quasi Steady-State Assumption. Examples of these comparisons for quasi-steady and dynamic maneuvers with fixed throttle and for dynamic maneuvers with variable throttle are presented in the following paragraphs.

SAENORM.COM : Click to view the full PDF of air5020a

7.6.1 Quasi Steady-State Maneuvers: Figure 47 compares quasi steady-state (acceleration) data with steady-state data for a single exhaust turbofan configuration from Reference 7.4. Each engine used in the flight test program was calibrated in an Altitude Test Facility prior to conduct of the flight tests. Airflow for engine ram drag was deduced from a correlation of engine low-pressure rotor speed with test facility airflow measurements. Engine gross thrust was determined from a correlation of Nozzle Pressure Ratio (NPR) with test facility measurement of thrust (i.e., F/AP gas path method). All flight data were corrected to a common set of reference conditions, and vehicle excess thrust was determined using the energy method described in 7.3.3 incorporating velocity measurements from the vehicle inertial guidance system.

The quasi steady-state and steady-state data in Figure 47 show excellent agreement with approximately the same level of precision data scatter of 1%. The data presented in Figure 47 also contain results from sustained g turns (steady-state maneuvers performed at elevated normal acceleration) which also show agreement with the 1-g steady-state and quasi steady-state data. Within the range of time-dependent vehicle and engine conditions encountered during this flight test program, the Quasi Steady-State Assumption is validated.

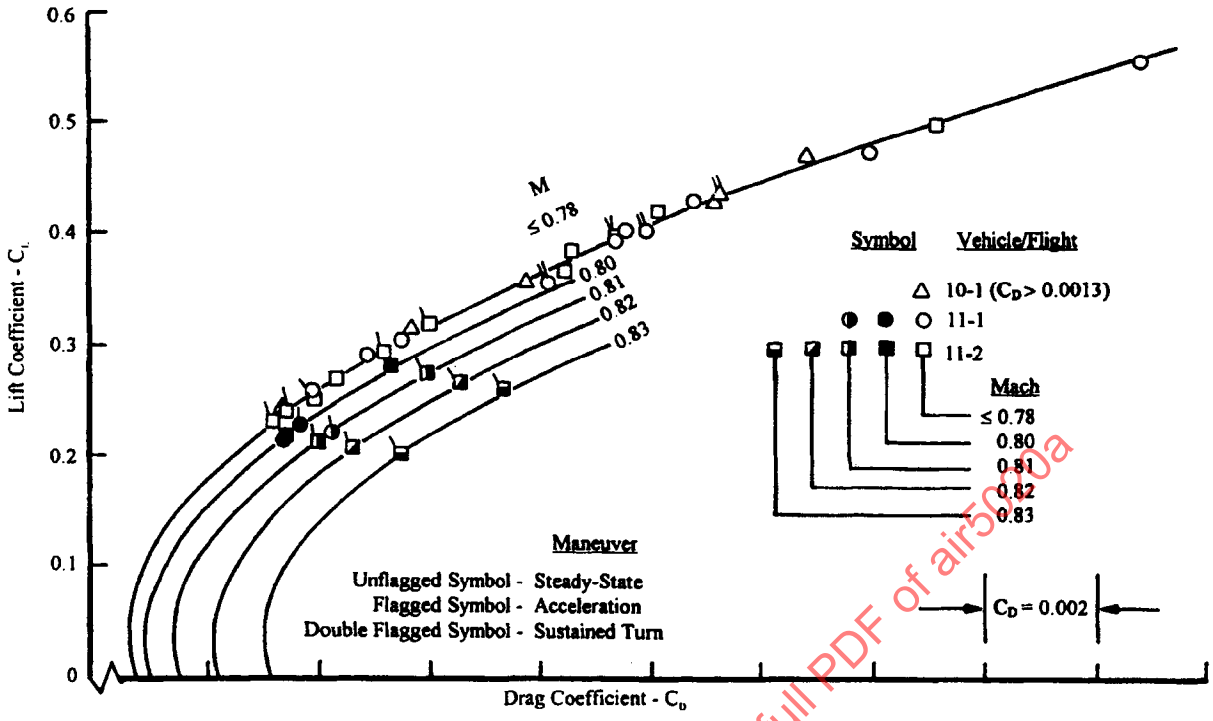

FIGURE 47 - Vehicle Drag Poles - Steady and Quasi Steady-State Flight Maneuvers

7.6.1 (Continued):

Figures 48 and 49 compare quasi steady-state (accelerations and climbs) and steady-state drag data for a mixed-flow, afterburning turbofan, twin-engine configuration reported in Reference 7.5. Calibration data were obtained from testing of separate engines in an altitude test facility. The generic calibration data were used with uncalibrated engines, incorporating the required instrumentation, in the flight portion of the program to compute in-flight thrust. Airflow for engine ram drag was determined from correlation of engine low-pressure rotor speed with test facility airflow measurements. Engine gross thrust was determined using the F/AP gas path method. Vehicle excess thrust was calculated using the Body Axes Accelerometer (BAA) method described in 7.3.2.

SAENORM.COM : Click to view the full PDF of air5020a

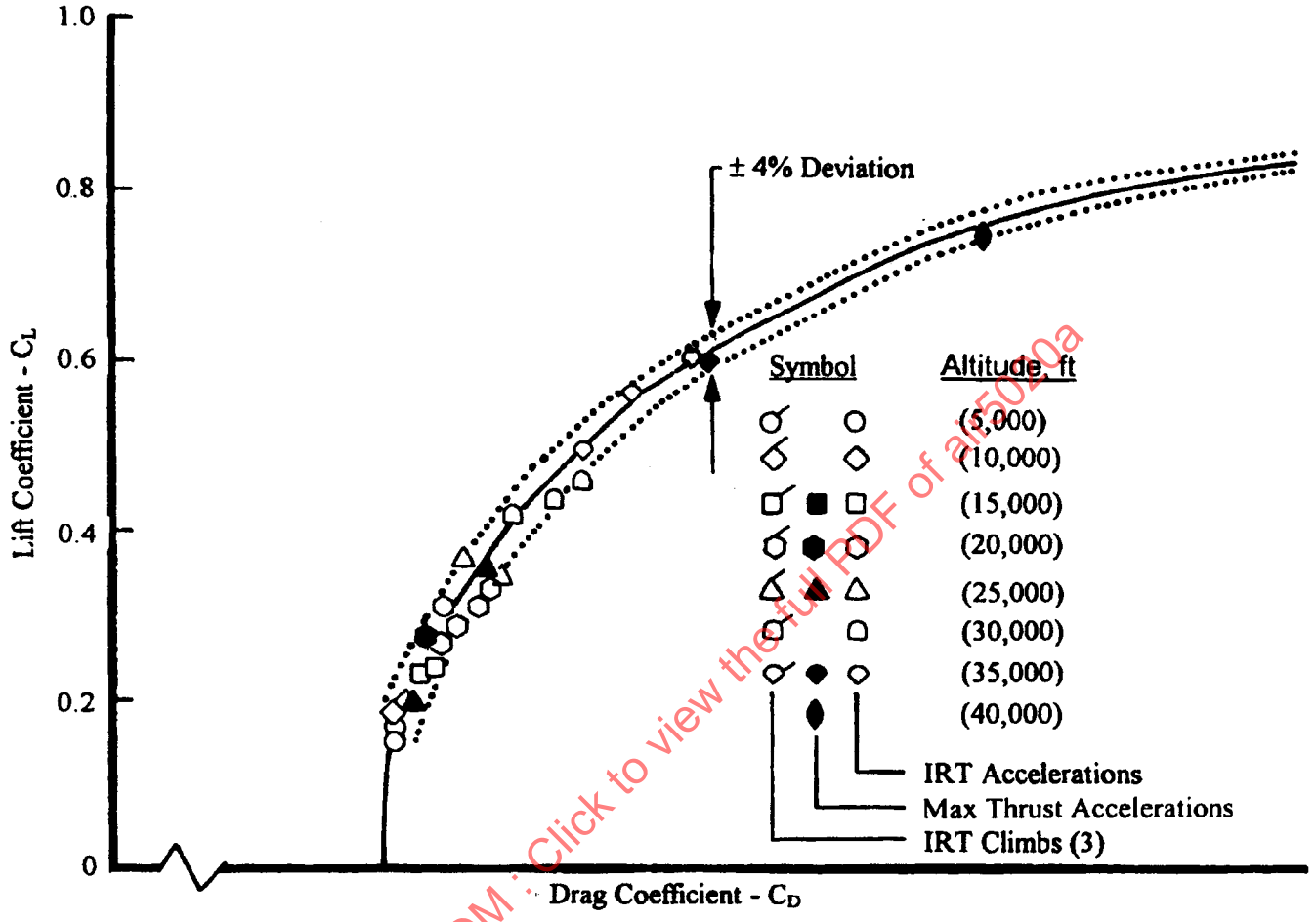

FIGURE 48 - Vehicle Drag Polar - Quasi Steady-State Flight Maneuvers at Mach = 0.7

SAENORM.COM : Click to view the full PDF of air5020a

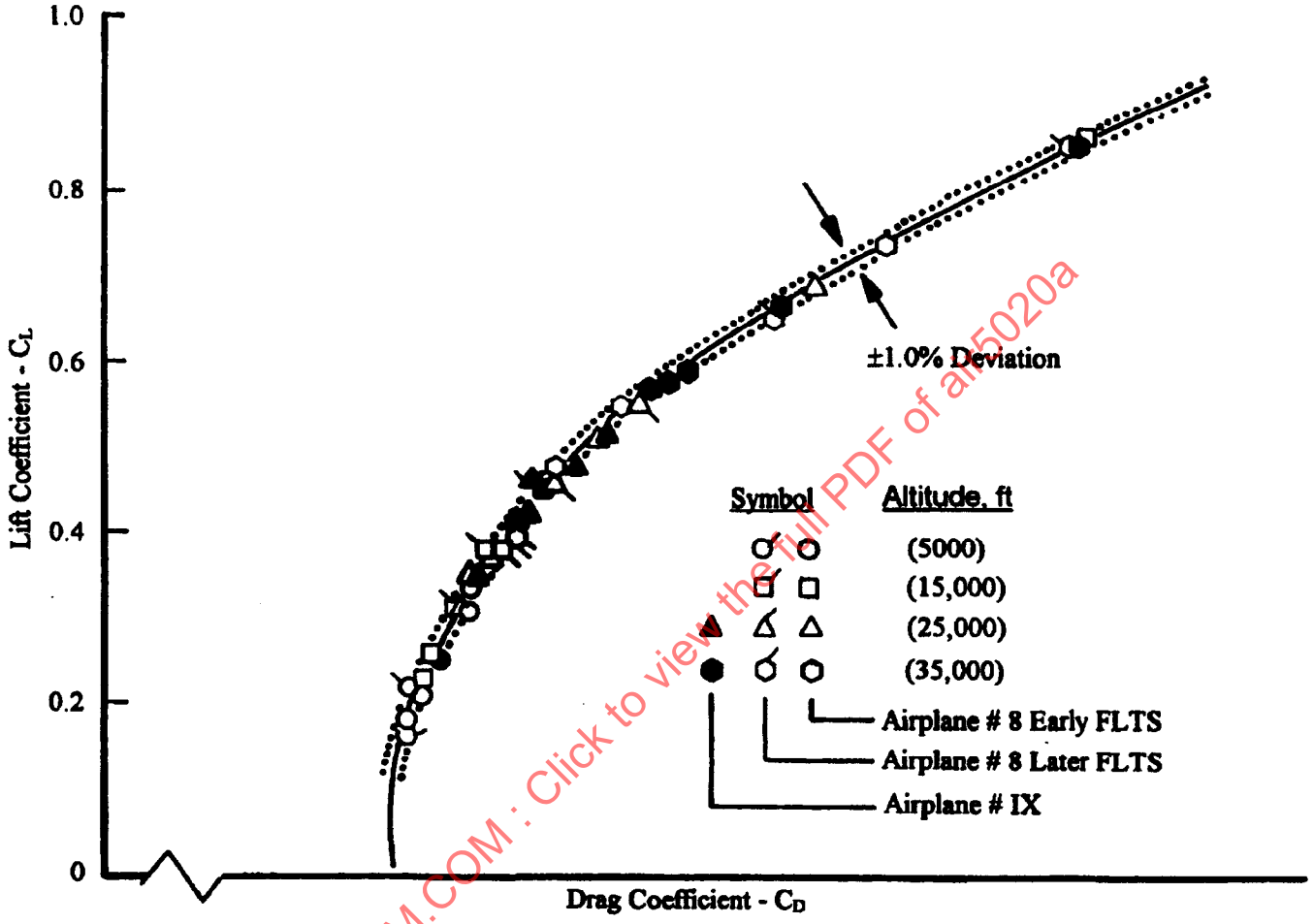

FIGURE 49 - Vehicle Drag Polar - Steady-State Flight Maneuvers at Mach 0.3 to 0.7

SAENORM.COM : Click to view the full PDF of air5020a

7.6.1 (Continued):

The fairing through the quasi steady-state data (Figure 48) is identical to the fairing through the steady-state data (Figure 49), except that 0.7 M drag divergence is included at lift coefficients greater than 0.6. The results show excellent drag level correlation between the quasi steady-state and steady-state drag measurement techniques, and again demonstrates the validity of the Quasi Steady-State Assumption for the range of time-dependent vehicle and engine conditions encountered during this program. It should be noted that the precision data scatter has increased from a level of ±1% for steady-state data in Figure 49 to approximately ±4% for the quasi steady-state data in Figure 48. Therefore, a larger quantity of quasi steady-state data is required to obtain the same level of confidence in the drag measurements than is required for the steady-state technique.

7.6.2 Dynamic Maneuvers - Fixed Throttle: Dynamic maneuver data from the References 7.4 and 7.6 flight programs are presented in Figures 50 and 51, respectively. The data in Figure 50 were obtained to investigate the applicability of the dynamic test technique to unmanned air vehicles. In addition to extending the range of drag polar definition, the results show good correlation with the segment of the drag polar defined by the steady-state and quasi steady-state test techniques (0.2 to 0.5C_L) in Figure 47. Although the data scatter is significant in Figure 50, the results suggest that the quality can be improved through more optimum control of pitch rate during the maneuver. Note that the data scatter is decreased near the peaks of the maneuver (low pitch rates) and increased in the vicinity of zero lift (high pitch rates).

The data in Figure 51 are the result of a conscious effort to perform the dynamic maneuver slowly, smoothly, and uniformly with pitch rates exceeding not more than 1.5 deg/s. The attention to performing the dynamic maneuver smoothly with low pitch rates explains the lower level of precision data scatter in Figure 51, which shows that the subsonic 0.7 M data are no worse than the quasi steady-state data scatter in Figure 48.

As evidenced by the results in this section and the statements in References 7.4 and 7.5, special attention must at least be made to the control of pitch rate during the dynamic maneuver to maintain the validity of the Quasi Steady-State Assumption. Pitch rate effects on the calculation of excess thrust may also contribute to the increase in data scatter. The dynamic maneuver results in this section agree favorably with the discussion of the limits of aircraft transients affecting aircraft performance in 3.3.

7.6.3 Dynamic Maneuvers - Variable Throttle: Dynamic maneuvers with variable throttle have not traditionally been used to obtain either aircraft or engine performance. However, during the Technology Demonstrator program of Reference 7.6, dynamic maneuvers (wind-up turns) were performed with both fixed and variable throttle. Figure 52 compares the results of a fixed-throttle wind-up turn, a fixed-throttle push-over-pull-up, and a variable-throttle wind-up turn. Center-of-gravity, Reynolds number, and control surface trim corrections were not applied to the test results; however, the maneuvers were flown at nominally the same conditions (0.5 M, 20,000-ft altitude) such that the corrections would be approximately the same for each of the maneuvers. Airflow for engine ram drag was based on an altitude test facility-developed airflow map as a function of low-pressure rotor speed. Engine gross thrust was determined using the $F/W\sqrt{T}$ gas path method utilizing the generic engine test calibration scheme. Excess thrust was determined using the Body Axes Accelerometer (BAA) method of 7.3.2.

SAENORM.COM : Click to view the full PDF of air5020a

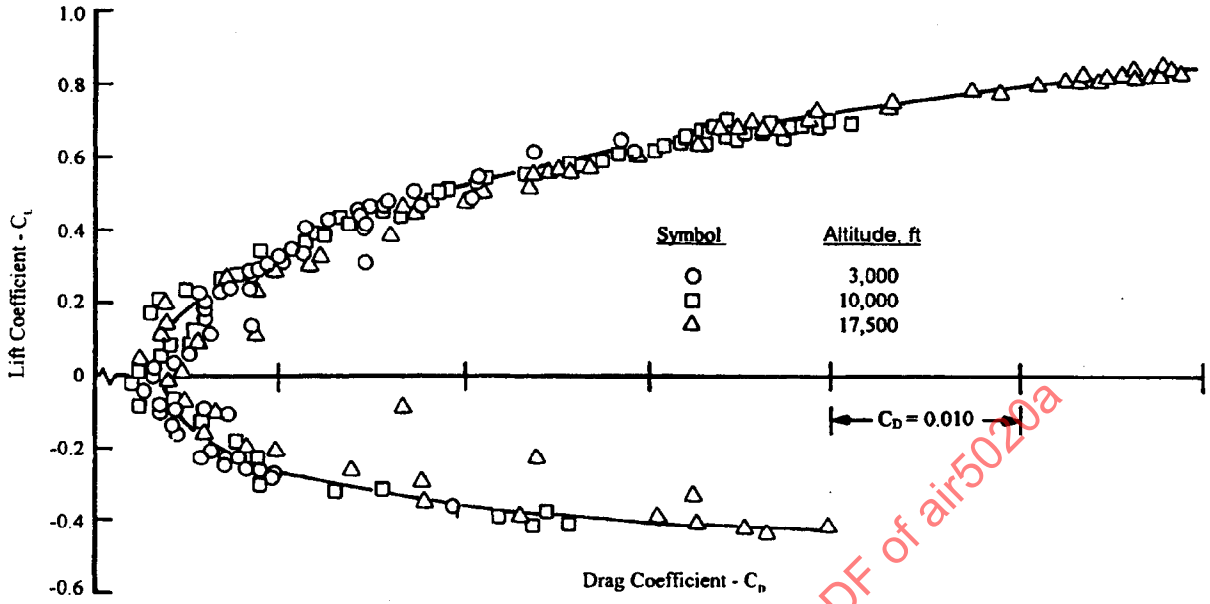

FIGURE 50 - Vehicle Drag Polar - Dynamic Push-Over/Pull-Up Flight Maneuvers at Mach = 0.7

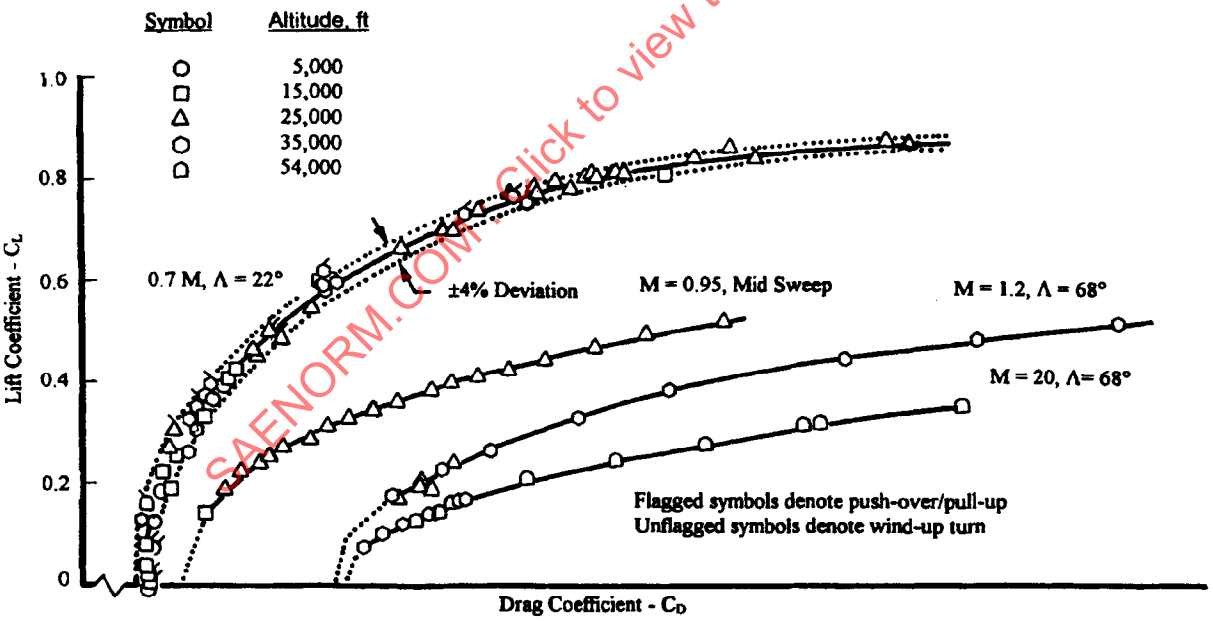

FIGURE 51 - Vehicle Drag Polars - Dynamic Flight Maneuvers

SAENORM.COM : Click to view the full PDF of air5020a

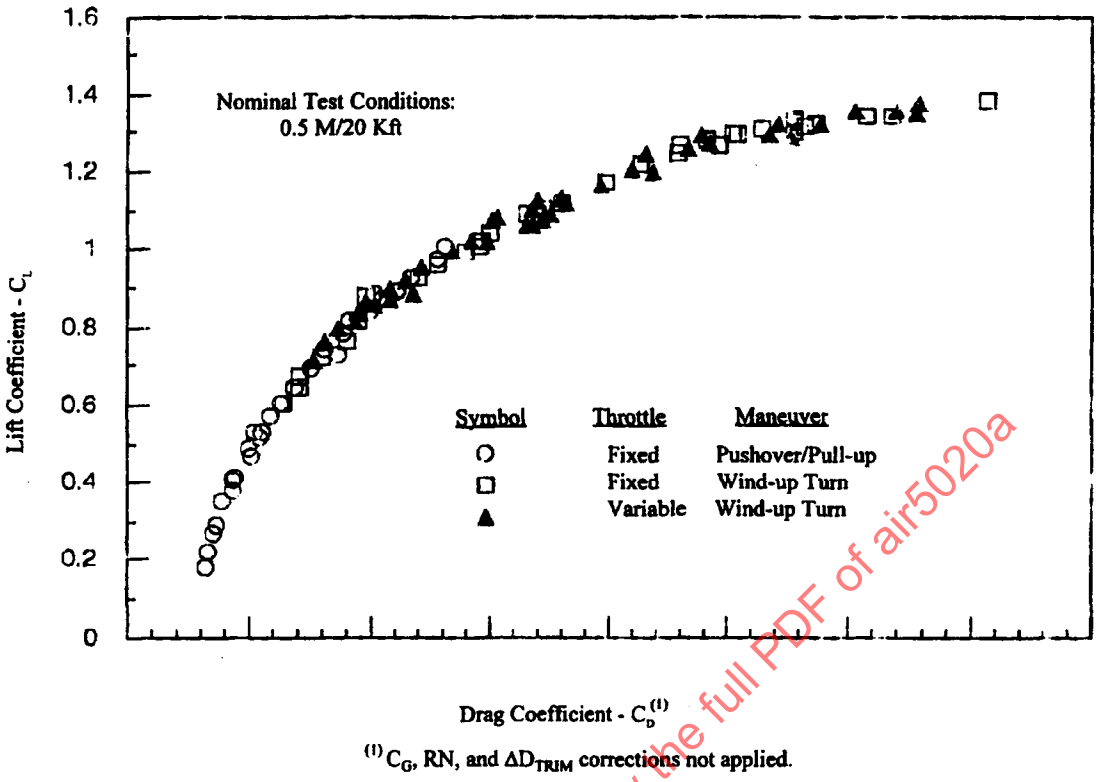

FIGURE 52 - Vehicle Drag Polar for Fixed and Variable Throttle Dynamic Aircraft Maneuvers

SAENORM.COM : Click to view the full PDF of air5020a

7.6.3 (Continued):

Although there are no steady-state data available for comparison, the variable- and fixed-throttle data correlate very well. This comparison does not validate the Quasi Steady-State Assumption. However, if other comparisons of fixed throttle correlate well with steady-state data (see 7.6.1 and 7.6.2), then it can be assumed that the variable-throttle data will also correlate.

Variable-throttle maneuvers offer the ability to better control the transient flight conditions of a maneuver by allowing both Mach number and altitude to be maintained which, in turn, allow lower pitch rate buildup to the target maximum g. This characteristic should prove useful in maintaining the validity of the Quasi Steady-State Assumption as discussed under the fixed-throttle dynamic maneuvers in 7.6.2.

7.6.4 Dynamic Maneuvers - Additional Considerations: Dynamic maneuvers at a fixed- or variable-throttle setting can have an effect on engine as well as vehicle performance measurements. During extreme maneuvering, inlet distortion can seriously degrade engine performance by producing large fluctuations in pressure and mass flow entering the engine. Ram recovery can be significantly reduced by inlet distortion. Figure 53 illustrates the effect of angle of attack on thrust. Thrust is shown as a ratio of the 0-deg angle-of-attack value for various flight conditions. These data were originally obtained in a wind tunnel and later validated with flight data.

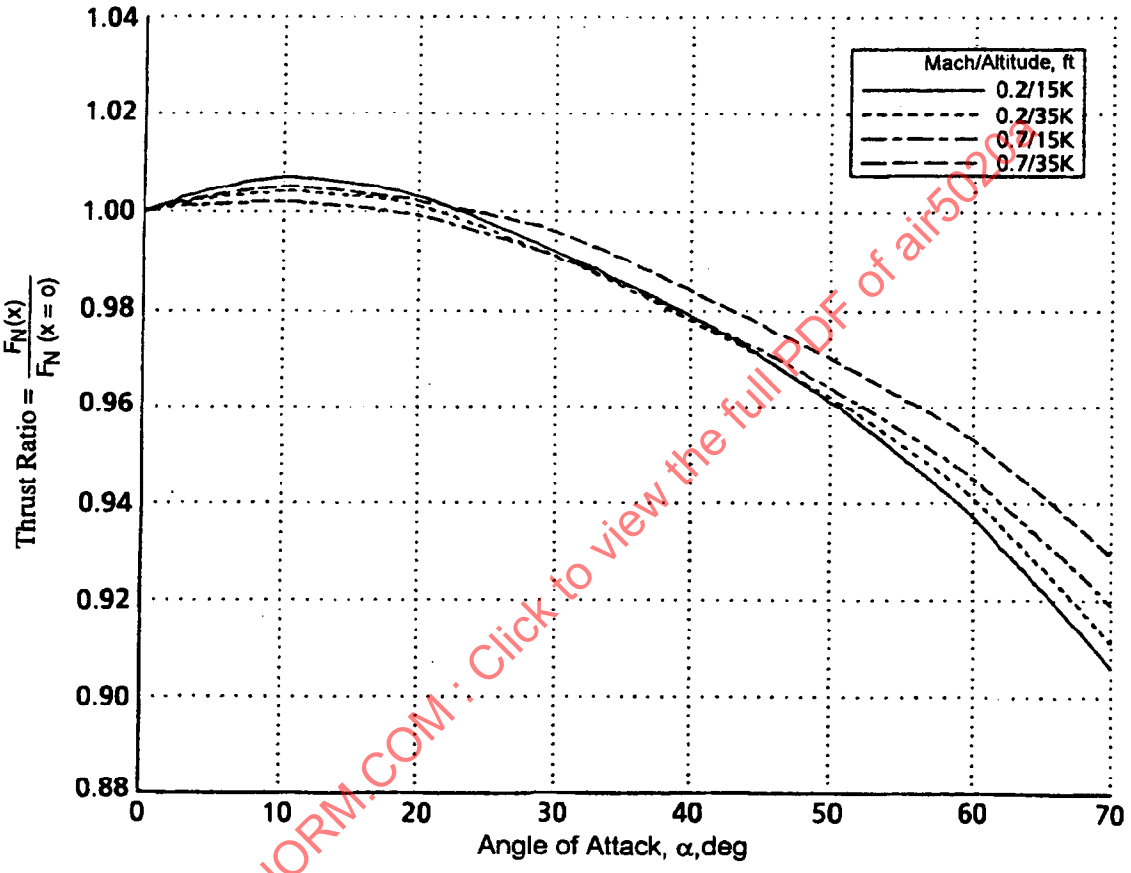

FIGURE 53 - Angle of Attack Effects on Engine Thrust

SAENORM.COM : Click to view the full PDF of air5020a

Most in-flight thrust models require an accurate understanding of the engine entrance conditions. The measurement of inlet distortion during flight is difficult because of the instrumentation and data acquisition challenges. Inlet pressure contours are obtained from an array of pressure probes recorded at high sample rates. Data analysis is also difficult because of the continual variation and large quantities of data.

7.6.4 (Continued):

The analysis of vehicle performance during dynamic maneuvering can require correction for trim drag effects, flow separation from lifting surfaces, and reversal of horizontal control surface lift. Large trim lift and drag corrections are caused by high maneuver rates or large changes in maneuver rate. If a maneuver is performed at a high rate, generally large longitudinal control surface deflections are required to generate the commanded pitch rates and accelerations. The large control surface deflections must be corrected back to the trimmed (zero pitch rate and accelerations) condition with resulting large corrections in trim lift/drag. Figure 54, developed during the Reference 7.6 program, shows the effect of maneuver rate on the vehicle drag polar when the results are not corrected for trim effects. The aerodynamic configuration of Reference 7.6 has a three-surface pitch control system (forward canards, wing camber control, and trailing strake flaps) that optimize the ratio of lift over drag. The trim drag effects illustrated in this example were caused by the slow tracking rate of the control surface scheduling during wind-up turn maneuvers.

SAENORM.COM : Click to view the full PDF of air5020a

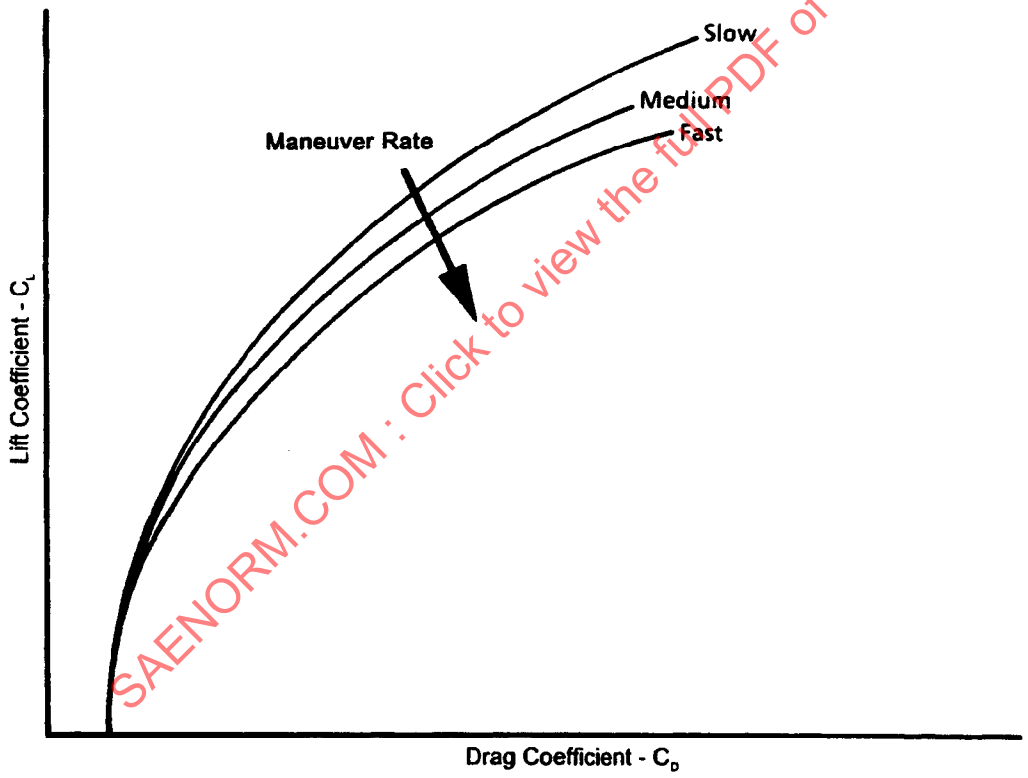

FIGURE 54 - Maneuver Effects on Variable Drag Polar for Wind-Up Turns at Various Rates

7.6.4 (Continued):

The reversal of control surface lift can also cause difficulties when analyzing dynamic vehicle performance maneuvers. For a conventional, stable aircraft, the horizontal control surface is downloaded. That is, for trimmed flight, the control surface has negative lift relative to the flight path. In performing a dynamic push-over maneuver, it is possible, particularly at aft center-of-gravity conditions, to upload the horizontal control surface. When this occurs, the control surface drag has gone through its minimum value (see Figure 55). Most incremental correction schemes assume it is still decreasing, causing an error in the correction (in this case in the wrong direction). If the tail lift were known precisely, the correction could be made properly, but correcting through the minimum drag point remains difficult.

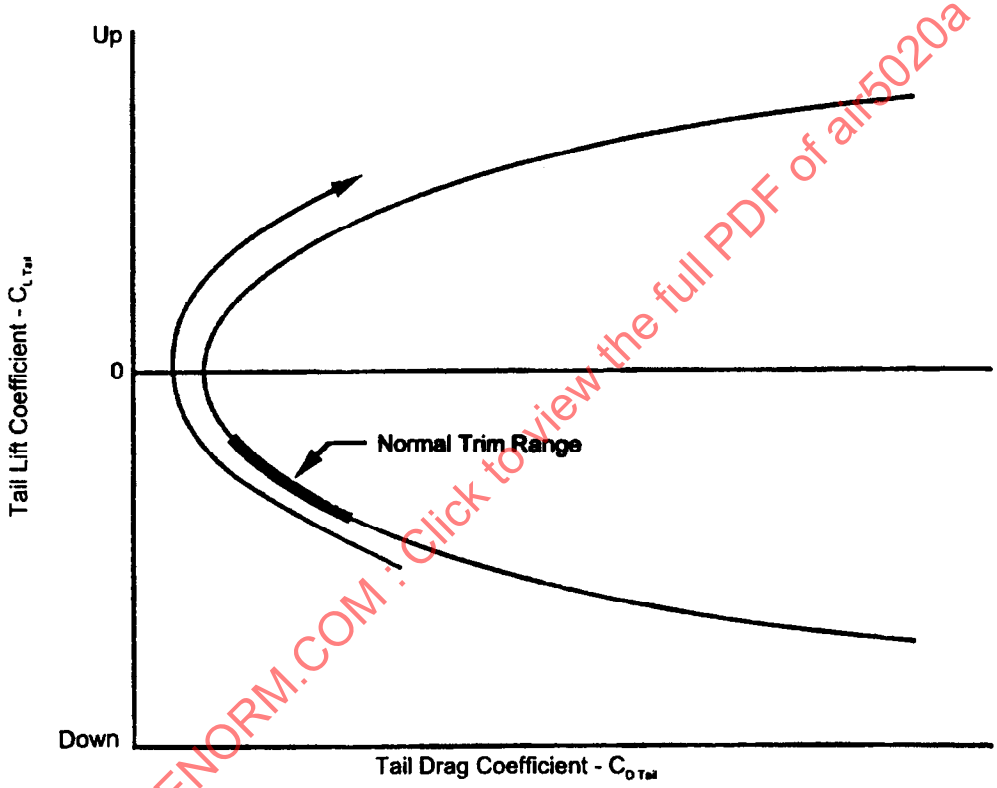

SAENORM.COM : Click to view the full PDF of air5020a

FIGURE 55 - Horizontal Tail Lift and Drag Coefficients

Another problem associated with dynamic vehicle performance is that of aerodynamic hysteresis associated with flow separation. This phenomenon is not easily recognized, but does exist (see Reference 7.7). Once flow has separated from the surface, it will normally reattach at a much lower angle of attack. Also, the repeatability of the reattachment location is not always consistent and may be time-dependent. In effect, this is an airflow hysteresis. Figure 56 illustrates this phenomenon based on data obtained during the Reference 7.8 flight program.

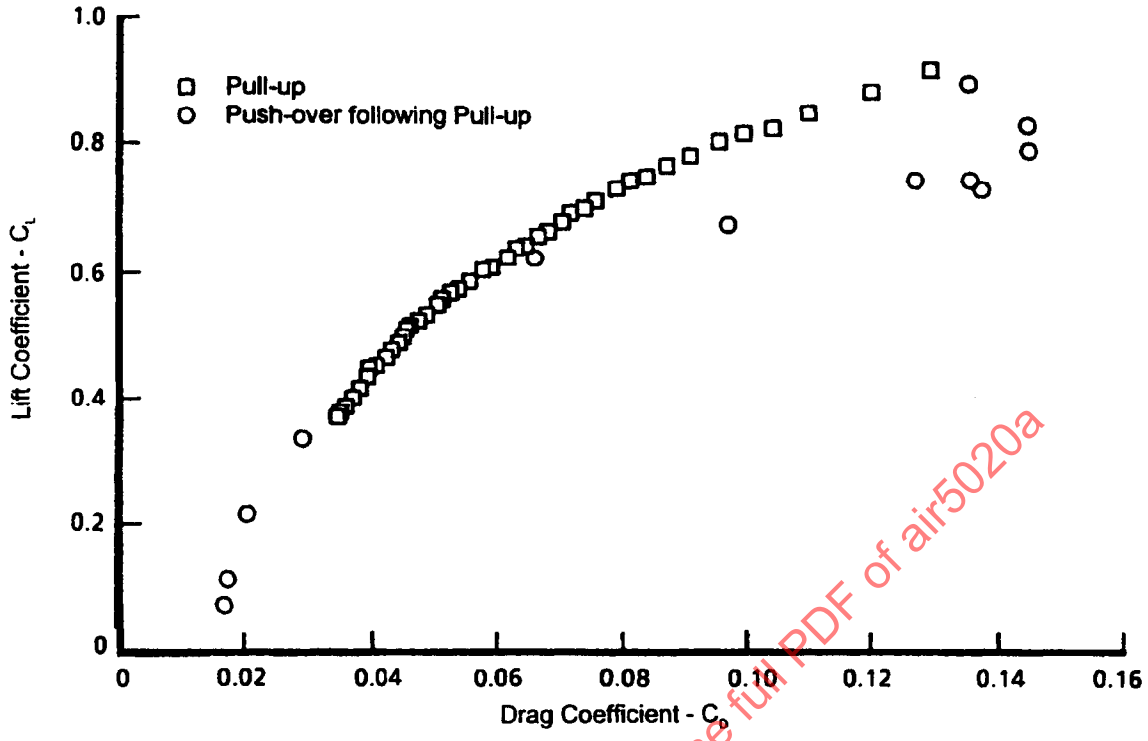

FIGURE 56 - Airflow Hysteresis Effects on Variable Drag Polar for Push-Over Following a Pull-Up at M = 0.85

7.7 Validation of Transient Thrust Measurement:

Flight test analysis techniques were developed to evaluate the accuracy of in-flight thrust measurement during transient engine operation. Thrust accuracy was assessed by comparing engine and aircraft performance response during varying throttle perturbations at quasi steady-state flight conditions. This approach relies on an accurate measure of aircraft excess thrust, F_{EX}, to evaluate the computed installed propulsive force, F_{IPF}, using the relationship of Equation 45:

$$F_{EX} = F_{IPF} - D_{AFS} \quad \text{(Eq.45)}$$

During stabilized flight conditions, drag can be assumed constant. This provides two important relationships for dynamic evaluation:

$$\Delta F_{EX} = \Delta F_{IPF} \quad \text{(Eq.46)}$$

and

$$\Delta F_{EX} / \Delta t = \Delta F_{IPF} / \Delta t \quad \text{(Eq.47)}$$

SAENORM.COM : Click to view the full PDF of air5020a

7.7 (Continued):

Two transient throttle maneuvers were formulated to use the above relationships. Throttle steps at various rates were used to compare the change in F_{IPF} to F_{EX}. Throttle frequency sweeps were used to evaluate the effect throttle rate has on calculated thrust. Both techniques give insight into the accuracy of calculated F_{IPF} during variable-throttle usage. Examples of each are presented using current in-flight thrust methodology utilized during recent flight test programs. The instrumentation and data acquisition systems used to obtain the data presented in this section were designed for typical vehicle performance testing. No attempt was made to optimize it for the dynamic performance application. These examples are presented only for the purpose of illustrating the time variant inflight thrust validation techniques.

7.7.1 Throttle Transients - Step Inputs: Throttle steps of various rates were performed on a low-bypass turbofan engine installed in an advanced technology demonstrator during stabilized aircraft flight conditions. Figure 57 illustrates three throttle rates: fast, medium, and slow for typical throttle step inputs. Similar transients were developed for throttle chops from maximum and intermediate rated thrusts. Actual throttle rates would be tailored to the specific engine system or thrust method being evaluated.

SAENORM.COM : Click to view the full PDF of air5020a

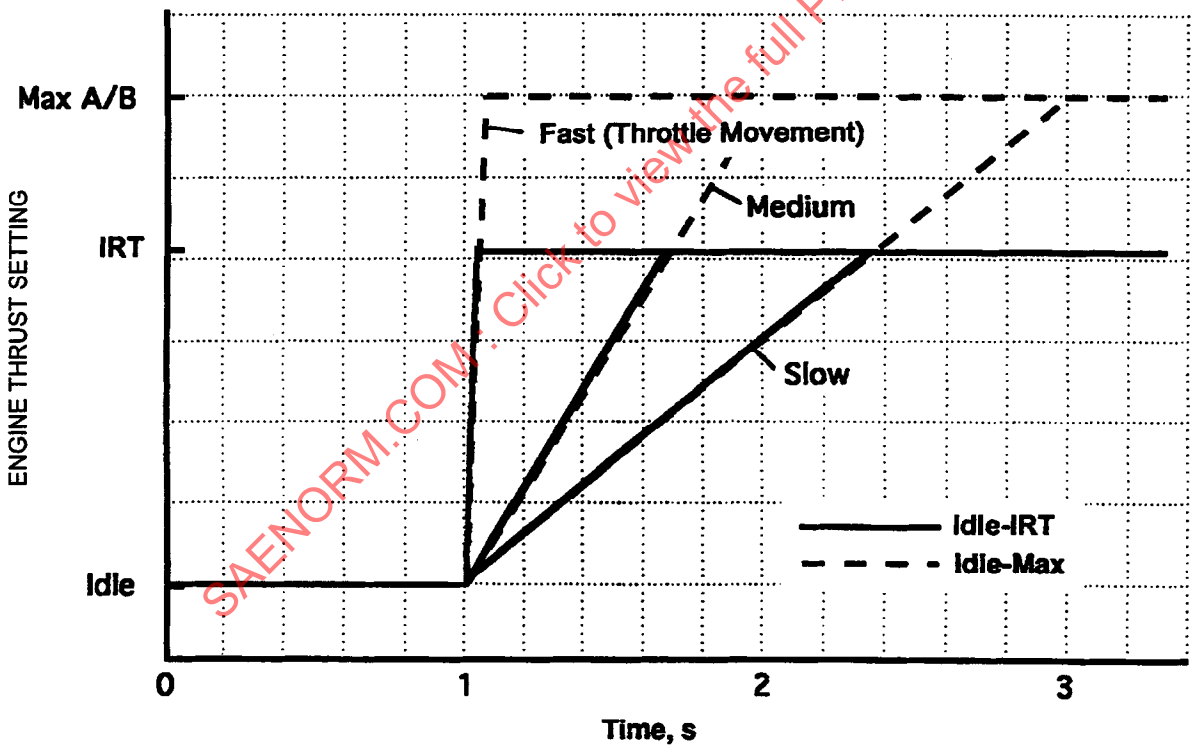

FIGURE 57 - Comparison of Throttle Transient Rates for Dynamic F_{IPF} Analysis

7.7.1 (Continued):

Thrust accuracy was evaluated by comparing the change in net propulsive force, ΔF_{IPF}, to the change in aircraft measured excess thrust, ΔF_{EX}, during the transients. Figure 58 shows the time-history response of various aircraft and engine parameters obtained during a series of throttle transients. The maneuver was initiated with the aircraft stabilized at the indicated flight conditions and the throttle set at the power required for level flight, PLF. After stabilization, the throttle was advanced to Max thrust at a medium rate, held for 10 s, then decreased to intermediate rated thrust, IRT, held until afterburner cancellation was complete, then reduced to idle.

Thrust was calculated using the conventional mass flow-temperature version of the gas path method (see 4.2). It was supplied by the engine manufacturer and intended for quasi-steady-state applications. Figure 59 provides a comparison of F_{IPF} to F_{EX} for the throttle transient presented above. It also includes the ideal line computed from the dynamic relationship presented in Equation 46. The results show this particular thrust model tends to overpredict F_{IPF} while the throttle is advanced and underpredicts it while throttling back. This tendency can be attributed to the accel/decel scheduling of fuel flow during the transient. The thrust model uses measured fuel flow, fan inlet temperature, and compressor speed (Figure 58) to calculate a temperature rise and mass flow rate through the engine. The model assumes a steady-state fuel-air ratio, thermal stabilization, and an energy balance between the turbines and fan/compressor components. Because these assumptions do not hold during a throttle transient, the model overestimates nozzle mass flow and nozzle throat temperature during throttle advancements and underpredicts both values during throttle reductions. The tendency is more pronounced the faster the throttle transient rate.

Comparisons of F_{IPF} versus F_{EX} calculated during various throttle rates are shown in Figure 60. An obvious difference occurs between afterburner and dry power transients. Afterburner transients are more sensitive to throttle rate, particularly during throttle chops. The primary reason for this is the use of power lever angle (PLA) to select when the afterburner is on or off. The thrust calculation logic does not account for augmentor transition time. This limitation is most noticeable during the Max thrust to IRT throttle step (Figure 60A), where afterburner fuel flow is prematurely zeroed out by the thrust model when the engine throttle power lever angle, PLA, initially reaches the IRT setting. For the fast throttle transient rate, this results in an initial 4,000-lbf reduction in calculated F_{IPF}, or a 40% error. A similar problem can occur during throttle advancements from nonafterburner to afterburner operation if excessive noise exists on the afterburner flowmeter when no fuel flows through it. In this case the model uses the noise as the afterburner fuel flow value resulting in an overestimation of F_{IPF}. Figure 60B illustrates this during the PLF to Max thrust transients. For a short period while afterburner operation is being initiated, F_{IPF} is influenced by the incorrect fuel flow value feeding the afterburner logic in the model. Calculated net thrust takes a sudden drop as soon as minimum afterburner operation is achieved because the afterburner fuel flowmeter is now operating normally. Figure 61 summarizes the effect of using PLA as a logical test for afterburner operation on the assumed fuel flow value in the thrust model.

SAENORM.COM : Click to view the full PDF of air5020a

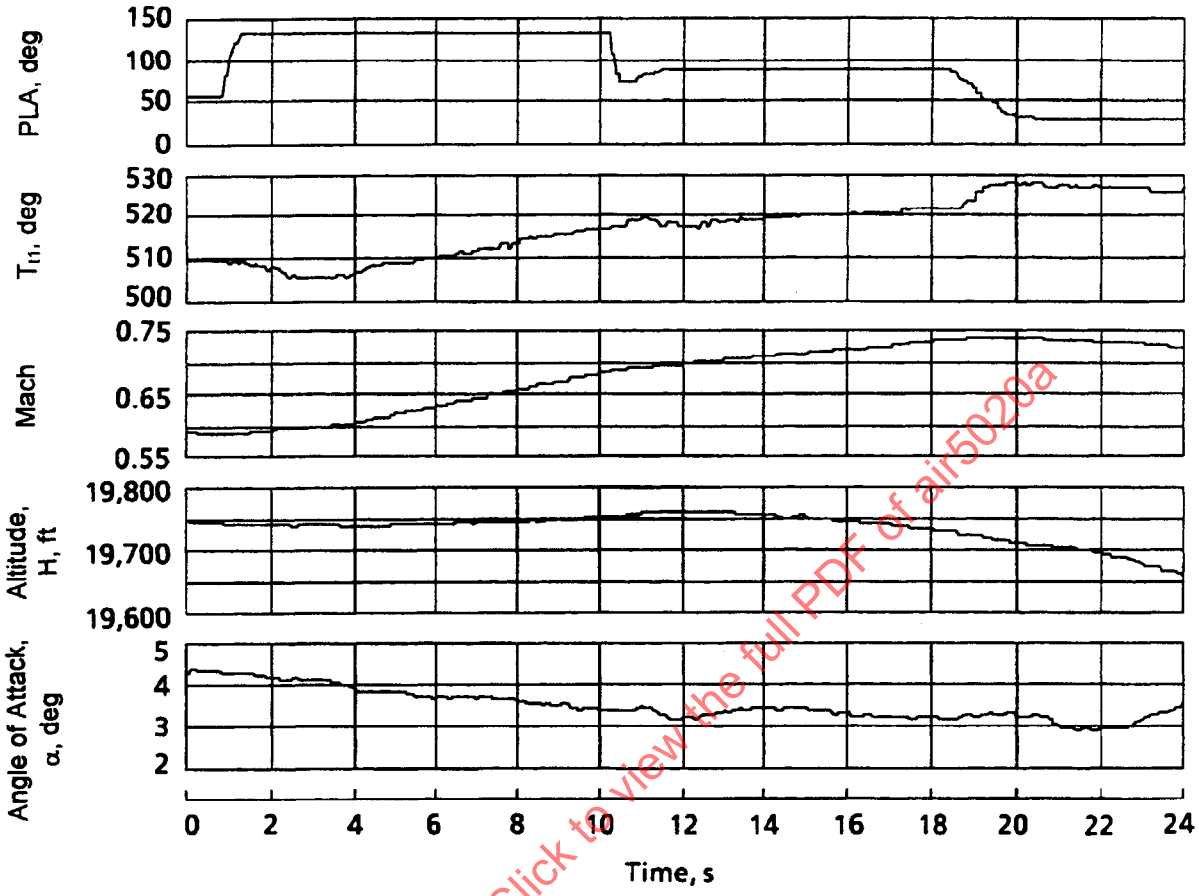

FIGURE 58A - Aircraft Flight Conditions

SAENORM.COM : Click to view the full PDF of air5020a

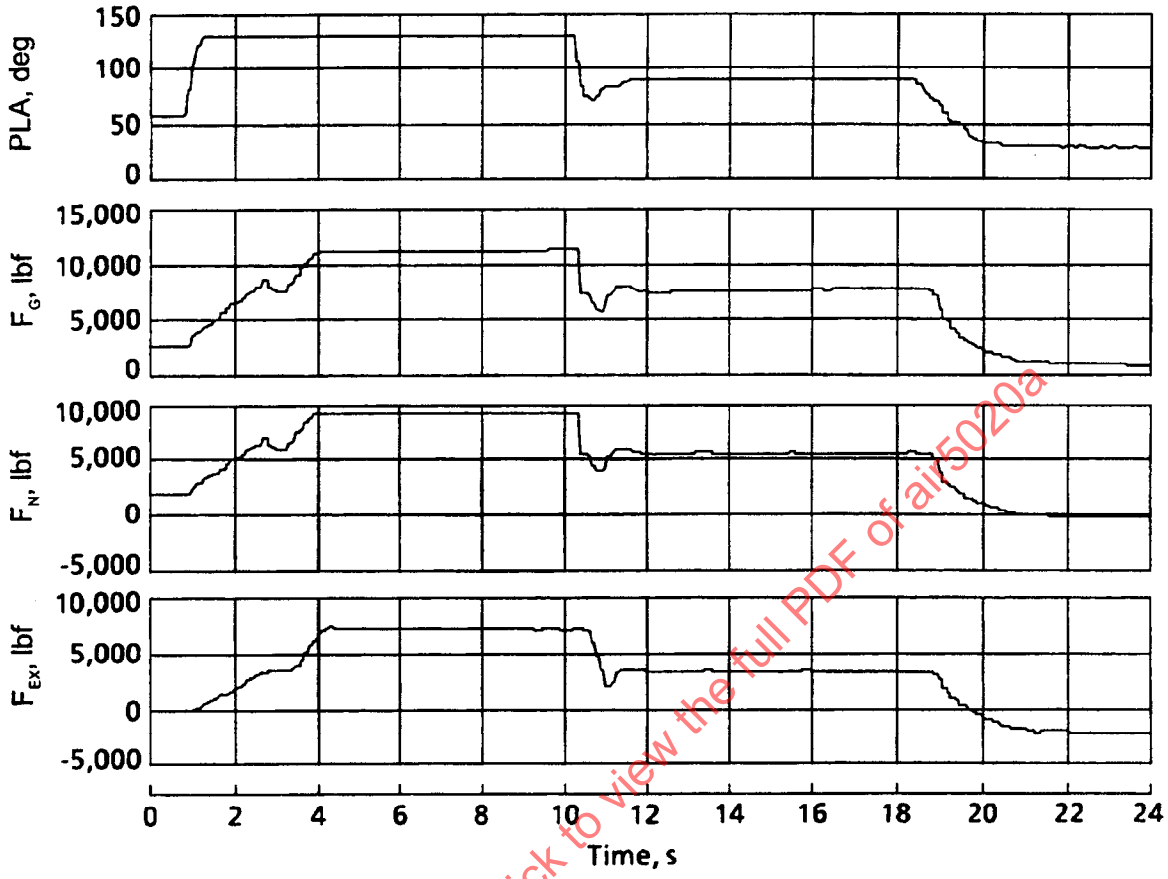

FIGURE 58B - Engine and Aircraft Performance Values

SAENORM.COM : Click to view the full PDF of air5020a

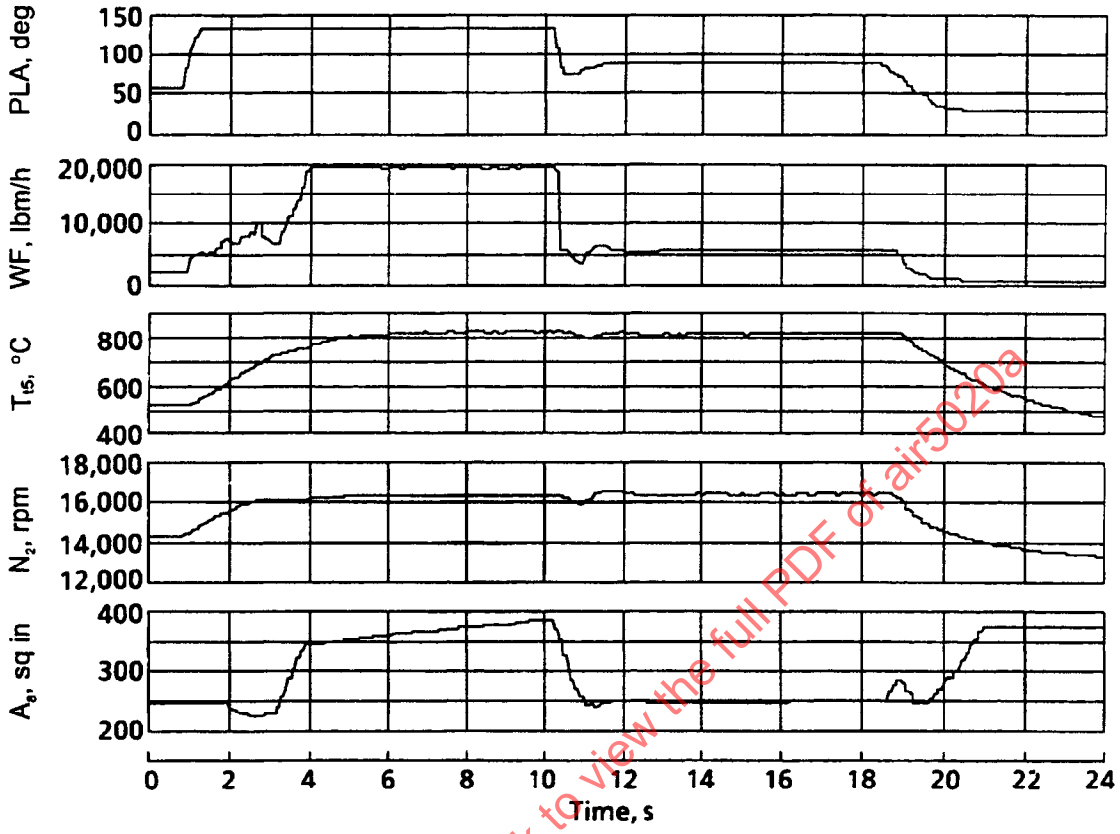

FIGURE 58C - Engine Parameter Values

FIGURE 58 - Throttle Transient Time Histories

SAENORM.COM : Click to view the full PDF of air5020a

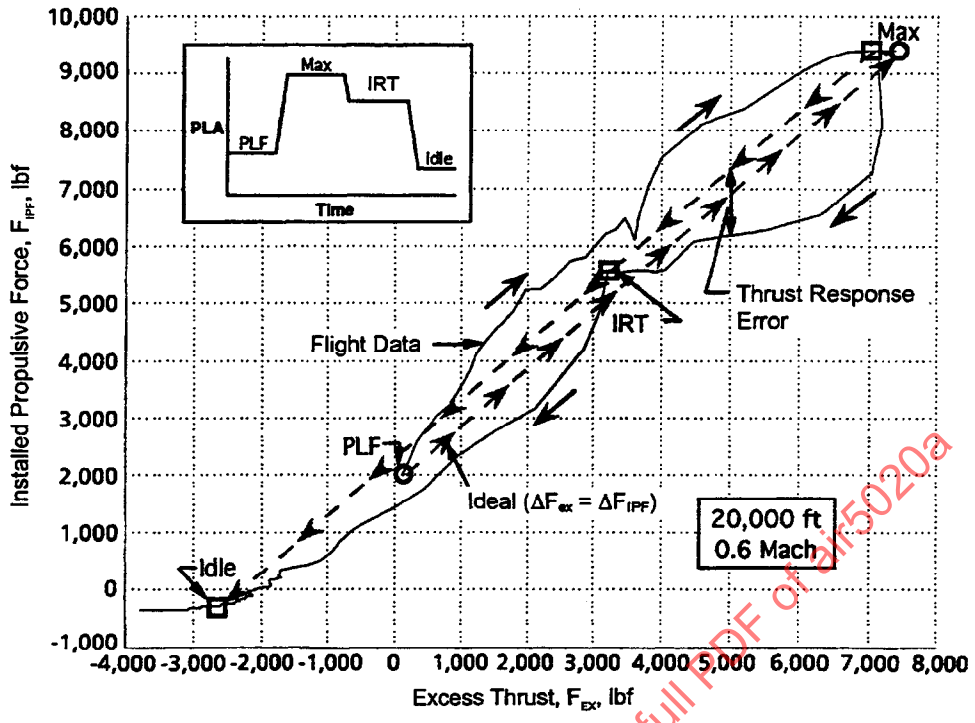

FIGURE 59 - Comparison of F_{IPF} and F_{EX} for a PLF-Max-IRT Throttle Transient

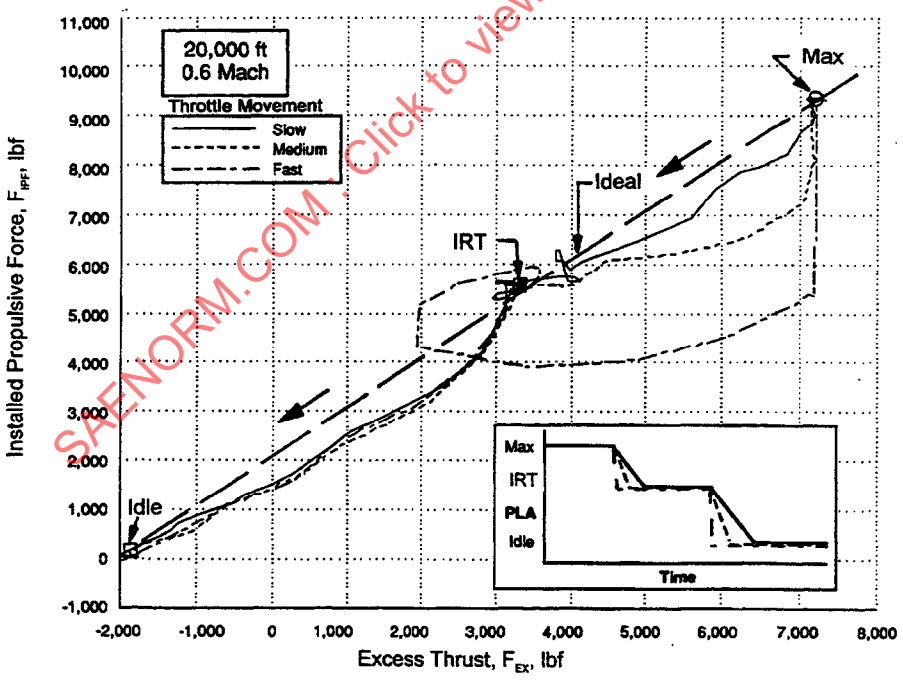

FIGURE 60A - Max to IRT to Idle

SAENORM.COM : Click to view the full PDF of air5020a

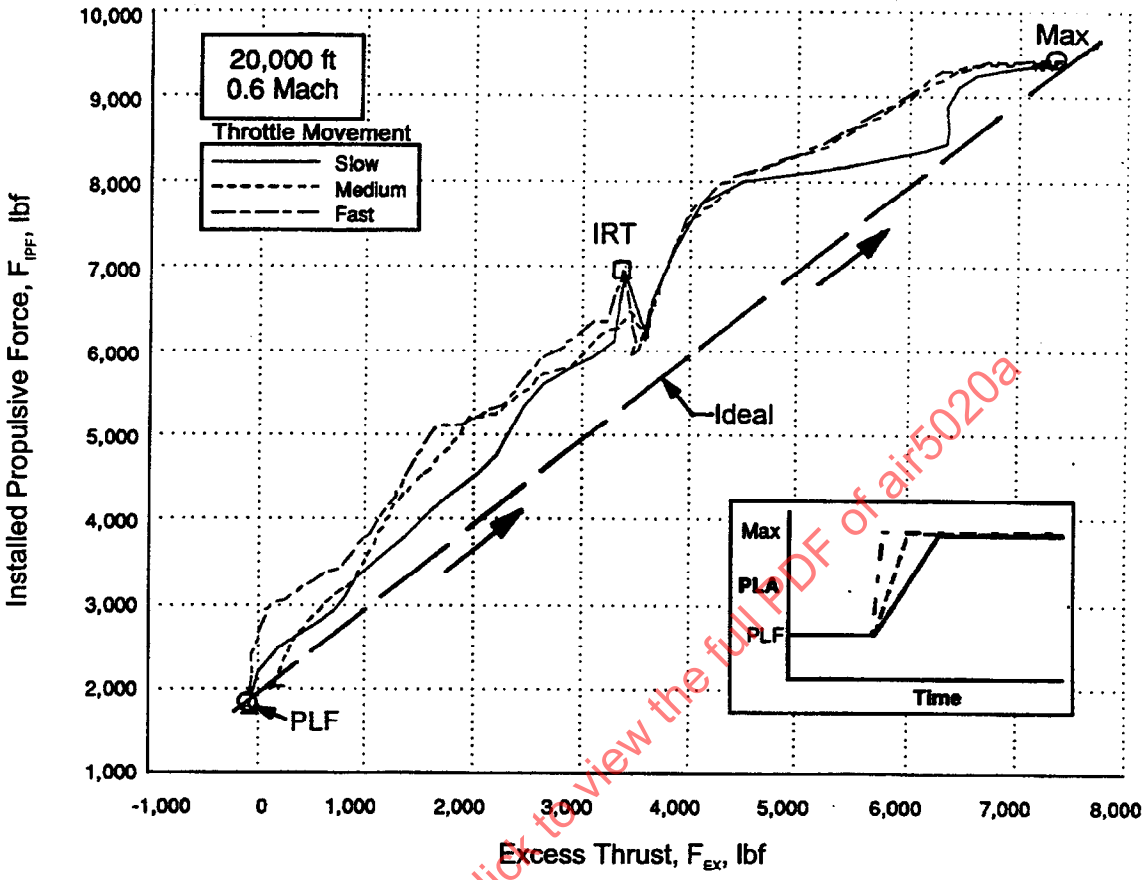

FIGURE 60B - PLF to Max

SAENORM.COM : Click to view the full PDF of air5020a

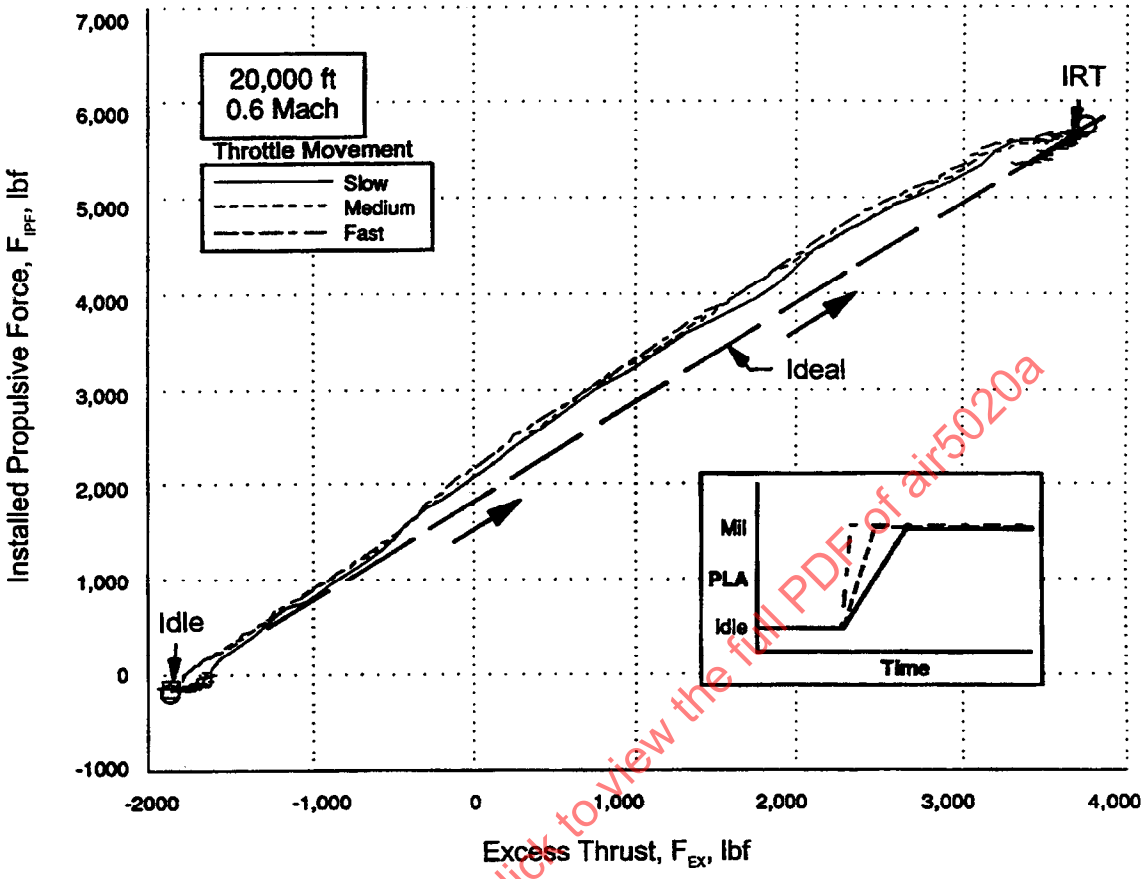

FIGURE 60C - Idle to IRT

FIGURE 60 - Comparison of Various Throttle Rates on FIPF Versus FEX

SAENORM.COM : Click to view the full PDF of air5020a

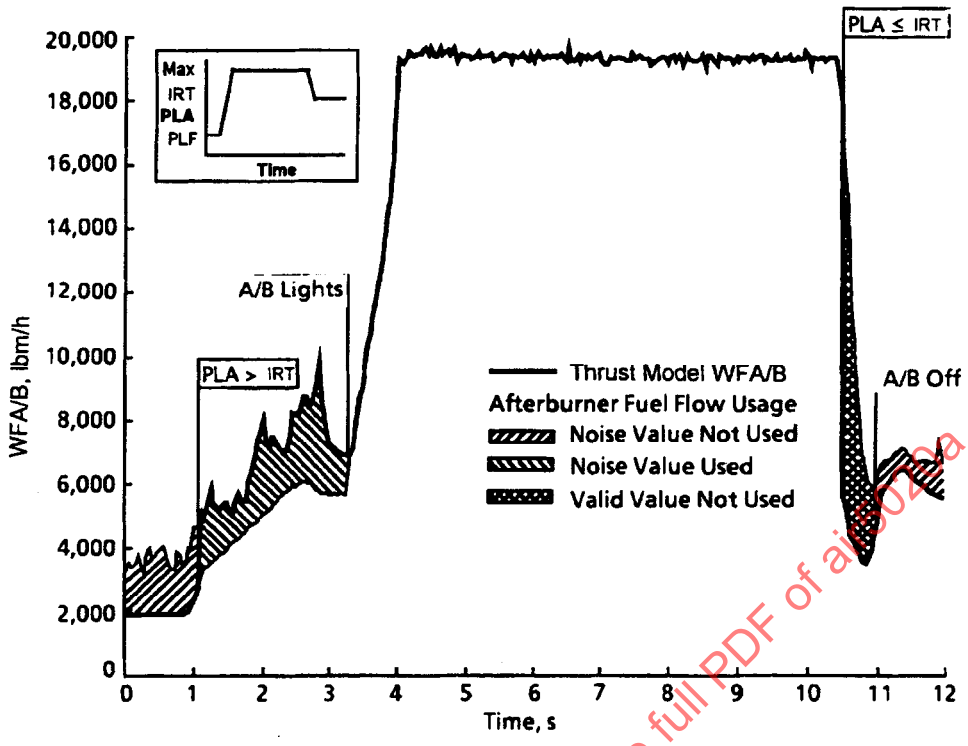

FIGURE 61 - Problems With Fuel Flow Calculation Caused by Using PLA as Afterburner Logic Test

7.7.1 (Continued):

The nonafterburner engine throttle step results in Figure 60 are noticeably affected by the engine accel/decel schedule, but show little sensitivity to throttle rate. The slow Idle-to-IRT transient (Figure 60C) differs from the ideal F_{IPF} value (based on change in F_{EX}) by up to 500 lb while the IRT-to-Idle transients (Figure 60A) deviate up to 1,000 lbf from the ideal value. Variations in F_{IPF} due to throttle rates are less than 100 lbf of each other, indicating that a possible throttle rate limiting condition exists in the engine control. This could be verified by repeating the maneuver at slower PLA rates.

A comparison of three various thrust calculation methods was made using the medium-rate throttle steps presented in Figure 58. In addition to the mass flow-temperature method ($F/W\sqrt{T}$) previously discussed, the gas path technique based on nozzle throat area and pressure (F/AP) was evaluated. The simplified gross thrust method (SGTM) developed for real-time application (4.1.2) was also tested. This method only uses augmentor-measured static and total pressures to calculate gross thrust. These three methods were calibrated in an altitude thrust facility where the steady-state gross thrust accuracies were determined to be 1.2%, 1.65%, and 1.8%, respectively, for $F/W\sqrt{T}$, F/AP, and SGTM (Reference 7.9). The transient F_{IPF} values calculated using these methods are compared in Figure 62. Small adjustments (biases) were made to the F/AP and SGTM thrust values to improve their agreement at steady-state conditions. Both the F/AP and SGTM methods show improved dynamic results over the $F/W\sqrt{T}$ method, particularly during dry power operation. This is

SAENORM.COM : Click to view the full PDF of air5020a

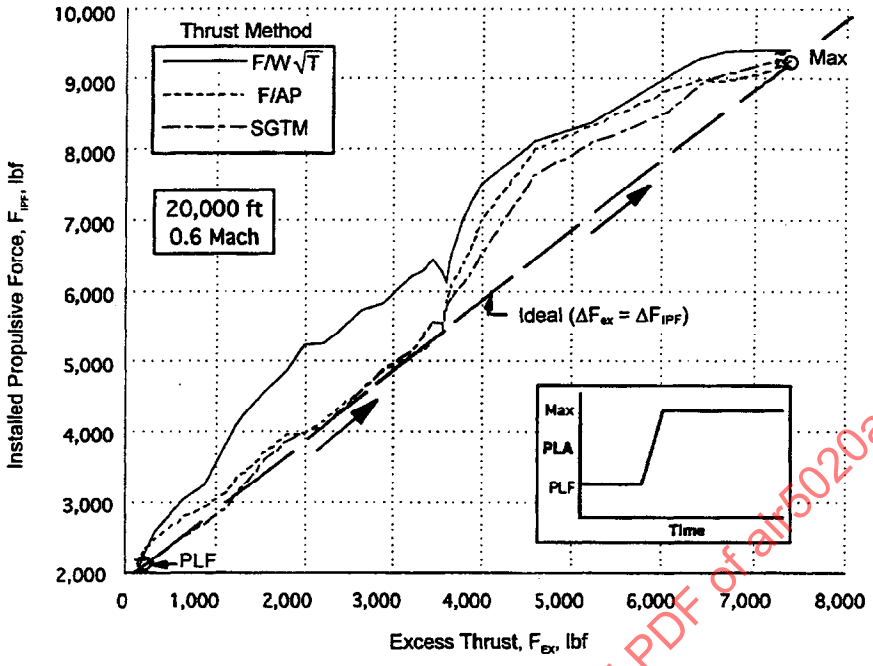

FIGURE 62A - PLF to Max

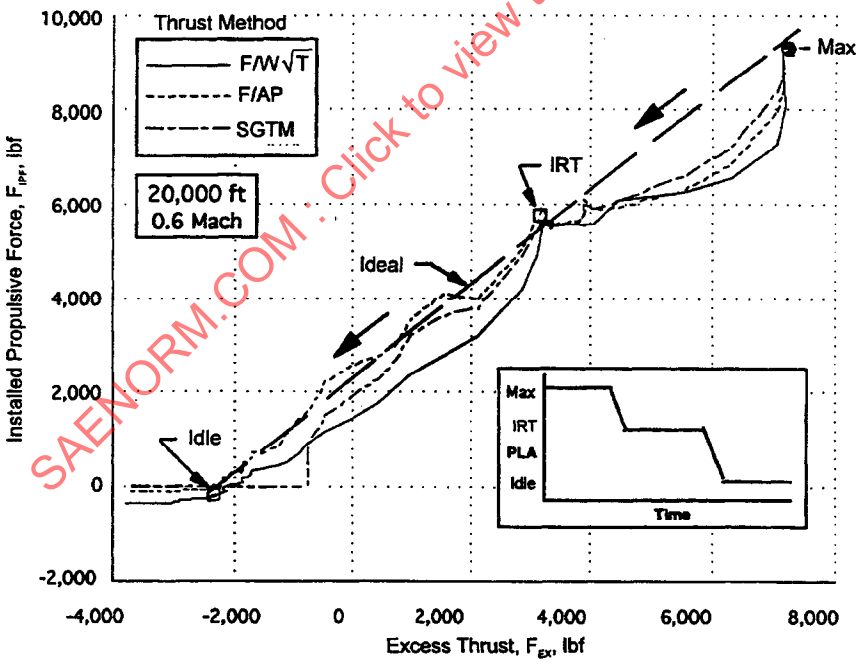

FIGURE 62B - Max-IRT-Idle

FIGURE 62 - Comparison of Various Thrust Calculation Techiques

SAENORM.COM : Click to view the full PDF of air5020a